

# Dissertation

Trace elements in Japanese precious corals as  
indicators for habitat and growth characteristics

Graduate School of Natural Science & Technology

Kanazawa University

Major Subject: Division of Material Science

Course: Material Information Analysis

School Registration No: 1023132312

Name : Nguyen Trong Luan

Chief Advisor: Prof. Hiroshi Hasegawa

## ABSTRACT

Japanese precious corals (JPCs) refer to Japanese red coral (*Paracorallium japonicum*), Japanese pink coral (*Corallium elatius*) and Japanese white coral (*Corallium konojoi*) are considered as ecologically as well as economically important natural resources of Japan, and are characterised by slow growth rates compared to other precious corals of other geographical locations. The study reveals that the trace elements in skeletons of precious corals are habitat-specific rather than species-specific. The Mg/Ca and Ba/Ca ratios in skeletons of precious corals, particularly, are the indicators of their habitats and environments. The study also show the spatial distribution of trace elements (S, P, Mg, and Sr) in the skeleton of *P. japonicum*. The distribution pattern of the trace elements, particularly Mg, S and P, illustrates linkage between the trace element distribution and the formation of growth bands in the coral skeleton.

The petrographic method is a popular technique for estimating the age and growth rates of corals based on growth ring density in their axial skeleton. The organic matrix staining (OMS) method, a modified method of petrographic method, has been used for measuring age and growth rate of the Mediterranean red coral (*Corallium rubrum*) by staining the organic matrix in the calcite skeleton. Since the OMS method is based on the concentration of organic matrix in the coral skeleton, this method may not be suitable for coral species with low organic matrix. In the present study, growth characteristics and growth rates of three Japanese precious corals (*Paracorallium japonicum*, *Corallium elatius* and *Corallium konojoi*) were determined based on the principles of the petrographic method using a VHX-1000 digital microscope, termed as

VHX-1000 hereafter, without staining the organic matrix in the axial skeleton. Compared to the organic matrix-stained cross-sections (slabs), growth rings in unstained slabs of the Japanese red coral were more clearly visible through the VHX-1000. This may be due to the low concentration of organic matrix in the Japanese precious corals compared to the Mediterranean red coral. Growth rates of Japanese precious corals differ significantly depending on coral species, habitat and environmental conditions. Diametric and linear growth rates of the Japanese red coral (*P. japonicum*) were slower ( $0.20\pm 0.08$ – $0.27\pm 0.01$  and  $2.22\pm 0.82$ – $6.66\pm 5.52$  mm yr<sup>-1</sup>, respectively) than the Japanese pink (*C. elatus*;  $0.30\pm 0.04$  and  $2.76\pm 2.09$  mm yr<sup>-1</sup>, respectively) and white (*C. konojoi*;  $0.44\pm 0.04$  and  $7.60\pm 0.75$  mm yr<sup>-1</sup>, respectively) corals. In addition, the diametric growth rate of the Japanese precious corals (*P. japonicum*) is slower ( $0.24\pm 0.05$ – $0.44\pm 0.04$  mm yr<sup>-1</sup>) than the Mediterranean red coral (*C. rubrum*;  $0.20$ – $0.62\pm 0.19$  mm yr<sup>-1</sup>).

Precious corals have been commercially exploited for many centuries all over the world. The skeletons of these corals consist of calcium carbonate, and have been used as amulets or gemstones since ancient times. Different *Corallium* species of Coralidae family (e.g., *C. rubrum*, *C. elatus*, *C. konojoi*, and *P. japonicum*) were collected from different locations of the Mediterranean Sea (off Italy) and Pacific Ocean (off Japan and off Midway Island), and trace elements in their skeletons were analyzed. Results show that trace element concentrations in the skeletons of *Corallium* spp. were attributable to their habitat and origin. In particular, Mg/Ca and Ba/Ca ratios in the skeletons of *Corallium* spp. from the Mediterranean Sea and Japanese and the Midway Islands' waters were found to be habitat-specific. This study also reveals that trace

elements in the skeletons can be used as ecological indicator of the coral's origin, and are expected to play an important part in the cultural study and sustainable management of precious corals. Findings of this study will also be of great relevance to the coral industry to authenticate and identify the habitat and origin of the corals.

This study also investigated the distribution of magnesium (Mg), phosphorus (P), sulfur (S) and strontium (Sr) using micro X-ray fluorescence ( $\mu$ -XRF), and the speciation of sulfur using X-ray absorption near edge spectroscopy (XANES) along the annual growth rings (AGRs) in the skeleton of Japanese red coral (*Paracorallium japonicum*). The Mg, P and S distribution in  $\mu$ -XRF mapping images correspond to the dark and light bands along the AGRs in microscopic images of the coral skeleton.  $\mu$ -XRF mapping data showed a strong positive correlation ( $r = 0.6$ ) between P and S distribution in the coral skeleton. A contrasting distribution pattern of S and Mg along the axial skeleton of the coral indicates a weak negative correlation ( $r = -0.2$ ) between these two elements. The distribution pattern of S, P and Mg in the axial skeleton of *P. japonicum* reveals linkage between the trace element distribution and the formation of dark/light bands along the AGRs. S and P were distributed in the organic matrix (OM) rich dark bands, while Mg was distributed in the light bands of the AGRs. XANES analysis showed that inorganic sulphate is the major species of S in the skeleton of *P. japonicum* with a ratio of 1:20 for organic and inorganic sulphate.

## **ACKNOWLEDGMENTS**

I am grateful to the many people who have made completing this research

I am very grateful to my advisor, Dr Hiroshi Hasegawa (Professor, Institute of Science and Engineering, Kanazawa University, Japan) for giving me the opportunity to work with him and for his cheerful attitude to work, his solemn instruction, valuable suggestions and constant encouragement during the entire period of the research work and in the preparation of this dissertation. Grateful acknowledgment is made to Dr. Nozomu Iwasaki (Professor, Faculty of Geo-environmental Science, Rissho University, Japan) for their support and many helpful discussion throughout this research.

I would like to thank Dr. M.Azizur Rahman, School of Environmental Sciences, University of Technology Sydney (UTS), Australia, for reviewing the manuscript and making a number of helpful suggestions. I am also grateful to Dr. Yusuke Tamenori and Dr. Toshio Ninomiya for their guidance and expertise with XRF and XANES measurement in his beam line during my visit and would like to thank Dr. Toshihiro Yoshimura (Atmospheric and Ocean Research Institute, University of Tokyo, Japan) and Ms. Satomi Takahashi (Rissho University) for his cooperation and comments. I would like to thank to Dr. Maki Teruya (Associate Professor, Institute of Science and Engineering, Kanazawa University, Japan) for his helps and supports throughout the course of my study. I would like to thank Mr. M.D Mamunur Rahman for his cooperation during the whole research period.

Thanks to the crews of the ROV 'Hakuyo 2000', 'Hakuyo 3000' and its mother vessel 'Shinsei Maru' and the SNK Ocean Co. Ltd for sample collection. The authors also thank the Kochi prefectural government for providing coral samples for

this study. This research was support partly by Japan Society for the Promotion of Science (JSPS) as Grant-in-Aid for Science Research (24310056 and 20310144) and a Research and Development Projects for Application in Promoting New Policy of Agriculture, Forestry and Fisheries (22032) in Japan. I really appreciate Soc Trang 150 Project, Mekong 1000 Project's financial support for my expenses within three years in Japan.

I am grateful to my friends and lab-mates for being encouraging and helpful.

Special thanks to my dear parents, sisters, brother and relatives for their encouragements, wishes and all kind of helps during my study.

**Nguyen Trong Luan**

**June, 2013**

# **Dedicated to My Family**

# TABLE OF CONTENTS

|  | <b>PAGE</b> |
|--|-------------|
| <b>ABSTRACT</b>  | i           |
| <b>ACKNOWLEDGEMENTS</b>  | iv          |
| <b>TABLE OF CONTENTS</b>   | vii         |
| <b>LIST OF TABLES</b>  | xi          |
| <b>LIST OF FIGURES</b>   | xii         |
| <b>CHAPTER 1: INTRODUCTION</b>   | <b>1</b>    |
| References   | 6           |
| <b>CHAPTER 2: LITERATURE REVIEW</b>  | <b>9</b>    |
| 2.1 Japanese precious coral species and distribution   | 9           |
| 2.2 Reproduction   | 12          |
| 2.3 Skeletal structure and feeding   | 13          |
| 2.4 Growth characteristics of DPCs   | 14          |
| 2.4.1 Growth banding   | 14          |
| 2.4.2 Age and growth rate  | 16          |
| 2.5 Trace element distribution in the skeletons of precious coral and its<br>roles in paleoenvironment reconstruct | 19          |
| References   | 26          |
| <b>CHAPTER 3: GROWTH CHARACTERISTICS AND GROWTH RATE<br/>ESTIMATION OF JAPANESE PRECIOUS CORALS</b>                | <b>31</b>   |
| 3.1 Introduction   | 31          |

|  |           |
|--|-----------|
| 3.2 Focus  | 33        |
| 3.3 Materials and Methods  | 34        |
| 3.3.1 Sample collection  | 34        |
| 3.3.2 Cross-section preparation of the coral skeleton  | 34        |
| 3.3.3 Staining of organic matrix in the coral skeleton   | 35        |
| 3.3.4 Determination of the age and growth rates of Japanese<br>precious corals   | 35        |
| 3.4 Results  | 37        |
| 3.4.1 Growth characteristics of Japanese precious corals   | 37        |
| 3.4.2 Age and diametric growth rates of Japanese precious corals   | 40        |
| 3.4.3 Linear growth rates of Japanese precious corals  | 41        |
| 3.5 Discussion   | 42        |
| 3.5.1 Growth characteristics of Japanese precious corals   | 42        |
| 3.5.2 Growth rates of Japanese precious corals   | 46        |
| 3.5.3 Correlation between number of growth rings and diameter  | 48        |
| 3.5.4 Determination of the ages and growth rates of Japanese<br>precious corals  | 50        |
| References   | 60        |
| <b>CHAPTER 4: RESULTS AND DISCUSSION:<br/>TRACE ELEMENTS IN <i>Corallium</i> spp. as INDICATORS FOR ORIGIN<br/>AND HABITAT</b> | <b>65</b> |
| 4.1 Introduction   | 65        |

|  |           |
|--|-----------|
| 4.2 Focus  | 68        |
| 4.3 Materials and Methods  | 69        |
| 4.3.1 Sampling sites   | 69        |
| 4.3.2 Chemical analysis of skeleton composition  | 69        |
| 4.3.3 Analysis of inorganic elements with electron probe<br>micro-analyzer (EPMA)  | 71        |
| 4.4 Results and Discussion   | 71        |
| 4.4.1 Trace element distribution in the skeletons of precious<br>coral   | 72        |
| 4.4.2 Trace element compositions reflecting the characteristics of<br>coral habitats   | 73        |
| References   | 80        |
| <b>CHAPTER 5: RESULTS AND DISCUSSION:</b>  | <b>84</b> |
| <b>DISTRIBUTION OF TRACE ELEMENT IN JAPANESE RED CORAL<br/>(<i>Paracorallium japonicum</i>) BY <math>\mu</math>-XRF AND SULFUR SPECIATION BY<br/>XANES: LINKAGE BETWEEN TRACE ELEMENT DISTRIBUTION<br/>AND GROWTH RING FORMATION</b> |           |
| 5.1 Introduction   | 84        |
| 5.2 Focus  | 88        |
| 5.3 Materials and Methods  | 88        |
| 5.3.1 Sample collection and preparation  | 88        |
| 5.3.2 Extraction of organic matrix from fraction   | 89        |
| 5.3.3 $\mu$ -XRF and XANES analysis  | 89        |

|  |            |
|--|------------|
| 5.4 Results and Discussion   | 90         |
| 5.4.1 $\mu$ -XRF analysis for trace element distribution in DPC<br>skeleton      | 90         |
| 5.4.2 Distribution of trace elements and the formation of annual<br>growth rings | 92         |
| 5.4.3 Speciation of S in Japanese red coral using XANES                          | 95         |
| References   | 102        |
| <b>CHAPTER 6: CONCLUSION</b>   | <b>107</b> |
| <b>APPENDIX</b>  | <b>110</b> |

| <b>LIST OF TABLES</b> |  | <b>PAGE</b> |
|-----------------------|--|-------------|
| <b>Table 1.1</b>      | Precious corals refers to about 31 species that belong to the <i>Corallium</i> and <i>Paracorallium</i> genera (Bayer & Cairns, 2003)  | 3           |
| <b>Table 2.1</b>      | Actual age and estimate obtain by staining the organic matrix and by the petrographic for five colonies collected from the experiment panels (Marschal et al, 2004)  | 18          |
| <b>Table 2.2</b>      | Biology of Japanese precious corals species  | 23          |
| <b>Table 3.1.</b>     | Diametric growth rates and ages of the Japanese red ( <i>Paracorallium japonicum</i> ), pink ( <i>Corallium elatius</i> ), and white ( <i>Corallium konojoi</i> ) corals collected from Japanese waters.             | 54          |
| <b>Table 3.2.</b>     | Linear growth rates of the Japanese red ( <i>Paracorallium japonicum</i> ), pink ( <i>Corallium elatius</i> ), and white ( <i>Corallium konojoi</i> ) corals collected from Japanese                                 | 55          |
| <b>Table 3.3.</b>     | Diametric and linear growth rate of Japanese precious corals (Luan et al., unpublished)  | 57          |
| <b>Table 3.4</b>      | Diametric growth rates of precious corals from different geographical locations estimated by different methods   | 58          |
| <b>Table 4.1.</b>     | Different types of precious corals collected for ICP-AES analysis. Samples were collected from Japanese waters, Midway Islands' waters and Mediterranean Sea from fishermen, coral traders, and research institutes. | 76          |

| <b>LIST OF FIGURES</b> |  | <b>PAGE</b> |
|------------------------|--|-------------|
| <b>Figure 2.1</b>      | Japanese precious corals. Above left : Shiro (white) ( <i>Corallium konojoi</i> ). Above right: Momo (Pink) ( <i>Corallium elatius</i> ). Below: Aka (red) ( <i>Paracorallium japonicum</i> )  | 11          |
| <b>Figure 2.2</b>      | A cross-section of the coral skeleton of DPC-19 ( <i>Paracorallium japonicum</i> ) (left). Two types of growth bands, light and dark, as seen under the VHX-1000 digital microscope. The dark bands indicate the zones of high organic matrix (OM) content,  | 15          |
| <b>Figure 2.3</b>      | Microscopic images of a corallium rubrum colony. A general view of cross section obtained using the petrographic and B the cross section after staining the organic matrix (Marschal et al., 2004)   | 15          |
| <b>Figure 2.4</b>      | Living colony of Mediterranean red coral ( <i>Corallium rubrum</i> ) (A). Axial skeleton of <i>C. rubrum</i> (B) and Sclerites of this coral (C)   | 25          |
| <b>Figure 3.1</b>      | Axial skeleton of Japanese red coral <i>Paracorallium japonicum</i> (DPC-18). Numbers on the skeleton indicate the sample sites, and the images are the cross-sections of the corresponding samples. The cross-sections were polished to make the growth rings clear to count them and estimate growth rate and age of the coral. The diameter of the core become wider at the younger part (tip; 1) than at the older part (base; 6) of the colony. | 38          |
| <b>Figure 3.2</b>      | The ratio of the core diameter and total (including the core)  | 39          |

diameter of the axis. The ratio increased with increasing distance of the axis cross-sections from the base to the tip of the colony. The cross-section numbers (CS4-CS1) in x-axis of the figure represent the consecutive slabs from the base to the tip of coral axis.

- Figure 3.3** (A) Two types of growth bands, light and dark, as seen under the VHX-1000 digital microscope. The dark bands indicate the zones of high organic matrix (OM) content, while the light bands represent the zones of low OM content in the coral skeleton. (B) A cross-section at the tip on the younger part of the coral skeleton (*Paracorallium japonicum*). The calcium carbonate deposited in the core on the younger part of the axis does not generate/form growth rings. 44
- Figure 3.4** Growth rings in thin cross-sections of the axial skeleton of different Japanese precious coral species under the VHX-1000 digital microscope. (A-B) red coral (*Paracorallium japonicum*), (C-D) pink coral (*Corallium elatius*), (E-F) white coral (*Corallium konojoi*). 45
- Figure 3.5** Correlation between the number of growth rings and the diameter of the base of Japanese precious corals (*Paracorallium japonicum*, *Corallium elatius*, and *Corallium konojoi*). 49
- Figure 3.6** Cross-section of the axial skeleton of the Japanese red coral (*Paracorallium japonicum*) observed under the VHX-1000 51

digital microscope without treatment (A), after treatment with 2% acetic acid solution for 4-5 h (B), and after staining the organic matrix in the skeleton with 0.05% Toluidine blue for 10-30 s (C). Magnified images of the internal region near center before and after staining the organic matrix with 0.05% Toluidine blue (D).

- Figure 4.1** Skeleton of Japanese white coral. Photograph of white coral (A), mapping analysis of Mg (B), Ca (C), Ba (D), and Sr (E) in the skeleton of precious white coral by EPMA. 78
- Figure 4.2** Distribution of Mg and Ba in skeleton of precious corals collected from different depth and geographical locations indicating the origin of the corals. Values are mean  $\pm$  SD. 79
- Figure 5.1** X-ray fluorescence spectrum of trace elements (Na, S, P, Mg and Sr) in powdered sample of Japanese red coral (DPC-19) skeleton measured at 2500 eV of excitation photon energy 97
- Figure 5.2** X-ray fluorescence spectrum of trace elements (Na, S, P, Mg and Sr) in Japanese red coral skeleton (DPC-19) using 2500 eV energy, 5s/point measuring time, and 10  $\mu$ m step size. White arrow (7 mm) is the position from where the section was taken for  $\mu$ -XRF analysis (A). Trace element spectrum in the sample (B). Relationship between the distributions of S and Mg (C) and S and P (D) in the skeleton of DPC-19 98
- Figure 5.3** Micro-XRF mapping analysis of Mg and S in axial skeleton of Japanese red coral (DPC-18). Cross section of DPC-18 skeleton 99

showing the position where the  $\mu$ -XRF analysis was performed (a). The magnification of the region of  $\mu$ -XRF analysis (b). Distribution maps of Mg and S in the skeleton of the coral (c). The colour bar represents the signal intensity with the blue and red color correspond to lower and higher distributions, and the black and red color regions in the maps indicate the lowest and highest distribution of the elements, respectively. Micro-XRF signal was collected at 10  $\mu$ m step size

**Figure 5.4** Micro-XRF mapping analysis of trace elements in polished cross section of Japanese red coral skeleton (DPC-19). Two copper rings of one mm diameter were used to select two positions on the cross section of the coral skeleton where the distribution of trace elements were detected. The colour bars represent the signal intensity with the blue and red color correspond to lower and higher distributions, and the black and red color regions in the maps indicate the lowest and highest distribution of the elements, respectively. Micro-XRF signal was collected at 10  $\mu$ m step size 100

**Figure 5.5** XANES spectra of sulfur (S) in axial skeleton and organic matter extract of DPC-19. XANES spectra of S reference compounds (A). Each of the cysteine and methionine spectra display a single peak at 2473 eV photon energy, while chondroitine, protamine, and gypsum show peaks at 2482 eV photon energy. Saccharine exhibits a single peak at 2477.5 eV 101

photon energy. Magnified view ( $\times 5$ ) of XANES spectra of S in axial skeleton and organic matter of DPC-19 (B) showing that sulfate is the main species of S and organic matter content in the DPC-19 skeleton is very low

## LIST OF CONFERENCES /FORUMS

1. **The Twelfth Asian Conference on Analytical Sciences**, August 22-24, 2013, Maidashi campus of Kyushu University , Fukuoka-city, Japan. (Presentation: **Luan Trong Nguyen**, M. Azizur Rahman, Toshihiro Yoshimura, Yusuke Tamenori, Teruya Maki, Nozomu Iwasaki, Hiroshi Hasegawa. “Determination of Growth Rings and Microstructure in Skeleton of Japanese Precious Corals”
2. **Forum of Division of Material Science**. November, 7.2011, Kanazawa University, Japan. (Presentation: **Luan Trong Nguyen**. “Distribution and Chemical Forms in Skeleton of Japanese precious corals by Micro-XRF and XANES analysis”
3. **Forum of Division of Material Science**. November, 5.2012, Kanazawa University, Japan. (Presentation: **Luan Trong Nguyen**. “Estimation of Growth Rate of Japanese Precious Red Coral, *Paracorallium japonicum*”)

# CHAPTER 1

## INTRODUCTION

Precious corals (PCs) belong to family Corallidae, class Anthozoa, subclass Octocorallia, order Scleractinia. They refer to roughly 31 species that belong to the *Corallium* and *Paracorallium* genera (Table 1.1) (Bayer and Cairns, 2003). They are found mainly in the Mediterranean Sea and Pacific Ocean (Japanese waters and off Taiwan, off the Midway Islands and off the Hawaiian Islands (Iwasaki and Suzuki, 2010). Many precious coral species are long-lived, grow slowly (diametric growth rate usually less than 1mm per year) and reaching more than 100 years of age (Andrews *et al.*, 2005; Luan *et al.*, 2013). Precious corals have been highly valued because their skeletons have been used as jewellery, souvenir industries, medicine and are one of the most valuable living marine resource (Nonaka and Muzik, 2009; Iwasaki and Suzuki, 2010; Tsounis *et al.*, 2010). Precious corals have attracted worldwide attention as sparse biological resources, and Corallidae have been recently proposed for inclusion in Appendix II of the Convention on International Trade in Endangered Species of Wild

Fauna and Flora (CITES) that regulates the international trade in endangered species by listing them in its appendices (Hasegawa and Yamada, 2010; Tsounis *et al.*, 2010; Hasegawa *et al.*, 2012)

Knowledge of the biology, growth rates, and durability of deep-sea corals (DSC) is important since they provide habitat to commercially important fishes and are under great threat from benthic fishing techniques (Witherell *et al.*, 2000; Roark *et al.*, 2006). Geochemical and isotopic data derived from DSC provide an understanding of past climate and environmental change (Roark *et al.*, 2006). Understanding of growth rates and ages of these long-lived DSC also contributes to our knowledge of their biology, ecology, and physico-chemical characteristics. In addition, conservation and management of marine ecosystems and DSC, and reconstruction of the paleo-environment using the paleoceanographic archive of DSC require knowledge of the growth rates and longevity of these organisms (Goldberg, 1991; Roark *et al.*, 2006).

Chemical analyses of carbonate skeletons in precious corals found that the mineralised hard tissues of precious corals are composed of a skeletal axis and spicules. Both spicules and skeletons of corals are mainly made of calcium carbonate (CaCO<sub>3</sub>) crystallized in the form of calcite and trace elements (Maté *et al.*, 1986; Hasegawa and Iwasaki, 2010). Precious corals are different from reef-building corals in that their skeletons are closely-packed with magnesium calcite, while the reef-building corals consist mostly of aragonite, and are porous because of its loosely-packed crystals (Hasegawa *et al.*, 2012).

Reef-building coral is better understood, and concentrations of trace elements in its carbonate skeletons have been determined. The validity of their use as indicators of past environmental conditions, such as water temperatures, nutrients and pollution

levels has been confirmed in earth and environmental science studies (Weber and Woodhead, 1970; Weber, 1973; Mitsuguchi *et al.*, 1996; Mitsuguchi *et al.*, 2001; Mitsuguchi *et al.*, 2003). In contrast, studies on trace elements in precious coral have been focused mostly on Mediterranean red coral (*C. rubrum*) (Weinbauer and Vellmirov, 1995; Weinbauer *et al.*, 2000). Studies on trace elements in other precious corals, especially the Japanese precious coral is limited.

---

**Table 1.1** Precious corals refer to about 31 species that belong to the *Corallium* and *Paracorallium* genera (Bayer & Cairns, 2003)

---

|                               |                              |                                     |
|-------------------------------|------------------------------|-------------------------------------|
| <i>Corallium abyssale</i>     | <i>Corallium niobe</i>       | <i>Corallium variabile</i>          |
| <i>Corallium borneense</i>    | <i>Corallium niveum</i>      | <i>Corallium sp. nov</i>            |
| <i>Corallium boshuense</i>    | <i>Corallium porcellanum</i> | <i>Paracorallium inutile</i>        |
| <i>Corallium ducale</i>       | <i>Corallium pusillum</i>    | <i>Paracorallium japonicum</i>      |
| <i>Corallium elatius</i>      | <i>Corallium regale</i>      | <i>Paracorallium nix</i>            |
| <i>Corallium halmaheirens</i> | <i>Corallium reginae</i>     | <i>Paracorallium salomonense</i>    |
| <i>Corallium imperiale</i>    | <i>Corallium rubrum</i>      | <i>Paracorallium stylasteroides</i> |
| <i>Corallium johnsoni</i>     | <i>Corallium secundum</i>    | <i>Paracorallium thrinax</i>        |
| <i>Corallium konojoi</i>      | <i>Corallium sulcatum</i>    | <i>Paracorallium tortuosum</i>      |
| <i>Corallium maderense</i>    | <i>Corallium tricolor</i>    |                                     |
| <i>Corallium medea</i>        | <i>Corallium vanderbilti</i> |                                     |

---

## Objectives of the Study

The aim objective of this thesis was to describe the growth rate and growth characteristics of Japanese precious corals. Concentration and distribution of trace elements in precious corals related to their origin and habitat were investigated as well. In addition, we also have examined the linkage between the distribution pattern of trace elements and the formation of annual growth rings along the coral skeleton.

The detailed thesis aims can be summarised as follows:

1. To investigate the skeletal structure, estimating growth rates and ages of three Japanese precious corals *Paracorallium japonicum*, *Corallium elatius*, *Corallium konojoi* using a high resolution VHX-1000 digital microscope.
2. To compare growth rings in the stained (the staining the organic matrix in the skeleton with toluidine blue) with unstained cross section.
3. To investigate if concentration and distribution of trace elements in precious corals related to their origin and habitat.
4. To investigated the distribution of magnesium (Mg), phosphorus (P), sulfur (S) and strontium (Sr) using micro X-ray fluorescence ( $\mu$ -XRF), and the speciation of sulfur using X-ray absorption near edge spectroscopy (XANES) along the annual growth rings in the skeleton of Japanese red coral (*Paracorallium japonicum*).

## Organization of the Study

Chapter 2 provides an overall view of the findings of biological and biochemical research on precious corals, introduces classification, ecology of corals, growth characteristics and trace elements distribution in the skeleton of corals.

Chapter 3 describes the growth characteristics and growth rates of Japanese precious corals by examining their skeletal structure and estimating growth rates using digital microscope. Comparison between the growth rings in both stained (toluidine blue, organic matrix staining methods) and unstained slabs of the corals

Chapter 4 discusses about the trace elements in *Corallium* Spp as indicator for origin and Habitat.

Chapter 5 is distribution of trace elements in Japanese red coral by  $\mu$ -XRF and sulfur speciation by XANES focus on the linkage between trace element distribution and growth ring formation.

Chapter 6 provides a summary of overall experiments and scope of the future research.

## References

- Andrews, A., Cailliet, G., Kerr, L., Coale, K., Lundstrom, C., DeVogelaere, A., 2005. Investigations of age and growth for three deep-sea corals from the Davidson Seamount off central California. In: Freiwald, A., Roberts, J.M. (Eds.), Cold-Water Corals and Ecosystems. Springer, Berlin, pp. 1021-1038.
- Bayer, F.M., Cairns, S.D., 2003. A new genus of the scleraxonian family Coralliidae (Octocorallia: Gorgonacea). Proc. Biol. Soc. Wash. 116, 222-228.
- Goldberg, W.M., 1991. Chemistry and structure of skeletal growth rings in the black coral *Antipathes fiordensis* (Cnidaria, Antipatharia). Hydrobiologia 216, 403-409.
- Harvell, C.D., Kim, K., Burkholder, J.M., Colwell, R.R., Epstein, P.R., Grimes, D.J., Hofmann, E.E., Lipp, E.K., Osterhaus, A., Overstreet, R.M., 1999. Emerging marine
- Hasegawa, H., Iwasaki, N., 2010. Chemical analyses of carbonate skeletons in precious corals. Biohistory of Precious corals.
- Hasegawa, H., Rahman, M.A., Luan, N.T., Maki, T., Iwasaki, N., 2012. Trace elements in *Corallium* spp. as indicators for origin and habitat. J. Exp. Mar. Biol. Ecol. 414-415, 1-5.
- Iwasaki, N., H. Hasegawa, T. Suzuki, Yamasa, a.M., 2009. Biology of Japanese *Corallium* and *Paracorallium*, paper presented at Proceedings of the First International Workshop on *Corallium* Science, Management, and Trade. NOAA Technical Memorandum NMFS-OPR-43 and CRCP-8, Silver Spring, MD, Hong Kong, China., 149.
- Iwasaki, N., Suzuki, T., 2010. Biology of precious corals. In: Iwasaki, N. (Ed.), Biohistory of precious corals- scientific,cultural and historical perspectives.

- Tokai Univeristy Press, Tokai, Japan.
- Jackson, J.B.C., Kirby, M.X., Berger, W.H., Bjorndal, K.A., Botsford, L.W., Bourque, B.J., Bradbury, R.H., Cooke, R., Erlandson, J., Estes, J.A., 2001. Historical overfishing and the recent collapse of coastal ecosystems. *Science* 293, 629-637.
- Luan, N.T., Rahman, M.A., Maki, T., Iwasaki, N., Hasegawa, H., 2013. Growth characteristics and growth rate estimation of Japanese precious corals. *J. Exp. Mar. Biol. Ecol.* 441, 117-125.
- Maté, P., Revenge, S., Masso, C., 1986. Estudio preliminar de la composicion quimica del coral rojo (*Corallium rubrum* L.) de distintas zonas del Mediterraneo Espanol. *Bol. Inst. Esp. Oceanogr.* 3, 53-60.
- Mitsuguchi, T., Matsumoto, E., Abe, O., Uchida, T., Isdale, P.J., 1996. Mg/Ca thermometry in coral skeletons. *Science* 274, 961.
- Mitsuguchi, T., Uchida, T., Matsumoto, E., Isdale, P.J., Kawana, T., 2001. Variations in Mg/Ca, Na/Ca, and Sr/Ca ratios of coral skeletons with chemical treatments: implications for carbonate geochemistry. *Geochim. Cosmochim. Acta* 65, 2865-2874.
- Musick, J.A., 1999. Ecology and conservation of long-lived marine animals. In: Musick, J.A. (Ed.), *Life in the Slow Lane: Ecology and Conservation of Long-Lived Marine Animals*. American Fisheries Society, Maryland, USA, pp. 1-10.
- Nonaka, M., Muzik, K., 2009. Recent harvest records of commercially valuable precious corals in the Ryukyu Archipelago. *Mar. Ecol. Prog. Ser.* 397, 269-278.
- Roark, E.B., Guilderson, T.P., Dunbar, R.B., Ingram, B.L., 2006a. Radiocarbon-based ages and growth rates of Hawaiian deep-sea corals. *Mar. Ecol. Prog. Ser.*
- Seki, K., 1991. Study of precious coral diver survey with open circuit air SCUBA

diving at 108 m. *Ann. Physiol. Anthropol.* 10(3), 189-192.

Tsounis, G., Rossi, S., Aranguren, M., Gili, J.M., Arntz, W., 2006. Effects of spatial variability and colony size on the reproductive output and gonadal development cycle of the Mediterranean red coral (*Corallium rubrum* L.). *Mar. Biol.* 148, 513-527.

Weber, J.N., 1973. Incorporation of strontium into reef coral skeletal carbonate. *Geochim. Cosmochim. Acta* 37, 2173-2190.

Weinbauer, M., Brandstätter, F., Velimirov, B., 2000. On the potential use of magnesium and strontium concentrations as ecological indicators in the calcite skeleton of the red coral (*Corallium rubrum*). *Mar. Biol.* 137, 801-809.

Weinbauer, M.G., Velimirov, B., 1995. Calcium, magnesium and strontium concentrations in the calcite sclerites of Mediterranean gorgonians (Coelenterata: Octocorallia). *Estuar. Coast. Shelf Sci.* 40, 87-104.

Witherell, D., Pautzke, C., Fluharty, D., 2000. An ecosystem-based approach for Alaska groundfish fisheries. *ICES J. Mar. Sci.* 57, 771-777.

# CHAPTER 2

## LITERATURE REVIEW

Precious corals are a group of about 31 species that belong to the *Corallium* and *Paracorallium* genera. Trade has mainly focused on species that are in highest demand by the jewellery, art objects, medicine such as *Corallium rubrum* from the Mediterranean and North East Atlantic, and *C. Secundum*, *C. konojoi*, *C. elatius*, *C. regale* and *Paracorallium japonicum* from the Pacific (2003). Three Japanese precious corals are *Paracorallium japonicum* (aka sango), *C. elatius* (momo sango), *C. konojoi* (shiro sango) belong to this precious group. In this thesis we focus on these species.

### 2.1 JAPANESE PRECOUS CORAL SPECIES AND DISTRIBUTION

Japanese precious corals (JPCs) refer to Japanese red coral (*Paracorallium japonicum*), Japanese pink coral (*Corallium elatius*) and Japanese white coral (*Corallium konojoi*), which are distributed and harvested in waters near Japan (Iwasaki

*et al.*, 2009). The first studies in Japan of JPCs (Kishinouye, 1903, 1904; Seki, 1991) found that *P. japonicum* habitat at depths of 76 to 280 m on the rocky bottom in Sagami Bay, Pacific coast of Japan, in the waters from the Ogasawara Islands to Taiwan and off the coast near the Goto Islands, Nagasaki. It was measured up to 30 cm in height. In the waters near Wakayama, Pacific coast of Japan, from the Ogasawara Islands to the northern South China Sea and off the Goto Islands, Nagasaki, *C. elatius* distributed on the rocky bottom at a depth of 100 – 276 m , with a height of up to 1.1m and 1.7 m in width and weighed 67 kg (Iwasaki and Suzuki, 2010). *C. konojoi* distributed on the rocky bottom at a depth of 76 to 276 m in the waters of Wakayama, pacific coast of Japan, in the waters from the Ogasawara Islands to the northern South China Sea and off the Goto Islands, Nagasaki, with a height of up to 30 cm (Seki, 1991; Nonaka *et al.*, 2006). .

In Japan, JPC fishing for *P. japonicum*, *C. elatius*, *C. konojoi* began in Kochi during the 19<sup>th</sup> century and maintain the present day in Kochi, Kagoshima and the Ryukyu Archipelago (Nonaka and Muzik, 2009). Different areas have different fishing methods. For example, in order to collect the coral, the fishermen in Kochi drag a kind of tangle net with a stone weight the sea, while manned or unmanned underwater vehicles are used to exploit the coral in Kagoshima and off Okinawa. Coral fisheries in Japan authorized by prefecture governors and fishing methods, areas and periods are different in prefectures. In a case of manned or manned underwater vehicles, fishermen follow self imposed minimum size limits that allow them to harvest corals only above a certain size (Iwasaki *et al.*, 2009).



Fig. 2.1 Japanese precious corals. Above left : Shiro (white) (*Corallium konojoi*). Above right: Momo (Pink) (*Corallium elatius*). Below: Aka (red) (*Paracorallium japonicum*)

## 2.2. REPRODUCTION

Precious coral species have both sexual and asexual production. Concerning gorgonian sexual reproduction, Ribes *et al* (2007) reported that there are 3 types. Firstly, fertilization occurs when eggs and sperms are released into the water. Secondly, eggs are fertilized and develop into larvae within female polyp. Thirdly, eggs are fertilised and develop into larvae on the surface of the mother colonies. Red coral (*Corallium rubrum*) can attain sexual maturity from 2 – 10 years (Santangelo *et al.*, 2003; Torrents *et al.*, 2005) while Grigg (1993) reported that *C. secundum* needed 12- 13 years to attain maturity. Gallmetzer *et al.*, (2010) reported that sexual maturation between male and female of precious corals is different. Male can achieve sexual maturation only approximately 6 years, while those of female is 10 years. Early maturation in males could point to a strategy against possible sperm limitation in environments where the presence of constant currents or turbulences enhances the dilution of gametes released into the water and reduces the fertilization success, if not compensated by early and high sperm production (Gallmetzer *et al.*, 2010). Therefore, these information have been helpful for management of the species. For example, colonies achieve sexual maturity only after approximately 10 years, but need at least 20 years or more to reach a colony size able to ensure a higher reproductive potential (Garrabou and Harmelin, 2002; Marschal *et al.*, 2004; Torrents *et al.*, 2005)

This thesis focuses on Japanese precious corals. However, information on reproduction of this species is very limited. (Kishinouye, 1904) reported that the reproductive season of *P. japonicum* was spring. Eggs and spermatids of this species

collected in March and September and it is noted that eggs and spermatids in March were larger in number and bigger than in size than in September.

### 2.3. SKELETAL STRUCTURE AND FEEDING

Iwasaki and Suzuki (2010) reported that JPC live attached directly to the bottom of 10-20 m high rock, between rocks, on slopes of 20-30 m high sea cliffs and rocks scattered on the sandy bottom. Colonies of *C. elatius* and *C. Konojoi* usually growth in the shape of fan, oriented at right angles to the water current, and their outer branches, were polyps grow, curve inwards slightly toward the current (Nishijima and Kamura, 1969). Precious coral skeletons are a complex of protein or calcium carbonate, its task is considered as a support system (Kishinouye, 1903, 1904; Muzik and Wainwright, 1977). In fact, the axis must be hard to support colonies away from seabed as well as limiting impact of water velocities (Muzik and Wainwright, 1977). Iwasaki,(2010) also showed that the axial skeleton of precious coral is hard with a Mohs hardness of 3.5 and specific gravity of 2.6 to 2.7.

Jones *et al.*(1994) suggested that if precious coral colonises form a three-dimension structure and other marine organisms make it their habitat for creating communities. In the fact that numerous organisms , such as galatheid crabs, brittle stars, mollusks , polychaetes and zoanthids, live in the colonies (Kishinouye, 1904; Reimer *et al.*, 2008). Precious corals not only provide shelter but also feed on suspended matter coming down form ocean surface turns it into organic matter, and pass it down to benthic communities (Gili and Coma, 1998). Stable carbon and nitrogen isotope

composition of a JPC, its associated organisms, and plankton collected from the sea off Kagoshima, Japan were shown by [Iwasaki \(2010\)](#)

## 2.4 GROWTH CHARACTERISTICS OF JAPANESE PRECIOUS CORALS

### 2.4.1 Growth banding

In the fact the information on growth characteristics of precious corals and reef building corals were described by [\(Marschal et al., 2004; Vielzeuf et al., 2008\)](#). However, research on determining the growth characteristic of JPCs has been limited. Some growth characteristics of JPCs were described by [\(Luan et al., 2013\)](#). For instance, The skeletons of the JPC were narrow at the tip and wide at the base of colony. Distinct growth rings did not form in the core of skeleton (detailed discussion in Chapter 3)

Using digital microscope [\(Luan et al., 2013\)](#) reported that axis cross section of JPC showed light and dark bands. The light bands were wider than the dark bands. Growth rings of axis cross section (a few hundred micrometers) were clearly visible and identifiable under the VHX-1000 and It was difficult to identify the growth rings in thicker sections. These characteristics were confirmed by [\(Marschal et al., 2004\)](#). They reported that a growth band consist a thick light colour and a thin dark colour that forms during the late autumn and winter months, corresponding to slow growth seasons. The dark bands indicate the zones of high organic matrix (OM) concentration, while the wider light bands represent the zones of low OM concentration in the coral skeleton [\(Marschal et al., 2004; Vielzeuf et al., 2008\)](#).

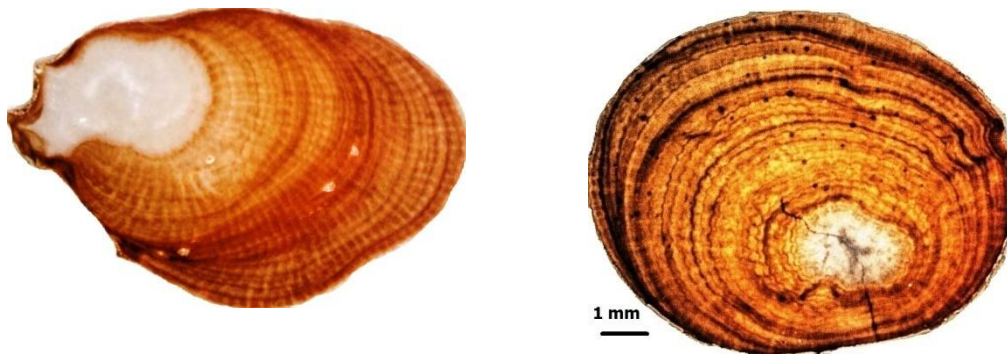


Fig. 2.2 A cross-section of the coral skeleton of DPC-19 (*Paracorallium japonicum*) (left). Two types of growth bands, light and dark, as seen under the VHX-1000 digital microscope. The dark bands indicate the zones of high organic matrix (OM) content

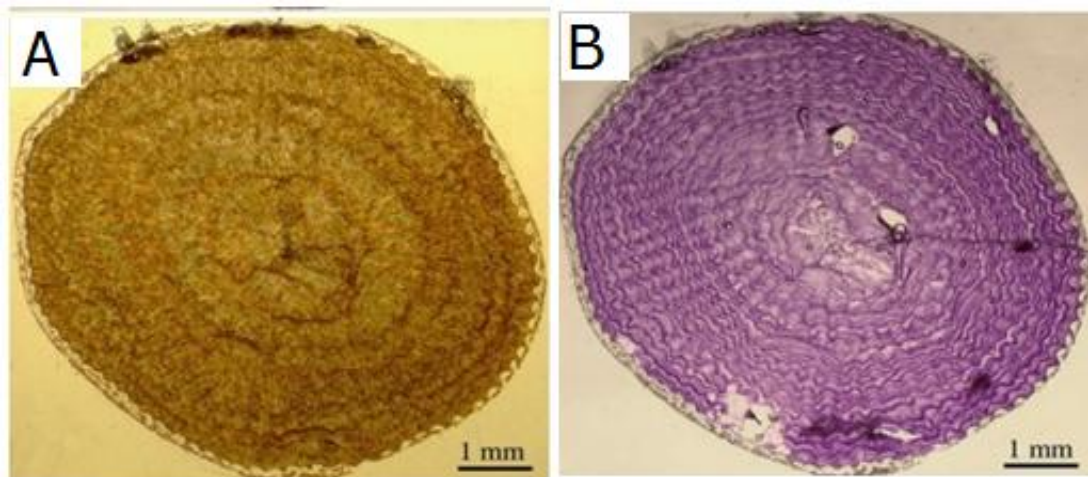


Fig 2.3. Microscopic images of a corallium rubrum colony. A general view of cross section obtained using the petrographic and B the cross section after staining the organic matrix (Marschal et al., 2004)

### 2.4.2 Age and Growth rate

For some species of coral, ages can be estimated by counting skeletal growth zones in cross sections of the axial skeleton (Grigg, 1974; Andrews *et al.*, 2002; Risk *et al.*, 2002b; Marschal *et al.*, 2004; Roark *et al.*, 2006).

The growth ring is annual and estimating age of corals based on counting the rings is more accurate than based on growth rate (Grigg, 1974). This author also suggested the number rings and estimates of age based on the growth age was suitable for young colonies.

Studies of age and growth characteristics of coral as shown by (Andrews *et al.*, 2002), those who counted growth rings in cross section to estimate age and growth and using a radiometric method to validate the estimated age and growth from ring counts. Risk *et al.*(2002a) and Casu *et al* (2008) also studied age of deep sea corals based on counting skeletal growth zones in cross sections of the axial skeleton. The results showed that the growth band of skeletons was approximately 10µm wide, which may be annual, and these authors suggested that the growth of these corals was very slow and long-lived.

Marschal *et al.*(2004) also reported that conventional petrographic method of direct microscope observation detected about 7 rings on the cross section of a 21 – 22 year old colony, while organic matrix staining method showed 17 – 18 rings. The organic matrix staining method showed underestimation of 3 – 4 rings in comparison with the actual age (Table 2.1)

However most these study focusing on reef-building corals or red coral (*C. rubrum*) and research on determining growth bands of JPCs is limited.

Growth rates of JPCs differ significantly depending on coral species, habitat and environmental conditions. Diametric growth rates of the *P. japonicum* were slow. Different species showed different growth rate eventhough the same species and the same habitat. For example the same species but one colony showed  $0.20\pm 0.08$ , while another one was  $(0.27\pm 0.01)$ . While linear growth rate of this species range from  $2.22\pm 0.82$ - $6.66\pm 5.52$  mm per year (Luan *et al.*, 2013). *C. elatius* showed a diametric growth rate of  $0.30\pm 0.04$  and linear growth rate of  $2.76\pm 2.09$  mm yr<sup>-1</sup>. The diametric and linear growth rate of *C. konojoi* showed a  $0.44\pm 0.04$  and  $7.60\pm 0.75$  mm yr<sup>-1</sup>, respectively (Luan *et al.*, 2013).

Other PC species have been found growth faster: for Mediterranean red coral (*C. rubrum*),  $0.35\pm 0.15$  (Marchal *et al.*, 2004);  $0.24 \pm 0.05$  (Gallmetzer *et al.*, 2010);  $0.62\pm 0.19$  (Bramanti *et al.*, 2005). Information on growth rate of other species are listed in Table 2.2

**Table 2.1:** Actual age and estimate obtain by staining the organic matrix and by the petrographic for five colonies collected from the experiment panels (Marschal et al, 2004)

| Colony | Age (years) | Age estimates (number of growth rings) |                     |
|--------|-------------|--|---------------------|
|        |             | Organic matrix staining                | Petrographic method |
| 1      | 21          | 18                                     | 7                   |
| 2      | 21          | 18                                     | 7                   |
| 3      | 22          | 18                                     | 7                   |
| 4      | 20          | 17                                     | 7                   |
| 5      | 20          | 16                                     | 5                   |

Marschal *et al* (2004) used staining organic matrix matrix method for aging *C. rubrum* (Fig. 2.3). . This method provided high resolution and clearer growth rings of *C. rubrum*. However, our recent study on *P. japonicum* showed that the annual growth rings were not more clearly visible in the stained slabs (using organic matrix staining method) than un-stained slab (using a high resolution VHX-1000 digital microscope) of skeleton of JPC because it is likely that the low concentration of organic matrix in the JPC (Luan *et al.*, 2013).

## 2.5 TRACE ELEMENT DISTRIBUTION IN THE SKELETONS OF PRECIOUS CORALS OF PRECIOUS CORAL AND ITS ROLES IN PALEOENVIRONMENT RECONSTRUCT.

Chemical analyses of carbonate skeletons in precious corals found that the mineralised hard tissues of precious corals are composed of axial skeleton and sclerites (Fig. 2.4). Both sclerites and skeletons of corals are mainly made of calcium carbonate (CaCO<sub>3</sub>) crystallized in the form of calcite and small amounts of trace elements also found (Maté *et al.*, 1986; Hasegawa and Iwasaki, 2010; Debreuil *et al.*, 2011)

Trace elements are incorporated in corals in the formation of skeleton and this can results in the production of growth rings composed of inorganic elements. In order to get this information, several studies have determined surface composition of the skeleton with other methods.

Using X-ray Fluorescence (XRF) method, Mg, Sr, Ba, I, and Mo concentrations have also been confirmed in *P. japonicum* by two-dimensional images (Hasegawa *et al.*, 2010). The results showed that strong correlation between Mg and

growth rings on the skeleton of *P. japonicum* obtained by XRF mapping analysis has been reported by Hasegawa et al. (2010), while a weak correlation between Sr concentration and growth rings on the skeleton of JPC obtained by XRF and Japanese white coral obtained by EPMA analysis (Hasegawa et al., 2012). Hasegawa et al (2012) also reported that Ca is distributed homogeneously while Mg concentration is distributed concentrically forming growth rings.

The Mg/Ca and Ba/Ca ratios in the skeletons of JPC can reflect the characteristics of corals habitats. Hasegawa et al (2012) reported that *P. japonicum*, *C. elatius*, *C. konojoi* co-habit in sea-floors around Japan and the Mg/Ca and Ba/Ca ratios in these three corals collected from the same area were within similar ranges without species-specific differences. Comparison between Mg/Ca and Ba/Ca ratios in corals from the Mediterranean Sea and Japanese waters and the sea around the Midway Islands, Hasegawa et al (2012) suggested that these trace element composition differed depending on their habitats (detailed discussion in the chapter 4)

Mg/Ca and Sr/Ca ratios in the skeletons of JPC of present study determined by EPMA analysis are well agreed with those in the skeletons of *C. rubrum* measured by XRF (Weinbauer and Vellmirov, 1995).

Luan et al.,(unpublished) investigated the distribution of magnesium (Mg), phosphorus (P), sulfur (S) and strontium (Sr) along annual growth rings of JPC skeleton using micro X-ray fluorescence ( $\mu$ -XRF). The results showed that The Mg, P and S distribution in  $\mu$ -XRF mapping images correspond to the dark and light bands along the AGRs in microscopic images of the coral skeleton. The report also showed the distribution pattern of S, P and Mg in the axial skeleton of JPC (*P. japonicum*) reveals linkage between the trace element distribution and the formation of dark/light bands

along the AGRs. S and P were distributed in the organic matrix (OM) rich dark bands, while Mg was distributed in the light bands of the AGRs (detailed discussion in the chapter 5).

Besides, the speciation of sulfur using X-ray absorption near edge spectroscopy (XANES) along the annual growth rings (AGRs) in the skeleton of *Paracorallium japonicum* were also investigated. The results revealed XANES analysis showed that inorganic sulphate is the major species of S in the skeleton of *P. japonicum* with a ratio of 1:20 for organic and inorganic sulphate (Luan et al., unpublished) (in the chapter 5)

Previous reports also suggested that trace elements roles in the skeleton of coral to reconstruct paleoenvironment. For instance, Weinbauer *et al* (2000b) showed that the Mediterranean red coral was sensitive to increase in temperature and light. The incorporation of Mg and Sr in the skeleton may be affected under changes in climate and increase in temperature and ultraviolet radiation. As a result, the Mg/Ca and Sr/Ca ratios of red coral skeletons has been considered as ecological indicator.

The variability of Mg, Sr and Ca concentrations in the skeleton types of the red coral (*C. rubrum*) based on X-ray fluorescence spectroscopy and microprobe analysis as a prerequisite for their use as ecological indicators (Weinbauer *et al.*, 2000a).

By using secondary ion mass spectrometry (SIMS), Heikoop *et al.*(2002) also reported a temperature dependency of skeletal Mg/Ca ratios in the precious coral, while Bond *et al* (2005) also using SIMS to analyze Mg/Ca ratios of high-Mg calcite loculi with skeleton of a shallow water gorgonian *Plexaurella dichotoma* from Bermusa and found a positive correction between Mg/Ca ratios and annual sea surface temperature.

Skeletal Mg/Ca ratio in deep-sea PCs have strong potential as a geochemical indicator for temperature (Suzuki *et al.*, 2010). These authors also analyzed chemical

compositions of *C. konojoi* which is collected off Kochi, Japan including skeletal Mg/Ca and Sr/Ca ratios. This result showed skeletal Mg/Ca ratios from core to the margin of the section declined by about  $10 \text{ mmol mol}^{-1}$  and this decrease in the Mg/Ca ratio corresponded to a cooling of approximately  $1.7\text{-}2.5^\circ\text{C}$  because Mg/Ca ratios depended on temperature with ratio of  $4\text{-}6 \text{ mmol mol}^{-1}\text{C}^{-1}$ , while the increase in oxygen isotope ratios from the centre to the margin along the transect was about 2‰, suggesting approximately  $8^\circ\text{C}$  of warming if typical temperature dependency of oxygen isotope ratios ( $-0.22\text{‰. C}^{-1}$ ) (Weinbauer *et al.*, 2000a)

The studies on biochemistry of PC in general and JPCs in particular is very limited so these studies provide vital important to better understanding about these species and marine organism as well.

**Table 2.2** Biology of Japanese precious corals species

| Species  | Location                           | Depth | Basal diameter (mm) | Linear growth rate | Diametric growth rate | Age             | Method   | Reference                   |
|--|------------------------------------|-------|---------------------|--------------------|-----------------------|-----------------|--|-----------------------------|
| <i>Paracorallium japonicum</i><br>(Japanese red coral) | Off Amami Island, Kagoshima, Japan | 207   | 4.20±1.48           | 5.68 ±2.6          | 0.24±0.02             | 17.60±6.3<br>5  | Petrographic method<br>(VHX-1000 digital microscope) | (Luan <i>et al.</i> , 2013) |
|  | Off Amami Island, Kagoshima, Japan | 212   | 13.05±6.58          | 5.82 ± 4.86        | 0.27±0.01             | 50.00±24.<br>79 | Petrographic method<br>(VHX-1000 digital microscope) | (Luan <i>et al.</i> , 2013) |
|  | Off Muroto, Kochi, Japan           | 94    | 8.23±5.60           | 1.78±0.67          | 0.20±0.08             | 44.50±24.<br>15 | Petrographic method<br>(VHX-1000 digital microscope) | (Luan <i>et al.</i> , 2013) |
|  | Off Kochi, Japan                   | 100   |                     |                    |                       |                 | OMS method   | (Iwasaki and Suzuki, 2010)  |
|  | Off Goyo, Japan                    | 140   |                     |                    |                       |                 | Infrared radiation                                   | (Iwasaki and Suzuki, 2010)  |

|  |                                       |         |             |              |   |           |             | method                          |                              |
|--|---------------------------------------|---------|-------------|--------------|---|-----------|-------------|---------------------------------|------------------------------|
| <i>Corallium elatius</i><br>(pink coral)           | Okinawa, Japan                        | 200-300 |             |              |   |           | 0.26-0.28   | Infrared radiation method       | (Bruckner and Roberts, 2009) |
|  | Okinawa, Japan                        | 100-300 |             |              |   |           | 0.15        | <sup>210</sup> Pb dating method | (Hasegawa and Yamada, 2010)  |
|  | Off Ryukyu Islands, Okinawa, Japan    | 200-300 | 17.00±13.20 | 2.76<br>1.70 | ± | 0.30±0.04 | 53.50±33.19 |                                 | (Luan <i>et al.</i> , 2013)  |
| <i>Corallium konojoi</i><br>(Japanese white coral) | Japan to northern Philippines Islands | 50-382  |             |              |   |           | 0.58        |                                 | (Iwasaki and Suzuki, 2010)   |
|  | Off Ashizuri, Kochi, Japan            | 108     | 7.18±4.21   | 7.15<br>0.53 | ± | 0.44±0.04 | 16.25±9.43  |                                 | (Luan <i>et al.</i> , 2013)  |

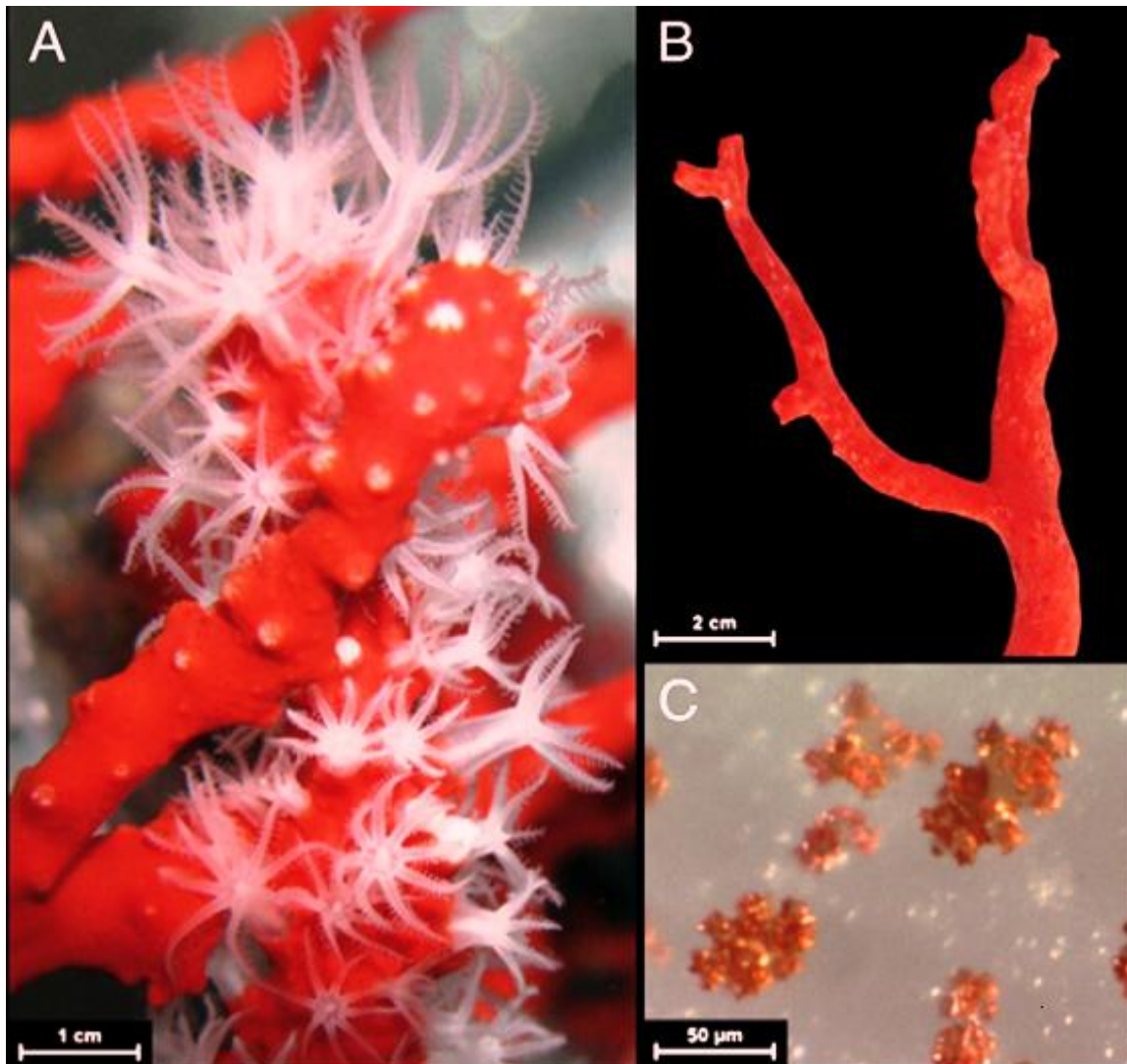


**Fig. 2.4** Living colony of Mediterranean red coral (*Corallium rubrum*) (A). Axial skeleton of *C. rubrum* (B) and Sclerites of this coral (C) (Debreuil *et al.*, 2011)

## REFERENCES

- Andrews, A.H., Cordes, E.E., Mahoney, M.M., Munk, K., Coale, K.H., Cailliet, G.M., Heifetz, J., 2002. Age, growth and radiometric age validation of a deep-sea, habitat-forming gorgonian (*Primnoa resedaeformis*) from the Gulf of Alaska. *Hydrobiologia* 471, 101-110.
- Bayer, F.M., Cairns, S.D., 2003. A new genus of the scleraxonian family Coralliidae (Octocorallia: Gorgonacea). *Proc. Biol. Soc. Wash.* 116, 222-228.
- Bond, Z.A., Cohen, A.L., Smith, S.R., Jenkins, W.J., 2005. Growth and composition of high-Mg calcite in the skeleton of a Bermudian gorgonian (*Plexaurella dichotoma*): Potential for paleothermometry. *Geochemistry, Geophysics, Geosystems* 6, 1-10.
- Bramanti, L., Magagnini, G., De Maio, L., Santangelo, G., 2005. Recruitment, early survival and growth of the Mediterranean red coral *Corallium rubrum* (L 1758), a 4-year study. *J. Exp. Mar. Biol. Ecol.* 314, 69-78.
- Bruckner, A.W., Roberts, G.G. (Eds.), 2009. *Proceedings of the First International Workshop on Corallium Science, Management, and Trade*. Silver Spring, Hong Kong.
- Casu, M., Casu, D., Lai, T., Cossu, P., Curini-Galletti, M., 2008. A molecular tool for genetic surveys in the red coral (*Corallium rubrum*): An Inter-Simple Sequence Repeats (ISSRs) perspective. *Biochem. Syst. Ecol.* 36, 77-83.
- Debreuil, J., Tambutté, S., Zoccola, D., Segonds, N., Techer, N., Allemand, D., Tambutté, É., 2011. Comparative analysis of the soluble organic matrix of axial skeleton and sclerites of *Corallium rubrum*: Insights for biomineralization. *Comparative Biochemistry and Physiology Part B: Biochemistry and Molecular Biology* 159, 40-48.

- Gallmetzer, I., Haselmair, A., Velimirov, B., 2010. Slow growth and early sexual maturity: Bane and boon for the red coral *Corallium rubrum*. *Estuar. Coast. Shelf Sci.* 90, 1-10.
- Garrabou, J., Harmelin, J.G., 2002. A 20-year study on life-history traits of a harvested long-lived temperate coral in the NW Mediterranean: insights into conservation and management needs. *J. Anim. Ecol.* 71, 966-978.
- Grigg, R.W., 1974. Growth rings: Annual periodicity in two gorgonian corals. *Ecology* 55, 876-881.
- Grigg, R.W., 1993. Precious coral fisheries of Hawaii and the U.S. Pacific Islands. 55, 50-60.
- Gili, J.-M., Coma, R., 1998. Benthic suspension feeders: their paramount role in littoral marine food webs. *Trends in ecology & evolution (Personal edition)* 13, 316-321.
- Hasegawa, H., Iwasaki, N., 2010. Chemical analyses of carbonate skeletons in precious corals. *Biohistory of Precious corals*.
- Hasegawa, H., Iwasaki, N., Suzuki, A., Maki, T., Hayakawa, S., 2010. Distribution of trace elements in biogenic carbonate minerals of precious corals by X-ray fluorescence analysis. *Bunseki Kagaku* 59, 521-530.
- Hasegawa, H., Rahman, M.A., Luan, N.T., Maki, T., Iwasaki, N., 2012. Trace elements in *Corallium* spp. as indicators for origin and habitat. *J. Exp. Mar. Biol. Ecol.* 414-415, 1-5.
- Hasegawa, H., Yamada, M., 2010. Biology of precious coral. In: Iwasaki, N. (Ed.), *Biohistory of Precious corals-Scientific, Cultural and Historical Perspective*. University Press, Tokai, Japan, pp. 43-60.
- Heikoop, J.M., Hickmott, D.D., Risk, M.J., Shearer, C.K., Atudorei, V., 2002. Potential

- climate signals from the deep-sea gorgonian coral *Primnoa resedaeformis*. *Hydrobiologia* 471, 117-124.
- Iwasaki, N., 2010. Biohistory of precious corals- scientific,cultural and historical perspectives. In: Iwasaki, N. (Ed.). Tokai Univeristy Press, Tokai, Japan.
- Iwasaki, N., H. Hasegawa, T. Suzuki, Yamasa, a.M., 2009. Biology of Japanese Corallium and Paracorallium, paper presented at Proceedings of the First International Workshop on Corallium Science, Management, and Trade. NOAA Technical Memorandum NMFS-OPR-43 and CRCP-8, Silver Spring, MD, Hong Kong, China., 149.
- Iwasaki, N., Suzuki, T., 2010. Biology of precious corals. In: Iwasaki, N. (Ed.), Biohistory of precious corals- scientific,cultural and historical perspectives. Tokai Univeristy Press, Tokai, Japan.
- Jones, C.G., Lawton, J.H., Shachak, M., 1994. Organisms as ecosystem engineers *Oikos* (Kbh.). 373-338.
- Kishinouye, K.J., 1903. Preliminary note on the Coralliidae of Japan. *Zoologische Anzeiger* 26, 623-626.
- Kishinouye, K.J., 1904. Notes on the natural history of corals. . *Journal of Fishery Bureau* 14, 1-32.
- Luan, N.T., Rahman, M.A., Maki, T., Iwasaki, N., Hasegawa, H., 2013. Growth characteristics and growth rate estimation of Japanese precious corals. *J. Exp. Mar. Biol. Ecol.* 441, 117-125.
- Marschal, C., Garrabou, J., Harmelin, J.G., Pichon, M., 2004. A new method for measuring growth and age in the precious red coral *Corallium rubrum* (L.). *Coral Reefs* 23, 423-432.

- Maté, P., Revenge, S., Masso, C., 1986. Estudio preliminar de la composición química del coral rojo (*Corallium rubrum* L.) de distintas zonas del Mediterráneo Español. Bol. Inst. Esp. Oceanogr. 3, 53-60.
- Muzik, K., Wainwright, S., 1977. Morphology and Habitat of Five Fijian Sea Fans. Bull. Mar. Sci. 27, 308-337.
- Nishijima, S., Kamura, K.Y.S., 1969. Notes on the characteristics of precious coral grounds in the Ryukyu Islands... Bull. Jp. Soc. Fish. Oceanogr, 291-297.
- Nonaka, M., Muzik, K., 2009. Recent harvest records of commercially valuable precious corals in the Ryukyu Archipelago. Mar. Ecol. Prog. Ser. 397, 269-278.
- Nonaka, M., Muzik, K., Uchida, S., 2006. Capture, study and display of precious corals. 10<sup>th</sup> international Coral Reef Symposium, Okinawa, Japan, pp. 1821-1831.
- Reimer, J., Nonaka, M., Sinniger, F., Iwase, F., 2008. Morphological and molecular characterization of a new genus and new species of parazoanthid (Anthozoa: Hexacorallia: Zoantharia) associated with Japanese Red Coral. Coral Reefs 27, 935-949.
- Ribes, M., Coma, R., Rossi, S., Micheli, M., 2007. Cycle of gonadal development in *Eunicella singularis* (Cnidaria: Octocorallia): trends in sexual reproduction in gorgonians. Invertebr. Biol. 126, 307-317.
- Risk, M.J., Heikoop, J.M., Snow, M.G., Beukens, R., 2002a. Lifespans and growth patterns of two deep-sea corals: *Primnoa resedaeformis* and *Desmophyllum cristagalli*. Hydrobiologia 471, 125-131.
- Risk, M.J., Heikoop, J.M., Snow, M.G., Beukens, R., 2002b. Lifespans and growth patterns of two deep-sea corals: *Primnoa resedaeformis* and *Desmophyllum cristagalli*. Hydrobiologia 471, 125-131.

- Roark, E.B., Guilderson, T.P., Dunbar, R.B., Ingram, B.L., 2006. Radiocarbon-based ages and growth rates of Hawaiian deep-sea corals. *Mar. Ecol. Prog. Ser.* 327, 1-14.
- Santangelo, G., Carletti, E., Maggi, E., Bramanti, L., 2003. Reproduction and population sexual structure of the overexploited Mediterranean red coral *Corallium rubrum*. *Mar. Ecol. Prog. Ser.* 248, 99-108.
- Seki, K., 1991. Study of precious coral diver survey with open circuit air SCUBA diving at 108m. *Ann. Physiol. Anthropol.* 10, 189-199.
- Suzuki, A., Inoue, M., Yokoyama, Y., 2010. Chemical analyses of carbonate skeletons in precious corals
- In: Iwasaki, N. (Ed.), *Biohistory of Precious corals*  
Tokai University Press.
- Torrents, O., Garrabou, J., Marschal, C., Harmelin, J.G., 2005. Age and size at first reproduction in the commercially exploited red coral *Corallium rubrum* (L.) in the Marseilles area (France, NW Mediterranean). *Biol. Conserv.* 121, 391-397.
- Vielzeuf, D., Garrabou, J., Baronnet, A., Grauby, O., Marschal, C., 2008. Nano to macroscale biomineral architecture of red coral (*Corallium rubrum*). *Am. Mineral.* 93, 1799.
- Weinbauer, M.G., Brandstatter, F., Velimirov, B., 2000b. On the potential use of magnesium and strontium concentrations as ecological indicators in the calcite skeleton of the red coral (*Corallium rubrum*). *Mar. Biol.* 137, 801-809.
- Weinbauer, M.G., Vellmirov, B., 1995. Calcium, magnesium and strontium concentrations in the calcite sclerites of Mediterranean gorgonians (Coelenterata: Octocorallia). *Estuar. Coast. Shelf Sci.* 40, 87-104.

# CHAPTER 3

## RESULTS AND DISCUSSION

### **GROWTH CHARACTERISTICS AND GROWTH RATE ESTIMATION OF JAPANESE PRECIOUS CORALS**

#### **3.1. INTRODUCTION**

Precious corals which belong to the deep sea corals are some of the most valuable living marine resources, and are harvested in limited areas in the world. Precious corals are different from reef-building corals in that their skeletons are closely-packed with magnesium calcite, while the reef-building corals consist mostly of

aragonite, and are porous because of its loosely-packed crystals (Hasegawa *et al.*, 2012). Some of the important precious corals include *Corallium rubrum*, *Paracorallium japonicum*, *Corallium elatius*, *Corallium konojoi* and *Corallium secundum* (Tsounis *et al.*, 2010a; Tsounis *et al.*, 2010b). The *Corallium* spp. are distributed in the seas around Hawaii and the Midway Islands, (Grigg, 1993b). Japanese red (*P. japonicum*), pink (*C. elatius*), and white (*C. konojoi*) corals are distributed and harvested in waters near Japan (Iwasaki *et al.*, 2009b). *Paracorallium japonicum* can be up to 30 cm height, and is found at depths of 76-280 m on the rocky bottom in Sagami Bay (Pacific coast off Japan), in the waters from the Ogasawara Islands (Japan), and off the coast near the Goto Islands, Nagasaki (Japan) (Iwasaki and Suzuki, 2010). *Corallium elatius* is distributed on the rocky bottom at a depth of 100-276 m in the waters near Wakayama (Pacific coast of Japan), from the Ogasawara Islands (Japan) to the northern South China Sea, and off the Goto Islands, Nagasaki, Japan (Iwasaki and Suzuki, 2010). *Corallium elatius* can be up to 67 kg with a height up to 1.1 m and width up to 1.7 m (Iwasaki and Suzuki, 2010). *Corallium konojoi* can grow up to 30 cm, and is distributed on the rocky bottom at a depth of 76-276 m in the waters of Wakayama (Pacific coast of Japan), in the waters from the Ogasawara Islands (Japan) to the northern South China Sea, and off the Goto Islands, Nagasaki, Japan (Seki, 1991a; Nonaka *et al.*, 2004).

Growth rates and ages of DSC have been estimated and measured by different methods including tagging (Grigg, 1974), counting of annual growth rings in the axial skeleton (Grigg, 1974; Wilson *et al.*, 2002), and applying radiometric techniques such as U/Th,  $^{210}\text{Pb}$  and radiocarbon dating (Druffel *et al.*, 1990; Cheng *et al.*, 2000; Andrews *et al.*, 2002; Risk *et al.*, 2002; Adkins *et al.*, 2004; Adkins *et al.*, 2006; Griffin and Druffel, 2006). All these methods estimate the age of individual specimens by

extrapolating the calculated linear or diametric growth rates (DGRs) . Growth rates and ages of precious corals have also been determined by various methods such as organic matrix staining (OMS) in the axial skeleton (Marschal *et al.*, 2004; Gallmetzer *et al.*, 2010), *in situ* studies (Garrabou and Harmelin, 2002; Bramanti *et al.*, 2005), and  $^{14}\text{C}$  method (Roark *et al.*, 2006a).

The petrographic method is a popular method for observing growth ring density in thin cross-sections (CSs) of the axial coral skeleton in order to estimate growth rates and ages of precious corals (Grigg, 1974; Santangelo *et al.*, 1993; Andrews *et al.*, 2002). In the OMS method, the organic matrix in the thin CS of the axial calcareous skeleton of the Mediterranean red coral (*C. rubrum*) was employed to better identify growth rings, and the results showed that compared to the petrographic method, staining the organic matrix provided a clearer image of the growth rings (Marschal *et al.*, 2004). Japanese precious corals are famous from antiquity for their beauty and mysterious powers of their skeletons. To date, however, research on determining growth rates and longevity of these corals is limited.

### 3.2. FOCUS

In the present study, the growth characteristics of three Japanese precious corals were studied by examining their skeletal structure and estimating growth rates and ages based on growth ring counts in CSs of the axial skeleton using a high resolution VHX-1000 digital microscope, termed as VHX-1000 hereafter, without staining the organic matrix in the skeleton. In addition, growth rings in the stained (staining the organic matrix in the skeleton with toluidine blue (Marschal *et al.*, 2004) and unstained

CSs of the axial coral skeleton were observed through the VHX-1000. The clarity of growth rings in stained CSs was compared with those of unstained CSs to validate the advantages of non-destructive unstaining method over the OMS method in determining growth rates and ages of Japanese precious corals..

### 3.3.MATERIALS AND METHODS

#### 3.3.1. Sample collection

Five colonies of each of the three Japanese precious corals were collected from different locations of Japanese waters. Colony 1 (DPC-18) and colony 2 (DPC-19) are deep-sea red corals (*P. japonicum*), which were collected from 207 and 212 m depth, respectively, off Amami Islands, Kagoshima, Japan on March 08, 2009. Colony 3 (DPC-20) is also a red coral (*P. japonicum*) was collected from a different depth and location (100 m depth off Kochi, Japan) on October 09, 2011. Colony 4 (DPC-10), a pink coral (*C. elatius*), was collected from 200-300 m depth Ryukyu Islands, Okinawa, Japan, and colony 5 (DPC-21), white coral (*C. konojoi*), was collected at a depth of 100 m off Kochi, Japan on November 10, 2011.

#### 3.3.2. Cross-section preparation of the coral skeleton

Colonies were dried at room temperature of 25°C. One to three mm thick CSs of the axial coral skeleton of each colony were made using a NSK ElecterEmax (NE 129, Nakanishi Inc., Japan) at different points from the tip to the bottom of the skeleton

(Fig. 3.1). The CSs were then embedded and coated in epoxy resin to provide a protective cover for cutting, grinding, and polishing the CSs of the skeleton. The CSs were then mounted on glass slides and polished with 60, 120, 400, 800, 100, 1500 and 2000 SiC grid powder and 3M imperial polishing paper. The thin polished CSs (slabs) were then cleaned ultrasonically, rinsed in 100% ethyl alcohol, and dried. The polished surfaces of the slabs were kept free from dust prior to examination under the VHX-1000.

### **3.3.3. Staining of organic matrix in the coral skeleton**

Based on the petrographic method, [Marschal et al. \(2004\)](#) developed the OMS method for measuring growth rate and age of the Mediterranean red coral (*C. rubrum*) by staining the organic matrix in the calcite skeleton. In this method, the thin (100-150  $\mu\text{m}$ ) slabs of coral skeleton were decalcified using 2% acetic acid solution for 4–5 h. After a gentle rinse, the slabs were stained with 0.05% toluidine blue for 10-30 s. Slabs were occasionally stained several times to improve visualization of the organic matrix rings under the stereomicroscope. After decalcification, special care had to be taken in handling the slabs to avoid breakage of the organic matrix structure. In the present study, the organic matrix in the slabs of Japanese red coral (*P. japonicum*) was stained following the OMS method.

### **3.3.4 Determination of the age and growth rates of Japanese precious corals**

Growth rates of the Japanese precious corals were estimated on the basis of

growth ring density in the slabs considering that the growth rings are formed annually (Grigg, 1974; Wilson *et al.*, 2002; Marschal *et al.*, 2004). The number of growth rings in un-stained slabs of the Japanese red, pink and white corals was counted three times through a VHX-1000 (Keyence, Japan) to determine their ages and growth rates. In addition, the number of growth rings in both stained and unstained slabs of the Japanese red coral (*P. japonicum*) was counted through the VHX-1000 to compare the visibility of growth rings in the stained and unstained slabs. The magnification of the lens of the VHX-1000 was adjusted to 20-200x, and was set at nine different modes (normal mode, sharpening image mode, light shift, glare remove, sharpening image mode with glare removed, High Dynamic Range (HDR) with light shift, HDR1, HDR 2 and HDR3) in order to capture the best images in which growth rings were most visible. Diameter of the slabs was calculated from the average of four measures at different positions using digital microscope (one of advantageous functions of the digital microscope), while distance of the spots from the base of the skeleton, from where the slabs were taken, was measured with a ruler (with the nearest 0.05 mm). The DGRs ( $\alpha$ ) were calculated from the following equation-

$$\alpha = \frac{a}{b} \dots \dots \dots (i)$$

where,  $a$  is the diameter of the slab and  $b$  is the the number of growth rings in the slab of the coral skeleton. Linear growth rates ( $\beta$ ) of the corals were calculated from the following equation-

$$\beta = \frac{a - a'}{x - x'} \dots \dots \dots (ii)$$

where,  $(a - a')$  is the difference between two successive slabs and  $(x - x')$  is the decrease of growth ring number in those two successive slabs.

### 3.4. RESULTS

#### 3.4.1. Growth characteristics of Japanese precious corals

The skeletons of the Japanese red, pink and white corals were narrow at the tip and wide at the base of colony (Fig. 3.1). The diameter of the core in the younger part (tip) is wider than that in the older part (base) of the colony; and the ratio of the core and total (including the core) diameter in the axis CSs increased with increasing distance of the axis CSs from the base to the tip of the colony (Fig. 3.2). In addition, calcium carbonate deposited in the core of the younger parts did not form distinct growth rings (Fig. 3.3B).

Growth rings in horizontal thin (a few hundred micrometers) cross sections were clearly visible and identifiable under the VHX-1000; however, it was difficult to identify the growth rings in thicker sections. Under the VHX-1000, two types of growth bands, light and dark, were observed. The light bands were wider than the dark bands (Fig. 3.3A). No trace of growth rings was identified in the thin section of a branch tip of *P. japonicum* (Fig. 3.3B).

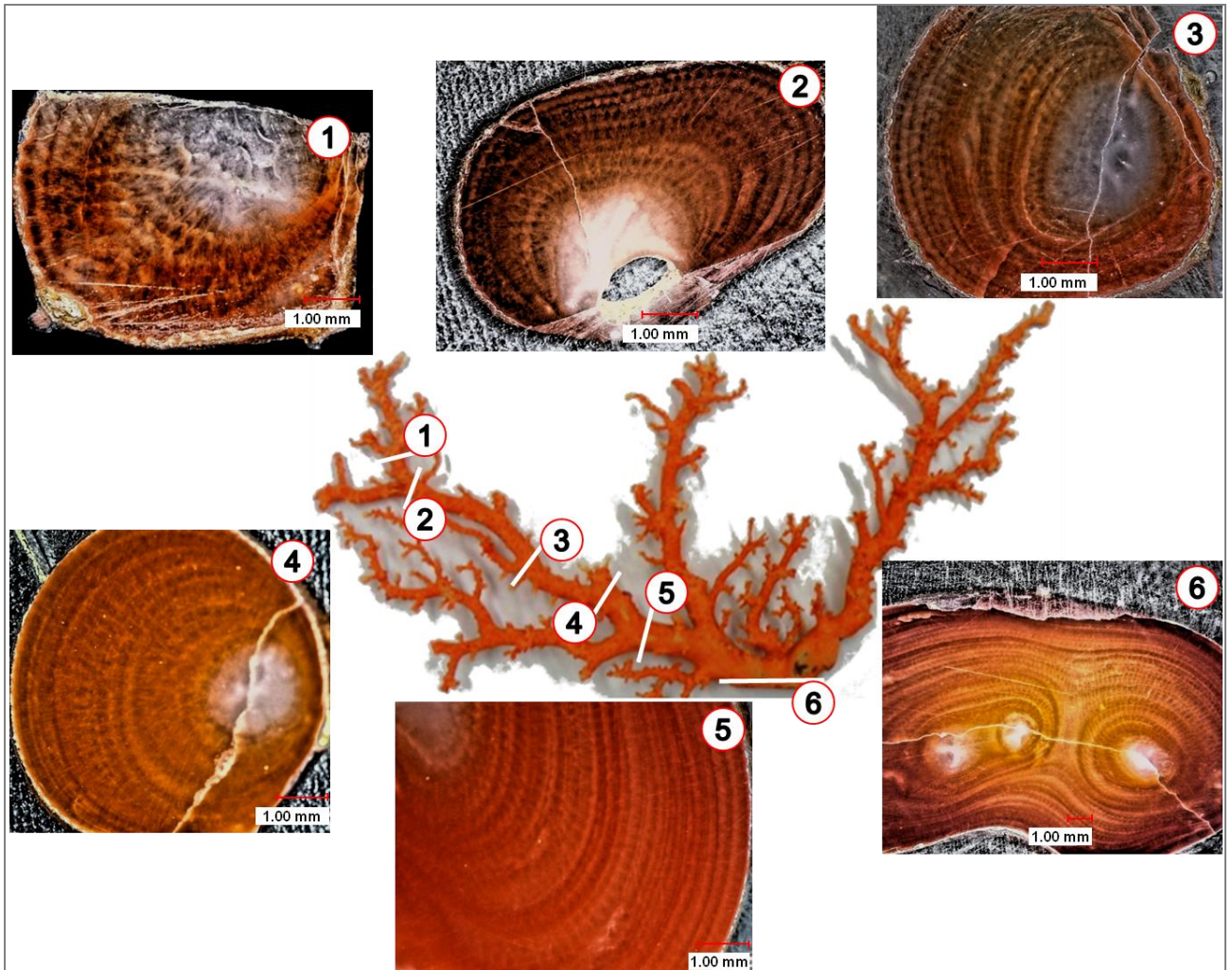


**Fig. 3.1.** Axial skeleton of Japanese red coral *Paracorallium japonicum* (DPC-18). Numbers on the skeleton indicate the sample sites, and the images are the cross-sections of the corresponding samples. The cross-sections were polished to make the growth rings clear to count them and estimate growth rate and age of the coral. The diameter of the core become wider at the younger part (tip;1) than at the older part (base; 6) of the colony.

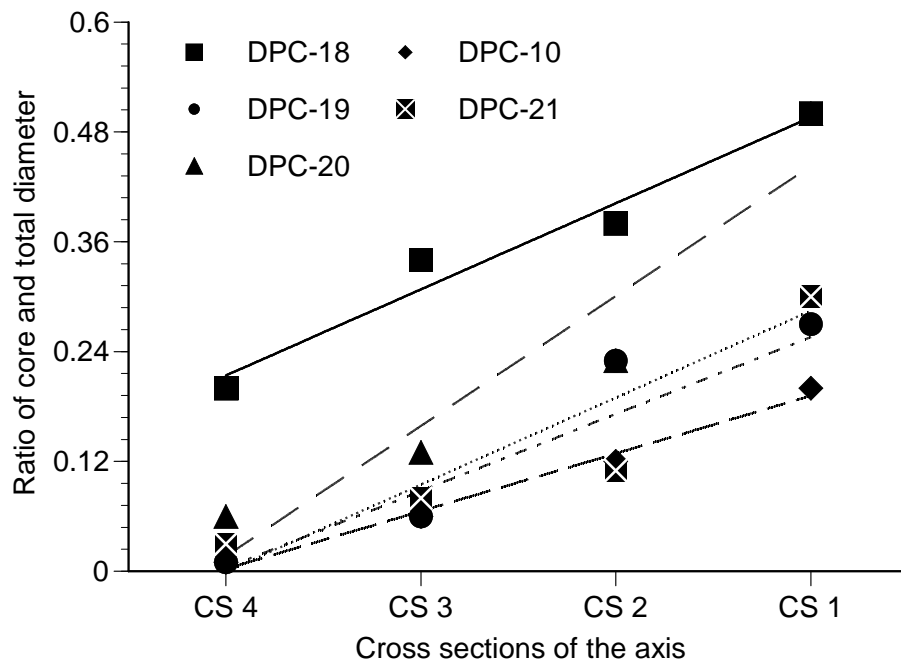


**Fig. 3.2.** The ratio of the core diameter and total (including the core) diameter of the axis. The ratio increased with increasing distance of the axis cross-sections from the base to the tip of the colony. The cross-section numbers (CS4-CS1) in x-axis of the figure represent the consecutive slabs from the base to the tip of coral axis.

### 3.4.2. Age and diametric growth rates of Japanese precious corals

#### 2.4.2.1. *Paracorallium japonicum* (Japanese red corals)

The diameter of DPC-18 ranged from 2.60 to 6.30 mm with an average of  $4.20 \pm 1.48$  mm. The number of annual growth rings in these CSs ranged between 10 and 26 indicating that the minimum estimated age of this colony is 10 years (yrs) and the maximum is 26 yrs with an average age of  $18 \pm 6$  yrs. The diametrical growth rate (DGR) of this colony was  $0.24 \pm 0.02$  mm yr<sup>-1</sup> (Table 3.1).

The diameter of CSs of colony DPC-19 was much bigger than the colony DPC-18 (ranging from 8.10 to 22.50 mm with an average of  $13.05 \pm 6.58$  mm) and the estimated age of this colony was older than that of DPC-18 (ranging from 29 to 83 yrs with an average of  $50 \pm 25$  yrs). However, the DGRs of these two colonies did not differ substantially, with an average of  $0.27 \pm 0.01$  mm yr<sup>-1</sup> for colony DPC-19 compared with  $0.24 \pm 0.02$  mm yr<sup>-1</sup> for colony DPC-18 (Table 3.1).

Colony DPC-20 had a diameter of  $8.23 \pm 5.60$  mm (range 3.70-16.40 mm). The average estimated age of this colony was  $44 \pm 24$  yrs ranging from 12 to 70 yrs. However, this colony showed the slowest average DGR ( $0.20 \pm 0.08$  mm yr<sup>-1</sup>) among the three Japanese red coral colonies studied (Table 3.1).

#### 3.4.2.2. *Corallium elatius* (Japanese pink coral)

The Japanese pink coral (*C. elatius*; colony DPC-10) showed a range of growth rates. The average age of this colony was  $54 \pm 33$  yrs with a range of 24-100 yrs, and the DGR was  $0.30 \pm 0.04$  mm yr<sup>-1</sup> with a range of 0.27 to 0.36 mm yr<sup>-1</sup> (Table 3.1). However, the average growth rate of this coral was higher than that of the Japanese red coral (*P.*

*japonicum*).

#### 3.4.2.3. *Corallium konojoi* (Japanese white coral)

The estimated average age of DPC-21 was  $16 \pm 9$  yrs with a range of 5-27 yrs, and the average growth rate was  $0.44 \pm 0.04$  mm yr<sup>-1</sup> ranging from 0.39 to 0.48 mm yr<sup>-1</sup>. The average of growth rate of this species was double that of the Japanese red coral (*P. japonicum*).

#### 3.4.3. Linear growth rates of Japanese precious corals

The number of growth rings in CSs at different heights from the base of the five colonies of three Japanese coral species provided a range of linear growth rates. The Japanese red coral (*P. japonicum*), DPC-18, DPC-19 and DPC-20 showed a decreasing pattern of linear growth rate from the tip to the base, except cross-section 1 of DPC-18. Japanese pink coral (*C. elatius*) also showed a same pattern, but the Japanese white coral did not (Table 3.2). DPC-18 and DPC-19 (Table 3.2), showed an average linear growth rate of  $5.68 \pm 2.60$  and  $5.82 \pm 4.86$  mm yr<sup>-1</sup>, respectively. The DPC-20 colony of the same coral species showed lower linear growth rate ( $2.22 \pm 0.67$  mm yr<sup>-1</sup>) than the colonies DPC-18 and DPC-19. The Japanese pink coral (*C. elatius*) showed a slower linear growth rate ( $2.76 \pm 1.70$  mm yr<sup>-1</sup>) compared to other species (Table 3.2). However, the linear growth of the Japanese white coral (*C. konojoi*) was much faster ( $7.15 \pm 0.53$ ) than all the other Japanese precious coral species studied

### 3.5. DISCUSSION

#### 3.5.1. Growth characteristics of Japanese precious corals

Japanese precious corals showed distinct growth characteristics. The axial skeletons of the corals were thinner at the tips than at the base of the colony, and the diameter of the core was wider at the tip which was the younger part than at the base which was the older part of the colony. An increasing pattern of the ratio of core diameter and diametric CS from the base to the tip of the colony was observed (Fig. 3.1), which concurs with the study of Tracey *et al.* (2007) for bamboo corals. However, why the core diameter of the coral axis increases toward the tip of the colony was not clearly demonstrated in previous studies. The reason for the increasing core diameter toward the tip of the coral colony is likely due to the fact that during the first few years of life, the calcium carbonate deposited in the core of the axis might not form growth rings (Marschal *et al.*, 2004). Therefore, the tip of younger parts of the colony almost shows an ratio of axial core size and diametric CS wider than that in the older parts.

Light bands in the thin CSs of the coral skeleton were wider than the dark bands (Fig. 3.3A). The dark bands indicate the zones of high organic matrix (OM) concentration, while the wider light bands represent the zones of low OM concentration in the coral skeleton (Marschal *et al.*, 2004; Vielzeuf *et al.*, 2008). The formation of dark and light bands depends on the availability of calcium and organic matter. The formation of growth rings in calcified material of marine organisms (e.g., intertidal barnacles and molluscs) can be entirely due to inorganic deposition, or can be defined by the alternation of a dark-colored organic layer followed by a lighter carbonate-rich

layer (Goldberg, 1991). In the skeletons of stony corals, sometimes the dark-colored organic layer is produced on emersion when calcium is unavailable (Dillon and Clark, 1980; Bourget, 1987), or due to the incorporation of inorganic foreign elements (Boto and Isdale, 1985). However, Bak and Laane (1987) argued that the black bands do not result from the inclusion of foreign material by the coral but are characterized by high concentrations of a dark fungus. Therefore, in some cases, the mechanism of growth band formation may be related to biological rather than physical cycles. In particular, the presence of annual growth rings in any species provides a powerful aid in interpreting their population dynamics (Grigg, 1974).

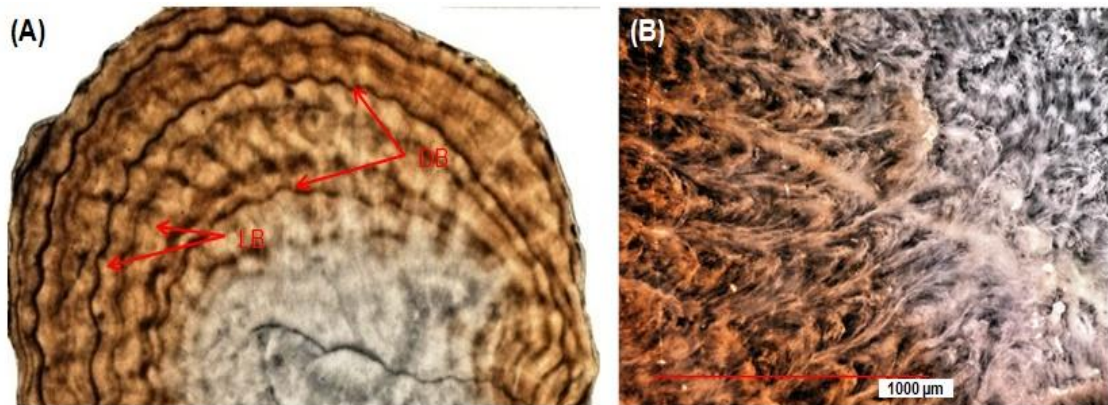


**Fig. 3.3.** (A) Two types of growth bands, light and dark, as seen under the VHX-1000 digital microscope. The dark bands indicate the zones of high organic matrix (OM) content, while the light bands represent the zones of low OM content in the coral skeleton. (B) A cross-section at the tip on the younger part of the coral skeleton (*Paracorallium japonicum*). The calcium carbonate deposited in the core on the younger part of the axis does not generate/form growth rings.

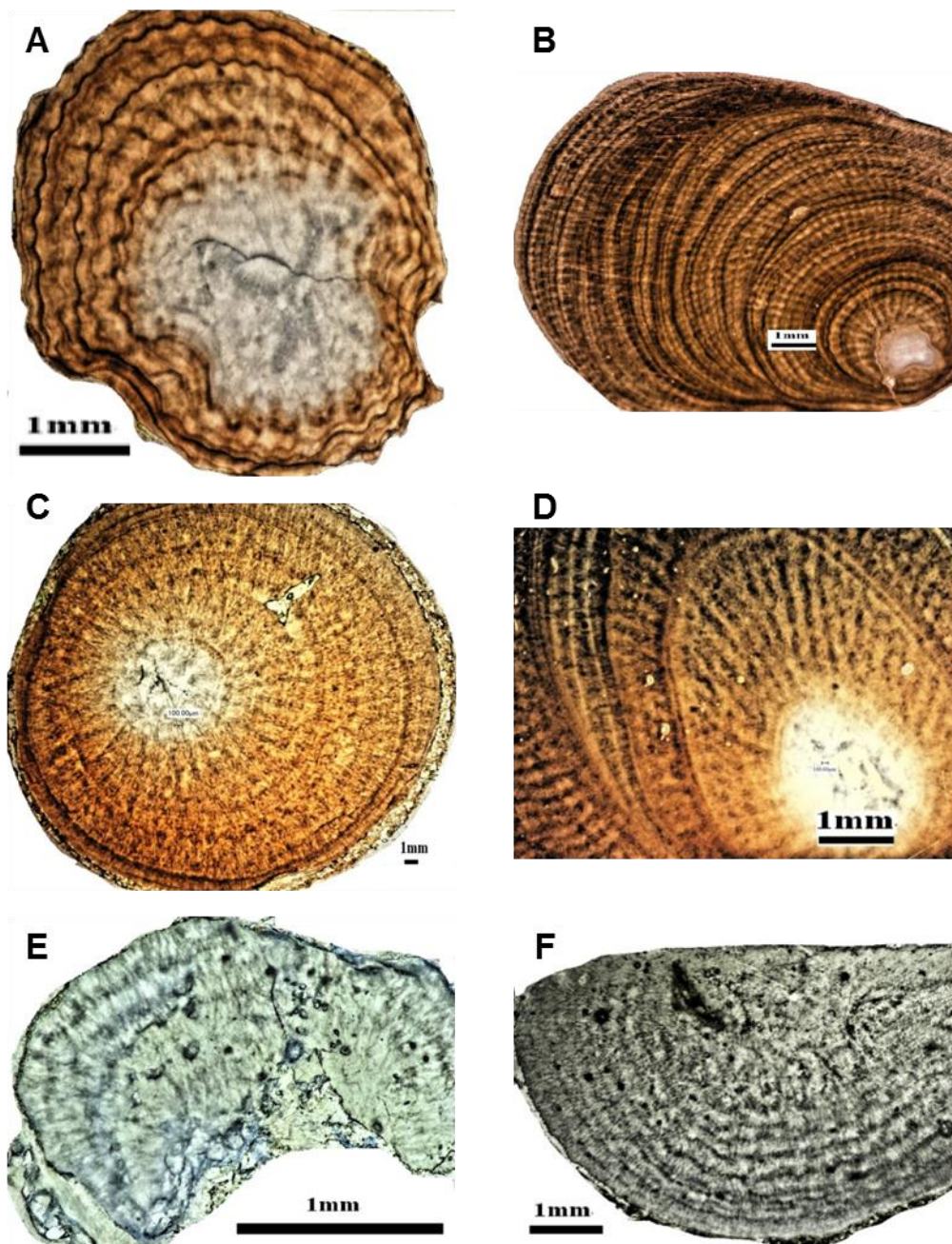


**Fig. 3.4.** Growth rings in thin cross-sections of the axial skeleton of different Japanese precious coral species under the VHX-1000 digital microscope. (A-B) red coral (*Paracorallium japonicum*), (C-D) pink coral (*Corallium elatius*), (E-F) white coral (*Corallium konojoi*)

### 3.5.2. Growth rates of Japanese precious corals

Diametric and linear growth rates of three Japanese precious coral species (*P. japonicum*, *C. elatius*, *C. konojoi*) were determined based on annual growth ring counting in the axial skeleton using the VHX-1000. Growth rings in thin CSs of the axial skeleton of different Japanese precious coral species under the VHX-1000 are presented in Figure 3.4. In general, DGR of Japanese precious corals is similar or slower than that of other precious corals species, but falls within the range of reported values for other precious coral species from other geographical locations (Table 3.4). The average DGRs of Japanese corals ranged between  $0.24 \pm 0.05$  and  $0.44 \pm 0.04$  mm yr<sup>-1</sup>, while the growth rates of Mediterranean red coral (*Corallium rubrum*) ranged between 0.20 and  $0.62 \pm 0.19$  mm yr<sup>-1</sup>. The DGR of the Mediterranean red coral (*C. rubrum*; 0.20 mm yr<sup>-1</sup>) collected from Pointe de La Revellata, France (Gallmetzer *et al.*, 2010) is similar to that of the Japanese red coral (*P. japonicum*;  $0.20 \pm 0.08$  mm yr<sup>-1</sup>) collected from off Kochi, Japan. A similar DGR (0.24 mm yr<sup>-1</sup>) was also observed for the Mediterranean red coral (*C. rubrum*, collected from Marseille, France) and the Japanese red coral (*P. japonicum*, collected from Amami Island, Kagoshima, Japan; Table 3.4). However, the Mediterranean red coral (*C. rubrum*) from Tuscany, Italy had higher DGR ( $0.62 \pm 0.19$  mm yr<sup>-1</sup>; (Bramanti *et al.*, 2005; Roark *et al.*, 2006a)) than that of the Japanese red coral.

The DGRs within the Japanese precious corals also differed substantially depending on coral species, habitat (depth and geographical location) and environmental conditions (Table 3.1). Colonies DPC-18 and DPC-19 of the Japanese red coral (*P. japonicum*) had average DGRs of  $0.24 \pm 0.02$  and  $0.27 \pm 0.01$  mm yr<sup>-1</sup>,

respectively. Both colonies were collected from the same geographical location (Amami Island, Kagoshima, Japan) but from slightly different depths (207 and 212, respectively). Colony DPC-20, which was collected from Kochi, Japan at a depth of 100 m had significantly lower DGR ( $0.20 \pm 0.08 \text{ mm yr}^{-1}$ ) than colonies DPC-18 and DPC-19 of the same species. A recent study (Luan et al., unpublished) showed that DGRs of colony showed a range of the growth rate of Japanese red coral (DPC-22) ( $0.30\text{-}0.56 \text{ mm yr}^{-1}$ ) was higher than DPC18 and DPC19 although all three colonies were collected the same location (Kagoshima, Japan) (Table 3.3). These results reveal that the growth rate of same coral species may differ for different geographical locations, environmental conditions and habitats. The present study also showed that the growth rates of colonies DPC-20 (*P. japonicum*) and DPC-21 (*C. konojoi*) differed substantially ( $0.20 \pm 0.08$  and  $0.44 \pm 0.04 \text{ mm yr}^{-1}$ , respectively) even though both coral species were collected from the same location (Kochi, Japan) and depth (100 m). Average growth rate of DPC-272 ( $0.36 \pm 0.05 \text{ mm yr}^{-1}$ ) and DPC-16 ( $0.38 \pm 0.03$ ) (Luan et al., unpublished) (Table 3.3) was higher the colony DPC-10 ( $0.30 \pm 0.04 \text{ mm yr}^{-1}$ ) but lower than the colony DPC-21 in this study. These results clearly demonstrate that different coral species show different growth rates even though the environmental conditions and habitat are the same.

The linear growth rates of the Japanese red coral (*P. japonicum*) and the Mediterranean red coral (*C. rubrum*) differed greatly. It was reported that the linear growth rates of the Mediterranean red coral ranged between  $1.78 \pm 0.67$  and  $1.83 \pm 0.15 \text{ mm yr}^{-1}$  (Garrabou and Harmelin, 2002; Bramanti et al., 2005), while the present study showed that the linear growth rates of the Japanese red coral ranged between  $2.22 \pm 0.67$  and  $5.82 \pm 4.86 \text{ mm yr}^{-1}$  (Table 3.2). Linear growth rates were also found to be differ considerably within the Japanese precious corals (Table 3.2). The results reveal that the

linear growth rates depend on the growth stages of the precious corals.

### **3.5.3. Correlation between number of growth rings and diameter**

In the present study, the ages and DGRs of three Japanese precious coral species were estimated based on the number of annual growth rings and the diameters of the axial skeleton. A significant positive correlation between the number of annual growth rings and the diameters of the axial skeletons was observed for the three coral species studied (Fig. 3.5). These results indicate consistent DGRs and increase of diameters of these Japanese precious corals.

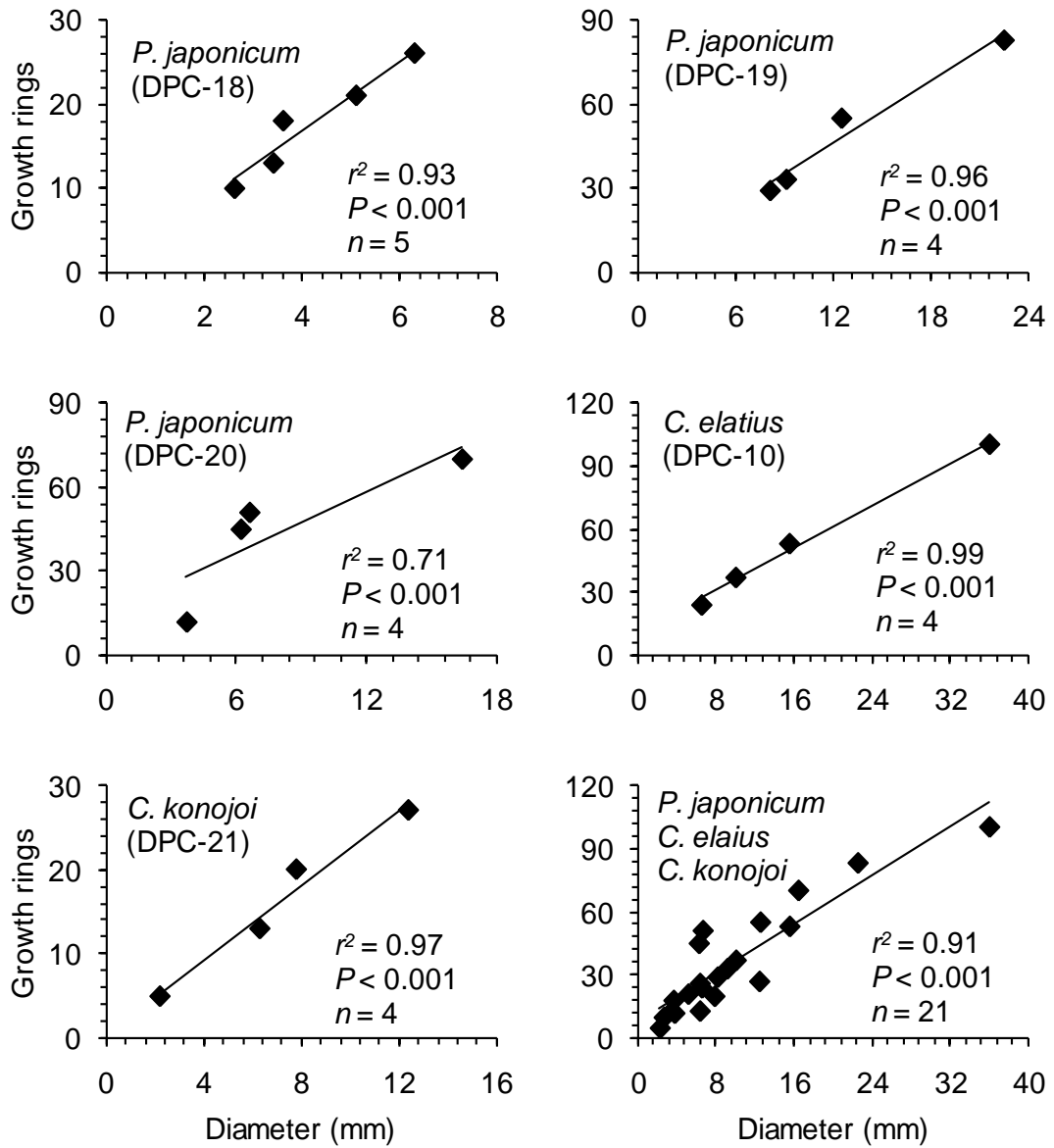


**Fig. 3.5:** Correlation between the number of growth rings and the diameter of the base of Japanese precious corals (*Paracorallium japonicum*, *Corallium elatius*, and *Corallium konojoi*).

#### 3.5.4. Determination of the ages and growth rates of Japanese precious corals

A number of methods has been employed for determining the age and growth rate of corals (Garrabou and Harmelin, 2002; Marschal *et al.*, 2004; Roark *et al.*, 2006a; Bruckner and Roberts, 2009). The petrographic method has been a popular method for estimating growth rates and ages of precious corals based on growth ring density in thin CSs of axial coral skeleton (Grigg, 1974; Santangelo *et al.*, 1993; Andrews *et al.*, 2002). However, Marschal *et al.* (2004) developed the OMS method (a modification of the petrographic method) for measuring growth rate and age of the Mediterranean red coral (*C. rubrum*) by staining the organic matrix in the calcite skeleton. Since the OMS method is mainly based on the concentration of organic matrix in the coral skeleton, it is uncertain whether this method is suitable for the determining the age and growth rates of corals having low concentrations of organic matrix. In the present study, growth rings on thin slabs of the Japanese red coral (*P. japonicum*) were observed through the VHX-1000 to determine age and growth rate of the coral based on the principles of the petrographic method. High dynamic range (HDR) is the most important function for light settings in the VHX-1000. This function first captures multiple images at several brightness levels and then integrates them into a single image with extremely high

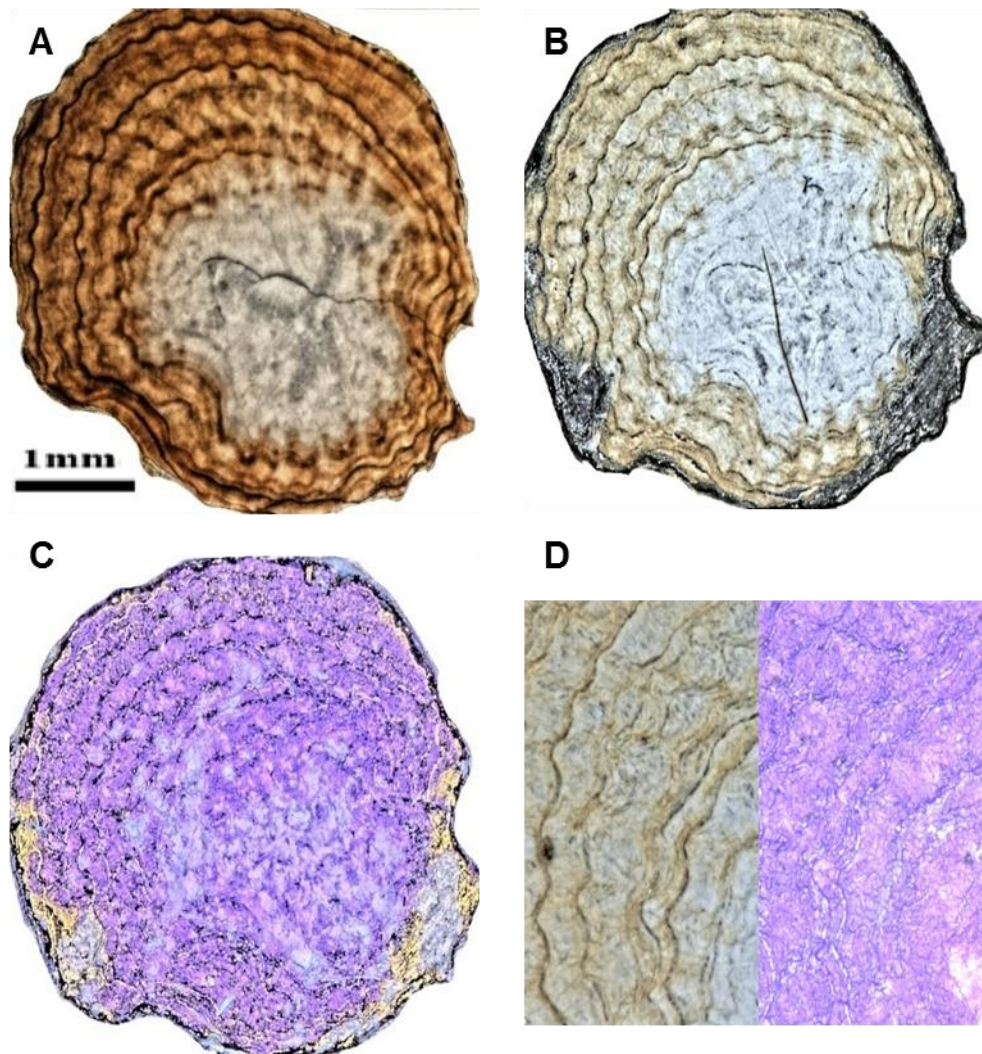


**Fig. 3.6:** Cross-section of the axial skeleton of the Japanese red coral (*Paracorallium japonicum*) observed under the VXH-1000 digital microscope without treatment (A), after treatment with 2% acetic acid solution for 4-5 h (B), and after staining the organic matrix in the skeleton with 0.05% Toluidine blue for 10-30 s (C). Magnified images of the internal region near center before and after staining the organic matrix with 0.05% Toluidine blue (D).

levels of color gradation (16-bit and 65536 levels of gray). Therefore, under the VHV-1000 digital microscope at high magnification (x200), minor rings are observed beside growth rings in the CSs of *P. japonicum*, and thus, this method produces an accurate image of the coral skeleton with clearly visible structures and growth rings.

Marschal et al. (2004) reported that compared to the polarisation microscopy method the OMS method provides high resolution and clearer growth rings in the Mediterranean red coral (*C. rubrum*). In the OMS method, thin (< 50  $\mu\text{m}$ ) slabs of the coral skeleton are soaked in 2% acetic acid for 4-5 h and then stained with 0.05% toluidine blue for 10-30 s; however, this treatment not only decalcifies but also destroys the organic matrix in the skeleton. Therefore, the thickness of slabs and the time of soaking in the acetic acid solution as well as the concentration of toluidine blue need to be considered. In the present study, growth rings in both stained (with 2% acetic acid solution for 4-5 h and 0.05% toluidine blue for 10-30 s) and unstained slabs of the Japanese red coral (*P. japonicum*) were observed through the VHX-1000 and the results were compared. The annual growth rings were more clearly visible in unstained slabs than the stained slabs (Fig. 3.6). This may be attributed to the low concentration of organic matrix in the Japanese red coral, which is likely to be due to different environmental conditions and habitats, such as weather patterns, ocean currents, depth, water temperatures, and nutriment availability. Therefore, the OMS method would be suitable for studying the age and growth rates of the Mediterranean red coral species as they have high organic matrix. However, this method is unsuitable for Japanese precious corals. Instead, the non-destructive method (without acetic acid treatment and without staining the organic matrix by toluidine blue) using the high resolution VHX-1000 would be a better choice for studying growth characteristics and estimating the age and

growth rates of Japanese precious corals.

**Table 3.1:** Diametric growth rates and ages of the Japanese red (*Paracorallium japonicum*), pink (*Corallium elatius*), and white (*Corallium konojoi*) corals collected from Japanese waters.

| Colony ID | Coral species                                       | <i>n</i> | Location                           | Depth (m) | Number of growth ring   | Diameter (mm)              | Diametric growth rate (mm yr <sup>-1</sup> ) | Age (yr.)               |
|-----------|---|----------|------------------------------------|-----------|-------------------------|----------------------------|--|-------------------------|
| DPC-18    | <i>Paracorallium japonicum</i> (Japanese red coral) | 5        | Off Amami Island, Kagoshima, Japan | 207       | 17.60±6.35<br>(10-26)   | 4.20±1.48<br>(2.60-6.30)   | 0.24±0.02<br>(0.20-0.26)                     | 17.60±6.35<br>(10-26)   |
| DPC-19    | <i>Paracorallium japonicum</i> (Japanese red coral) | 4        | Off Amami Island, Kagoshima, Japan | 212       | 50±24.79<br>(29-83)     | 13.05±6.58<br>(8.10-22.5)  | 0.27±0.01<br>(0.23-0.28)                     | 50.00±24.79<br>(29-83)  |
| DPC-20    | <i>Paracorallium japonicum</i> (Japanese red coral) | 4        | Off Muroto, Kochi, Japan           | 94        | 44.50±24.15<br>(12-70)  | 8.23±5.60<br>(3.70-16.4)   | 0.20±0.08<br>(0.13-0.31)                     | 44.50±24.15<br>(12-70)  |
| DPC-10    | <i>Corallium elatius</i> (Japanese pink coral)      | 4        | Off Ryukyu Islands, Okinawa, Japan | 200-300   | 53.50±33.19<br>(24-100) | 17.00±13.20<br>(6.50-36.0) | 0.30±0.04<br>(0.27-0.36)                     | 53.50±33.19<br>(24-100) |
| DPC-21    | <i>Corallium konojoi</i> (Japanese white coral)     | 4        | Off Ashizuri, Kochi, Japan         | 108       | 16.25±9.43<br>(5-27)    | 7.18±4.21<br>(2.2-12.4)    | 0.44±0.04<br>(0.39-0.48)                     | 16.25±9.43<br>(5-27)    |

**Table 3.2:** Linear growth rates of the Japanese red (*Paracorallium japonicum*), pink (*Corallium elatius*), and white (*Corallium*) corals collected from Japanese waters.

| Colony | Coral species                                       | Cross-section/<br>Slab <sup>a</sup> | Height from<br>base (mm) | Number of<br>growth<br>rings | Linear growth rate<br>(mm/year) <sup>b</sup> | Ref.       |
|--------|---|-------------------------------------|--------------------------|------------------------------|--|------------|
| DPC-18 | <i>Paracorallium japonicum</i> (Japanese red coral) | 1                                   | 139.0                    | 10                           | 3.33   | This study |
|        |   | 2                                   | 129.0                    | 13                           | 8.68   |            |
|        |   | 3                                   | 85.6                     | 18                           | 7.80   |            |
|        |   | 4                                   | 62.2                     | 21                           | 2.90   |            |
|        |   | 5                                   | 47.7                     | 26                           |  |            |
|        |   | Mean                                |                          |                              | 5.68 ± 2.6 (n = 4)                           |            |
| DPC-19 | <i>Paracorallium japonicum</i> (Japanese red coral) | 1                                   | 167.2                    | 29                           | 12.65  | This study |
|        |   | 2                                   | 116.6                    | 33                           | 3.03   |            |
|        |   | 3                                   | 49.9                     | 55                           | 1.78   |            |
|        |   | 4                                   |                          | 83                           |  |            |
|        |   |                                     |                          | Mean                         |  |            |
| DPC-20 | <i>Paracorallium japonicum</i> (Japanese red coral) | 1                                   | 163.7                    | 12                           | 3.01   |            |
|        |   | 2                                   | 64.3                     | 45                           | 2.28   |            |
|        |   | 3                                   | 50.6                     | 51                           | 1.37   |            |
|        |   | 4                                   | 24.5                     | 70                           |  |            |

|        |                          |      |       |     |                         |                                 |
|--------|--------------------------|------|-------|-----|-------------------------|---------------------------------|
|        |                          | Mean |       |     | $2.22 \pm 0.82 (n = 3)$ | This study                      |
| DPC-10 | <i>Corallium elatius</i> | 1    | 150.0 | 24  | 5.08                    |                                 |
|        | (Japanese pink coral)    | 2    | 84.0  | 37  | 2.13                    |                                 |
|        |                          | 3    | 50.0  | 53  | 1.06                    |                                 |
|        |                          | 4    |       | 100 | -                       |                                 |
|        |                          | Mean |       |     | $2.76 \pm 1.70 (n = 3)$ | This study                      |
| DPC-21 | <i>Corallium konojoi</i> | 1    | 157.0 | 5   | 6.98                    |                                 |
|        | (Japanese white coral)   | 2    | 101.2 | 13  | 6.60                    |                                 |
|        |                          | 3    | 55.0  | 20  | 7.86                    |                                 |
|        |                          | 4    |       | 27  | -                       |                                 |
|        |                          | Mean |       |     | $7.15 \pm 0.53 (n = 3)$ | This study                      |
| -      | <i>Corallium rubrum</i>  |      |       |     | $1.78 \pm 0.67$         | (Bramanti <i>et al.</i> , 2005) |
| -      | <i>Corallium rubrum</i>  |      |       |     | $1.83 \pm 0.15$         | (Garrabou and Harmelin, 2002)   |

<sup>a</sup> The descending numbers represent the position of the cross-section/slabs of the coral axis from the tip to the base.

<sup>b</sup> The linear growth rate was calculated from the ration of the distance between two successive slabs of the coral axis and the decrease of growth ring number for the distance between the two successive slabs (Eg.(ii)).

**Table 3.3:** Diametric and linear growth rate of Japanese precious corals (Luan et al., unpublished)

| Colony ID | Coral species | n | Location              | Depth (m)  | Number of growth ring  | Diameter (mm)              | Diametric growth rate (mm yr <sup>-1</sup> ) | Linear growth rate (mm yr <sup>-1</sup> ) |
|-----------|---------------|---|-----------------------|------------|------------------------|----------------------------|--|---|
| DPC-22    | Red coral     | 7 | Off Amami, Japan      | 207        | 12±7.30<br>(3-23)      | 4.17±1.89<br>(1.51-7.01)   | 0.40±0.10<br>(0.30-0.56)                     | 2.21±2.07<br>(0.13-6.10)                  |
| DPC-272   | Pink coral    | 5 | Off Ogasawara, Japan  | 1420 -1620 | 33.20±13.76<br>(14-52) | 12.47±6.10<br>(4.06-20.12) | 0.36±0.05<br>(0.29-0.42)                     | 3.81±3.27<br>(1.18-8.57)                  |
| DPC-16    | White coral   | 6 | Off Kagoshima, Japan- | 100 - 150  | 26±8.83<br>(13-40)     | 9.63±3.12<br>(5.05-14.12)  | 0.38±0.03<br>(0.32-0.41)                     | 5.87±2.74<br>(2.37-9.74)                  |

**Table 3.4:** Diametric growth rates of precious corals from different geographical locations estimated by different methods

| Family                       | Coral species   | Location                           | Depth (m) | Measurement method         | Diametric growth rate (mm yr <sup>-1</sup> ) | References                        |
|------------------------------|---|------------------------------------|-----------|----------------------------|--|-----------------------------------|
| Octocorallia;<br>Coralliidae | <i>Corallium rubrum</i> (Red coral)                         | Off Pointe de La Revellata, France | 36-42     | OMS* method                | 0.20   | (Gallmetzer <i>et al.</i> , 2010) |
|                              | <i>Corallium rubrum</i> (Red coral)                         | Off Marseille, France              | 27        | OMS* method                | 0.35±0.15                                    | (Marschal <i>et al.</i> , 2004)   |
|                              | <i>Corallium rubrum</i> (Red coral)                         | Off Marseille, France              | 27        | <i>in situ</i> method      | 0.24±0.05                                    | (Garrabou and Harmelin, 2002)     |
|                              | <i>Corallium rubrum</i> (Red coral)                         | Off Tuscany, Italy                 | 25-35     | <i>in situ</i> method      | 0.62±0.19                                    | (Bramanti <i>et al.</i> , 2005)   |
|                              | <i>Paracorallium japonicum</i> (Japanese Red coral, DPC-22) | Off Amami Island, Kagoshima, Japan | -         | <i>Petrographic method</i> | 0.40±0.10<br>(0.30-0.56)                     | Luan <i>et al.</i> , unpublished  |
|                              | Japanese pink coral(DPC-272)                                | Ogasawara Island, Japan            | -         | <i>Petrographic method</i> | 0.36±0.05<br>(0.29-0.42)                     | Luan <i>et al.</i> , unpublished  |

|                    |   |                       |             |                                 |                          |                                     |
|--------------------|---|-----------------------|-------------|---------------------------------|--------------------------|-------------------------------------|
|                    | Japanese white coral<br>(DPC-16)                          | -                     |             | <i>Petrographic method</i>      | 0.38±0.03<br>(0.32-0.41) | Luan <i>et al.</i> ,<br>unpublished |
|                    | <i>Corallium secundum</i><br>(Hawaiian pink coral)        | Off Hawaii            | 450         | <sup>14</sup> C dating method   | 0.17                     | (Roark <i>et al.</i> ,<br>2006a)    |
|                    | <i>Paracorallium japonicum</i><br>(Japanese red coral)    | Off Kochi,<br>Japan   | 100         | OMS* method                     | 0.30±0.08                | (Iwasaki and<br>Suzuki, 2010)       |
|                    | <i>Paracorallium japonicum</i><br>(Japanese red coral)    | Off Goyo, Japan       | 140         | Infrared radiation<br>method    | 0.34-0.50                | (Iwasaki and<br>Suzuki, 2010)       |
|                    | <i>Corallium elatius</i><br>(Japanese pink coral)         | Off Okinawa,<br>Japan | 100-300     | <sup>210</sup> Pb dating method | 0.15                     | Hasegawa and<br>Yamada, 2010        |
|                    | <i>Corallium elatius</i><br>(Japanese pink coral)         | Off Okinawa,<br>Japan | 200+30<br>0 | Infrared radiation<br>method    | 0.26-0.28                | (Bruckner and<br>Roberts, 2009)     |
| Hexacorallia;      | <i>Gerardia</i> sp. ( <i>Savalia</i> sp.)<br>(Gold coral) | Off Hawaii            | 450         | <sup>14</sup> C dating method   | 0.03                     | (Roark <i>et al.</i> ,<br>2006a)    |
| Parazoanthida<br>e |   |                       |             |                                 |                          |                                     |
| Antipathidae       | <i>Antipathes dichotoma</i><br>(Black coral)              | Off Hawaii            | 50          | <sup>14</sup> C dating method   | 0.26-2.28                | (Roark <i>et al.</i> ,<br>2006a)    |

\*OMS = Organic matrix staining

## REFERENCES

- Adkins, J.F., Griffin, S., Kashgarian, M., Cheng, H., Druffel, E.M., Boyle, E.A., Edwards, R.L., Shen, C.C., 2006. Radiocarbon dating of deep-sea corals. *Radiocarbon* 44(2), 567-580.
- Adkins, J.F., Henderson, G.M., Wang, S.L., O'Shea, S., Mokadem, F., 2004. Growth rates of the deep-sea scleractinia *Desmophyllum cristagalli* and *Enallopsammia rostrata*. *Earth Planet. Sci. Lett.* 227(3-4), 481-490.
- Andrews, A.H., Cordes, E.E., Mahoney, M.M., Munk, K., Coale, K.H., Cailliet, G.M., Heifetz, J., 2002. Age, growth and radiometric age validation of a deep-sea, habitat-forming gorgonian (*Primnoa resedaeformis*) from the Gulf of Alaska. *Hydrobiologia* 471(1), 101-110.
- Bak, R.P.M., Laane, R., 1987. Annual black bands in skeletons of reef corals (*Scleractinia*). *Mar. Ecol. Prog. Ser.* 38, 169-175.
- Boto, K., Isdale, P., 1985. Fluorescent bands in massive corals result from terrestrial fulvic acid inputs to nearshore zone. *Nature* 315(6018), 396-397.
- Bourget, E., 1987. Barnacle shells: Composition, structure and growth. In: Southward, A.J. (Ed.), *Barnacle Biology*. Balkema, Rotterdam, pp. 267-285.
- Bramanti, L., Magagnini, G., De Maio, L., Santangelo, G., 2005. Recruitment, early survival and growth of the Mediterranean red coral *Corallium rubrum* (L 1758), a 4-year study. *J. Exp. Mar. Biol. Ecol.* 314(1), 69-78.
- Bruckner, A.W., Roberts, G.G., 2009. Proceedings of the First International Workshop on *Corallium* Science, Management, and Trade. Silver Spring, Hong Kong, 153 pp.

- Cheng, H., Adkins, J., Edwards, R.L., Boyle, E.A., 2000. U-Th dating of deep-sea corals. *Geochim. Cosmochim. Acta* 64(14), 2401-2416.
- Dillon, J.F., Clark, G.R., 1980. Growth line analysis as a test for contemporaneity in populations. In: Rhoads, D.C., Lutz, R.A. (Eds.), *Skeletal Growth in Aquatic Organisms*. Plenum, New York, pp. 395-415.
- Druffel, E.R.M., King, L.L., Belastock, R.A., Buesseler, K.O., 1990. Growth rate of a deep-sea coral using  $^{210}\text{Pb}$  and other isotopes. *Geochim. Cosmochim. Acta* 54(5), 1493-1499.
- Gallmetzer, I., Haselmair, A., Velimirov, B., 2010. Slow growth and early sexual maturity: Bane and boon for the red coral *Corallium rubrum*. *Estuar. Coast. Shelf Sci.* 90(1), 1-10.
- Garrabou, J., Harmelin, J.G., 2002. A 20-year study on life-history traits of a harvested long-lived temperate coral in the NW Mediterranean: Insights into conservation and management needs. *J. Anim. Ecol.* 71(6), 966-978.
- Goldberg, W.M., 1991. Chemistry and structure of skeletal growth rings in the black coral *Antipathes fiordensis* (Cnidaria, Antipatharia). *Hydrobiologia* 216(1), 403-409.
- Griffin, S., Druffel, E.M., 2006. Sources of carbon to deep-sea corals. *Radiocarbon* 31(3), 533-543.
- Grigg, R.W., 1974. Growth rings: Annual periodicity in two gorgonian corals. *Ecology* 55(4), 876-881.
- Grigg, R.W., 1993. Precious coral fisheries of Hawaii and the US Pacific Islands. *Mar. Fish. Rev.* 55(2), 50-60.
- Harvell, C.D., Kim, K., Burkholder, J.M., Colwell, R.R., Epstein, P.R., Grimes, D.J.,

- Hofmann, E.E., Lipp, E.K., Osterhaus, A., Overstreet, R.M., 1999. Emerging marine diseases - climate links and anthropogenic factors. *Science* 285(5433), 1505-1510.
- Hasegawa, H., Rahman, M.A., Luan, N.T., Maki, T., Iwasaki, N., 2012. Trace elements in *Corallium* spp. as indicators for origin and habitat. *J. Exp. Mar. Biol. Ecol.* 414-415, 1-5.
- Iwasaki, N., Hasegawa, H., Suzuki, T., Yamasa, M., 2009. Biology of Japanese *Corallium* and *Paracorallium*. In: Bruckner, A.W., Roberts, G.G. (Eds.), The 1<sup>st</sup> International Workshop on *Corallium* Science, Management, and Trade. NOAA Technical Memorandum NMFS-OPR-43 and CRCP-8, Silver Spring, MD, Hong Kong, China, pp. 68-70.
- Iwasaki, N., Suzuki, T., 2010. Biology of precious corals. In: Iwasaki, N. (Ed.), *Biohistory of Precious corals- Scientific, Cultural and Historical Perspectives*. Tokai University Press, Tokai, Japan.
- Jackson, J.B.C., Kirby, M.X., Berger, W.H., Bjorndal, K.A., Botsford, L.W., Bourque, B.J., Bradbury, R.H., Cooke, R., Erlandson, J., Estes, J.A., 2001. Historical overfishing and the recent collapse of coastal ecosystems. *Science* 293(5530), 629-637.
- Marschal, C., Garrabou, J., Harmelin, J.G., Pichon, M., 2004. A new method for measuring growth and age in the precious red coral *Corallium rubrum* (L.). *Coral Reefs* 23(3), 423-432.
- Musick, J.A., 1999. Ecology and conservation of long-lived marine animals. In: Musick, J.A. (Ed.), *Life in the Slow Lane: Ecology and Conservation of Long-Lived Marine Animals*. American Fisheries Society, Maryland, USA, pp. 1-10.

- Nonaka, M., Muzik, K., Uchida, S., 2004. Capture, study and display of precious corals, 10<sup>th</sup> International Coral Reef Symposium, Okinawa, Japan, pp. 38-42.
- Risk, M.J., Heikoop, J.M., Snow, M.G., Beukens, R., 2002. Lifespans and growth patterns of two deep-sea corals: *Primnoa resedaeformis* and *Desmophyllum cristagalli*. *Hydrobiologia* 471(1), 125-131.
- Roark, E.B., Guilderson, T.P., Dunbar, R.B., Ingram, B.L., 2006. Radiocarbon-based ages and growth rates of Hawaiian deep-sea corals. *Mar. Ecol. Prog. Ser.* 327, 1-14.
- Santangelo, G., Abbiati, M., Giannini, F., Cicogna, F., 1993. Red coral fishing trends in the western Mediterranean Sea during the period 1981-1991. *Sci. Mar.* 57, 139-143.
- Seki, K., 1991. Study of precious coral diver survey with open circuit air SCUBA diving at 108 m. *Ann. Physiol. Anthropol.* 10(3), 189-192.
- Tracey, D.M., Neil, H., Marriott, P., Andrews, A.H., Cailliet, G.M., Sanchez, J.A., 2007. Age and growth of two genera of deep-sea bamboo corals (Family Isididae) in New Zealand waters. *Bull. Mar. Sci.* 81(3), 393-408.
- Tsounis, G., Rossi, S., Aranguren, M., Gili, J.M., Arntz, W., 2006. Effects of spatial variability and colony size on the reproductive output and gonadal development cycle of the Mediterranean red coral (*Corallium rubrum* L.). *Mar. Biol.* 148(3), 513-527.
- Tsounis, G., Rossi, S., Grigg, R., Santangelo, G., Bramanti, L., Gili, J.M., 2010. The exploitation and conservation of precious corals. *Ocean. Mar. Biol.* 48, 161-212.
- Vielzeuf, D., Garrabou, J., Baronnet, A., Grauby, O., Marschal, C., 2008. Nano to macroscale biomineral architecture of red coral (*Corallium rubrum*). *Am. Mineral.* 93(11-12), 1799-1815.
- Wilson, M.T., Andrews, A.H., Brown, A.L., Cordes, E.E., 2002. Axial rod growth and

age estimation of the sea pen, *Halipteris willemoesi* Kolliker. *Hydrobiologia* 471(1), 133-142.

Witherell, D., Pautzke, C., Fluharty, D., 2000. An ecosystem-based approach for Alaska groundfish fisheries. *ICES J. Mar. Sci.* 57(3), 771-777.

# CHAPTER 4

## RESULTS AND DISCUSSION

### TRACE ELEMENTS IN *Corallium* spp. as INDICATORS FOR ORIGIN AND HABITAT

#### 4.1. INTRODUCTION

Precious corals are some of the most valuable living marine resources, and are harvested only in limited areas in the world. They belong to the functional group of deep corals and are important structure-forming organisms that provide shelter for other organisms and increase marine biodiversity (Tsounis *et al.*, 2010a). Precious corals are different from reef-building corals in that their skeletons are closely-packed with high magnesium calcite, while the reef-building corals consist mostly of aragonite, and are

porous because of its loosely-packed crystals.

Taxonomically, precious corals belong primarily to three orders of the class Anthozoa, and the most valuable species are red and pink corals of the genus *Corallium* and *Paracorallium* (Tsounis *et al.*, 2010a). They are found mainly in the Mediterranean Sea and Pacific Ocean (Japanese waters and off Taiwan, off the Midway Islands and off the Hawaiian Islands) (Iwasaki and Suzuki, 2010). Some of the important precious corals include *Corallium rubrum*, *Paracorallium japonicum*, *Corallium elatius*, *Corallium konojoi* and *Corallium secundum* (Tsounis *et al.*, 2010a). The *Corallium* spp. are commonly known as deep-sea coral, and the red coral (*C. rubrum*) is produced in the Mediterranean Sea. The pink coral (*C. secundum*) is distributed in the seas around Hawaii and the Midway Islands, and also found in the waters close to the Midway Island (Grigg, 1993b).

Japanese red coral (*P. japonicum*), pink coral (*C. elatius*) and white coral (*C. konojoi*) are distributed and harvested in waters near Japan (Iwasaki *et al.*, 2009c). *Paracorallium japonicum* is found at depths of 76-280 m on the rocky bottom in Sagami Bay (Pacific coast of Japan), in the waters from the Ogasawara Islands (Japan), and off the coast near the Goto Islands, Nagasaki (Japan) (Seki, 1991a). *Corallium elatius* is distributed on the rocky bottom at a depth of 100-276 m in the waters near Wakayama (Pacific coast of Japan), from the Ogasawara Islands (Japan) to the northern South China Sea, and off the Goto Islands, Nagasaki, Japan (Iwasaki and Suzuki, 2010). *Corallium konojoi* is distributed on the rocky bottom at a depth of 76-276 m in the waters of Wakayama (Pacific coast of Japan), in the waters from the Ogasawara Islands (Japan) to the northern South China Sea, and off the Goto Islands, Nagasaki, Japan (Seki, 1991a; Nonaka *et al.*, 2004). *Corallium secundum* has been found to grow on flat

exposed substrata whereas *C. regale* prefer encrusted uneven rocky bottom habitat in the Hawaiian Islands, and both species are absent from the shelf areas (<400 m depth) (Grigg, 1974).

Some *Corallium* species have a hard calcium skeleton of intense red and others are pink and of pink (Iwasaki and Suzuki, 2010). Both spicules and skeletons of red coral (*C. rubrum*) are mainly made of calcium carbonate ( $\text{CaCO}_3$ ) crystallized in the form of calcite, though small amounts of other trace elements such as magnesium (Mg), strontium (Sr), iron (Fe), aluminum (Al) and sulphur (S) are also found (Maté *et al.*, 1986b). Previously, Velimirov and Bohm (1976) analyzed calcium (Ca) and Mg by atomic absorption spectroscopy and ethylenediaminetetraacetate (EDTA) titration with the aim of providing information on the mineral composition of gorgonians and the possible variations in different growth regions. They showed that  $\text{CaCO}_3$ ,  $\text{MgCO}_3$  and total mineral content increase markedly from branch to stem. Weinbauer and Velimirov (1995) determined Mg, Ca, and Sr in sclerites of four Mediterranean gorgonians and suggested that Mg/Ca and Sr/Ca ratios were very low (0.064-0.098 and 0.004-0.0025, respectively). They also revealed that calcium concentrations did not vary with geographical origin, while the variations of Mg/Ca and Sr/Ca ratios were related to water depth. Besides, there was a direct relationship between Mg concentration and temperature, and the Mg/Ca ratios increased significantly with the ambient water temperature (Weinbauer and Vellmirov, 1995).

Reef-building coral is better understood, and concentrations of trace elements in its carbonate skeletons have been determined. The validity of their use as indicators of past environmental conditions, such as water temperatures, nutrients and pollution levels has been confirmed in earth and environmental science studies (Weber and

Woodhead, 1970; Weber, 1973; Mitsuguchi *et al.*, 1996; Mitsuguchi *et al.*, 2001; Mitsuguchi *et al.*, 2003). In contrast, studies on trace elements in precious coral have been focused mostly on Mediterranean red coral *C. rubrum* (Weinbauer and Vellmirov, 1995; Weinbauer *et al.*, 2000). Studies on trace elements in other precious corals, especially the Japanese white coral (*C. konojoi*), from various locations is limited. Research on precious corals in Japanese waters has recently been started.

Precious corals have attracted worldwide attention as sparse biological resources, and Corallidae have been recently proposed for inclusion in Appendix II of the Convention on International Trade in Endangered Species of Wild Fauna and Flora (CITES) that regulates the international trade in endangered species by listing them in its appendices. The problem is that appendix II permits the export and/or import of corals from well managed stocks, while it prohibits that corals from unmanaged areas can pass the costumes borders. Therefore, appropriate scientific methods for the authentication of the uniqueness and origin of Corallidae are necessary to protect the coral resources and international trade. This refers both to geographical and bathymetric origin, because shallow coral maybe protected in one area, while deeper stocks may be harvested for commercial uses.

## 4.2. FOCUS

In the present study, trace element concentrations in the skeletons of *Corallium* spp. of Corallidae family from different geographical locations (origins) were determined to investigate if the concentrations and distribution of trace elements were related to their origin and habitat. The identification of the origin of the corals via trace

metal analysis will provide the opportunity to reveal smuggling of illegal corals with fake papers.

### 4.3. MATERIALS AND METHODS

#### 4.3.1. Sampling sites

Samples were collected from Japanese waters, the Midway Islands' waters and the Mediterranean Sea (off Italy) from fishermen, coral traders, and research institutes. A deep-sea coral (*Corallium* sp.) was collected by Marine Geological Research Vessel "HakureiMaru" cruise GH85-1 conducted by the National Institute of Advanced Industrial Science and Technology. Two specimens of Japanese red coral (*Paracorallium japonicum*) were collected by a manned submersible "Hakuyo" from the Kochi Prefectural Deep Seawater Laboratory. The species and the locations from where the samples were collected are shown in Table 4.1.

Corals of the Mediterranean Sea and Japanese waters were sampled from a depth of < 150 m, while some samples of the Midway Islands were collected from a depth of 400-500 m and the other were from a depth of 900-1200 m (deep-sea coral). White coral (*Corallium konojoi*; Fig. 4.1) was collected from a depth of 100 m, off Cape Muroto, Kochi, Japan, in July 2004.

#### 4.3.2. Chemical analysis of skeleton composition

Barium (Ba), Ca, Mg, and Sr concentrations were analyzed in skeleton of the corals. Each of the skeleton was ground in an agate mortar into a particle size of 5 mm

in diameter and 0.1 g of it was taken into 10-mL polypropylene test tubes with three replications. The skeletons of precious corals were then cleaned following sequential methods of ultrasonic, oxidation, and reduction treatments (Shen, Boyle, 1988). At first the samples were treated with ultrasonic waves in 1 mL of purified water and then in 1 mL of 0.2 M nitric acid for 10 min each. The samples were rinsed with purified water between the treatments. This procedure was repeated three times. After drying at room temperature, they were ground further in the agate mortar and were sieved through a 25-50 Teflon mesh screen of a polypropylene sieve. The samples were then selected from three different sieved samples in the same colony ( $n = 3$ ).

After ultrasonic cleaning, the samples in 10-mL polypropylene test tubes were oxidized by addition of 1 mL solution prepared from 1:1 (v/v) 30% hydrogen peroxide ( $\text{H}_2\text{O}_2$ ) and 0.2 M sodium hydroxide (NaOH). They were then placed in a steam and an ultrasonic bath for 2 min each for a total of 10 repeats. They were then sequentially treated with ultrasonic waves in 1 mL of 0.2 M nitric acid for 3 min, in 1 mL of purified water for 10 min and in 1 mL of 0.2 M nitric acid for 3 min, and then the oxidation treatment was applied once again. A reduction treatment was followed by oxidation treatment in which the samples were treated with 1 mL solution containing 97% hydrogen, concentrated ammonia, and 0.3 M citric acid in the ratio of 1:6:3. They were then placed in a hot ( $70^\circ\text{C}$ ) and an ultrasonic bath for 2 min each for a total of 16 repeats. Finally the samples were cleaned by repeating oxidation treatments, treating ultrasonic waves (2-min) in 1 mL of 0.2 M nitric acid three times, and rinsing twice in 1 mL of 0.2 M nitric acid. Then the samples were dissolved in 1 mL of 2 M nitric acid.

The sample solutions were diluted to 1000 times with 0.5 M nitric acid, and the determination of trace element concentrations in the samples were carried out by

inductively coupled plasma atomic emission spectroscopy (ICP-AES, Perkin Elmer, Optima 3300XL) in triplicates using a calibration curve method.

#### **4.3.3. Analysis of inorganic elements with electron probe micro-analyzer (EPMA)**

Each skeleton sample with dried organic tissues attached on the surface of white coral (*C. konojoi*) was embedded in polyester resin for EPMA. The skeletons were cut at 5 mm intervals perpendicular to the growth direction using a diamond saw, and one of the thin slices was ground to 100-200  $\mu\text{m}$  with 600, 1000, and 2000 grits silicon carbide abrasive papers. The surface of the samples was then polished to a mirror finish using an alumina wrapping sheet (Marumoto Kogyo, Japan) with a particle diameter of 0.1  $\mu\text{m}$ , and was coated with a 10- $\mu\text{m}$  carbon film by evaporative deposition of carbon. EPMA was performed using an EPMA-8705 (Shimadzu Corporation, Japan). Two-dimensional images of elemental distribution were obtained by stage mapping the sample along the  $x$  and  $y$  axes with 29  $\mu\text{m}$  raster spacing. Measurement parameters were set as follows: accelerating voltage at 15 keV, beam current at 0.3  $\mu\text{A}$ , and a measurement time 0.04 sec. for Ca and Sr, and 0.22 s. for Mg and Ba.

### **4.4. RESULTS AND DISCUSSION**

#### **4.4.1. Trace element distribution in the skeletons of precious coral**

Ca and Mg measurements in the cross-section of white coral (*C. konojoi*)

skeleton reveal that Ca is distributed homogeneously (Fig. 4.1C), while Mg concentration is distributed concentrically forming growth rings (Fig. 4.1B). About 38 growth rings of Mg were observed in tiers on a 6 mm radius. If these growth rings are formed annually, the radial growth rate of this white coral will be  $0.32 \text{ mm yr}^{-1}$ . This rate agrees with the radial growth rate of the same coral obtained through infrared spectroscopy using synchrotron radiation as well as through  $^{210}\text{Pb}$  dating (Hasegawa *et al.*, 2010). As in *C. rubrum*, annual rings can also be observed by staining the organic matrix with toluidine blue. Vielzeuf *et al.* (2008) performed EPMA mapping on the skeleton of *C. rubrum* and found a negative correlation between Mg concentrations and the organic matter, except in the center part of the skeleton, indicating that Mg concentrations corresponded to annual rings. Thus, Mg growth rings can be considered as annual rings of precious coral.

Mg-rich layers grow in warm seasons, and the variations in Mg concentrations in the skeleton are very likely to be related to water temperatures. Weinbauer and Velimirov (1995) compared the Mg/Ca ratios in the skeletons of several *C. rubrum* species from different depths and found a positive correlation between the Mg/Ca ratios and water temperatures. Variations in Mg concentrations within an individual coral skeleton can be assessed as the Mg/Ca molar ratio. The Mg/Ca ratio in white coral varies from 10 to 15% of the mean values, while that in *C. rubrum* obtained from EPMA study of Weinbauer *et al.* (2000) varied from 13 to 30%.

Other than these elements, Sr, Ba, I, and Mo concentrations have also been confirmed in Japanese red coral by two-dimensional images produced in a synchrotron-radiation X-ray Fluorescence (XRF) study (Hasegawa *et al.*, 2010). These elements are distributed homogeneously across the cross-sections of the skeleton, and

the variations of their concentrations are lower compared to Mg concentration. Weak correlation between Sr concentration and the number of growth rings on the skeleton of Japanese red coral obtained by XRF mapping analysis has been reported by Hasegawa et al. (2010). The present study also reveals a weak correlation between Sr concentration and growth rings on the skeleton of white coral obtained by EPMA analysis (Fig. 4.1E). The millimeter-scale variations of the Sr/Ca ratio do not correspond to those of growth rings, which is between 100 and 200 $\mu\text{m}$ . On the other hand, the Sr/Ca ratio in the skeletons of *C. rubrum* has been reported to vary significantly in proportion to skeleton density (Weinbauer et al., 2000).

#### **4.4.2. Trace element compositions reflecting the characteristics of coral habitats**

The Mg/Ca and Ba/Ca ratios in the skeletons of *C. rubrum*, Japanese red, pink and white corals, and Midway corals are shown in Fig. 4.2. Japanese red, pink and white corals co-habit in sea-floors around Japan. The Mg/Ca and Ba/Ca ratios in these three corals collected from the same area were within similar ranges without species-specific differences. On the other hand, Mg/Ca and Ba/Ca ratios in corals from the Mediterranean Sea, Japanese waters and the sea around the Midway Islands differed depending on their habitats (Fig. 4.2) except Sr/Ca ratio ( $0.31\text{-}0.33 \times 10^{-2} \text{ mol mol}^{-1}$ ). Mg/Ca and Sr/Ca ratios in the skeletons of precious corals (*C. rubrum* and Japanese red, pink and white corals) of present study determined by EPMA analysis are well agreed with those in the skeletons of *C. rubrum* measured by XRF (Weinbauer and Vellmirov, 1995). This study also showed that Ba/Ca ratio in the Midway deep-sea corals is higher

compared to that in other samples.

The Mg/Ca ratios in precious corals of the Mediterranean Sea and Japanese waters ranged from  $10\text{-}15 \times 10^{-2} \text{ mol mol}^{-1}$ , while those in pink and white corals of the Midway Islands were in the ranges of  $9\text{-}11 \times 10^{-2} \text{ mol mol}^{-1}$  and  $8\text{-}9 \times 10^{-2} \text{ mol mol}^{-1}$  for 400-500 m and 900-1200 m (deep-sea corals), respectively. Because Mg and Ca are the major salts in seawater, and Mg/Ca ratio is almost constant in all parts of the ocean, it is extremely unlikely that the observed variations in the Mg/Ca ratio were influenced by the Mg/Ca ratio in seawater. In a previous study, [Weinbauer and Velimirov \(1995\)](#) observed that the Mg/Ca ratio in the skeletons of *C. rubrum* was usually related to ocean's depth. They incorporated other reports and estimated that the Mg/Ca ratio in *C. rubrum* was directly proportional to water temperature, increasing by  $0.004\text{-}0.006 \text{ mol mol}^{-1}$  per  $1 \text{ }^\circ\text{C}$ . Water temperatures near the sediments, where the coral samples for the present study were collected (Table 4.1), were in the range of  $13\text{-}24 \text{ }^\circ\text{C}$  in the Mediterranean Sea and Japanese waters, and  $8\text{-}11$  and  $2\text{-}3 \text{ }^\circ\text{C}$  at a depth of 400-500 m and 900-1200 m in the Midway Islands, respectively. The difference in the water temperature could be predicted by the Mg/Ca ratios assuming that an increase of  $0.004\text{-}0.006 \text{ mol mol}^{-1}$  Mg/Ca ratio per  $1 \text{ }^\circ\text{C}$  was applicable to all precious corals in the subclass Octocorallia. The difference in temperature between the Mediterranean Sea/Japanese waters and the Midway shallow area is  $2\text{-}16 \text{ }^\circ\text{C}$ , and between the Mediterranean Sea/Japanese waters and the Midway deep area is  $10\text{-}22 \text{ }^\circ\text{C}$ , which can be calculated as  $0.008\text{-}0.096$  and  $0.040\text{-}0.132 \text{ mol mol}^{-1}$  of Mg/Ca ratios, respectively. Because these figures are close to the difference in the Mg/Ca ratios in this study (Fig. 4.2), variations in the Mg/Ca ratio of precious corals are likely to be explained by difference in water temperature during coral formation.

Ba/Ca ratio in the Midway coral from a depth of 900-1200 m was significantly higher ( $10-15 \times 10^{-6} \text{ mol mol}^{-1}$ ) than that of Midway coral from a depth of 400-500 m ( $5-8 \times 10^{-6} \text{ mol mol}^{-1}$ ) and Japanese corals from a depth of 100-150 m ( $2-6 \times 10^{-6} \text{ mol mol}^{-1}$ ). In contrast, the Ba/Ca ratios in *C. rubrum* showed a wider range ( $4-14 \times 10^{-6} \text{ mol mol}^{-1}$ ). The proportions of Mg, Ca, and Sr concentrations, the major constituents of seawater, are almost identical to those in seawater, while Ba concentration increases with the depth of the ocean. For example, dissolved Ba concentrations of 30-40 mol kg<sup>-1</sup> at 50-200 m, 40-55 mol kg<sup>-1</sup> at 400-500 m, and 90-110 mol kg<sup>-1</sup> at 900-1200 m were reported from *Corallium* (what species) in the North Pacific (Chow and Goldberg, 1960; Boyle *et al.*, 1976). These figures agree well with the Ba/Ca ratios in the skeletons of analyzed precious corals collected from the waters around Japan and around the Midway Islands.

**Table 4.1:** Different types of precious corals collected for ICP-AES analysis. Samples were collected from Japanese waters, Midway Islands' waters and Mediterranean Sea from fishermen, coral traders, and research institutes.

| Species                        | Common name        | Collection sites                | Habitat (m) | Number of Samples ( <i>n</i> ) |
|--------------------------------|--------------------|---------------------------------|-------------|--------------------------------|
| <i>Corallium rubrum</i>        | Red coral          | Off Italy, Mediterranean Sea    | <100        | 4                              |
|                                |                    | Mediterranean Sea               | <100        | 15                             |
| <i>Paracorallium japonicum</i> | Japanese red coral | Goto Islands, Japan             | 140         | 1                              |
|                                |                    | Amami Islands, Japan            | 100-150*    | 2                              |
|                                |                    | Off Cape Muroto, Kochi, Japan   | 100-150*    | 7                              |
|                                |                    | Off Cape Ashizuri, Kochi, Japan | 100-150*    | 2                              |
| <i>Corallium elatius</i>       | Pink coral         | Ogasawara Islands, Japan        | 100-150*    | 10                             |
|                                |                    | Amami Islands, Japan            | 100-150*    | 3                              |
|                                |                    | Off Cape Muroto, Kochi, Japan   | 100-150*    | 6                              |
|                                |                    | Goto Islands, Japan             | 100-150*    | 1                              |
| <i>Corallium konojoi</i>       | White coral        | Ogasawara Islands, Japan        | 100-150*    | 2                              |
|                                |                    | Goto Islands, Japan             | 100-150*    | 2                              |

|                       |                               |                               |                      |    |
|-----------------------|-------------------------------|-------------------------------|----------------------|----|
|                       |                               | Off Cape Muroto, Kochi, Japan | 100                  | 1  |
|                       |                               | Ogasawara Islands, Japan      | 1420-1620            | 1  |
| <i>Corallium</i> spp. | Deep sea coral                | Midway***                     | 400-500 or 940-1100* | 19 |
|                       | Deep sea pink coral           | Midway***                     | 400-500 or 940-1100* | 8  |
|                       | Deep sea white coral (garnet) | Midway***                     | 400-500 or 940-1100* | 2  |

\* Estimated depth.

\*\* Collected at St.4762 on GH85-1cruise conducted by the National Institute of Advanced Industrial Science and Technology.

\*\*\* Collected from northwestern (31°16'-36°47'N, 171°02'-175°55'E, 400-500 m) or northeastern (32°31'-32°58'N, 175°03'W-175°18'W, 940-1100 m) waters of Midway.

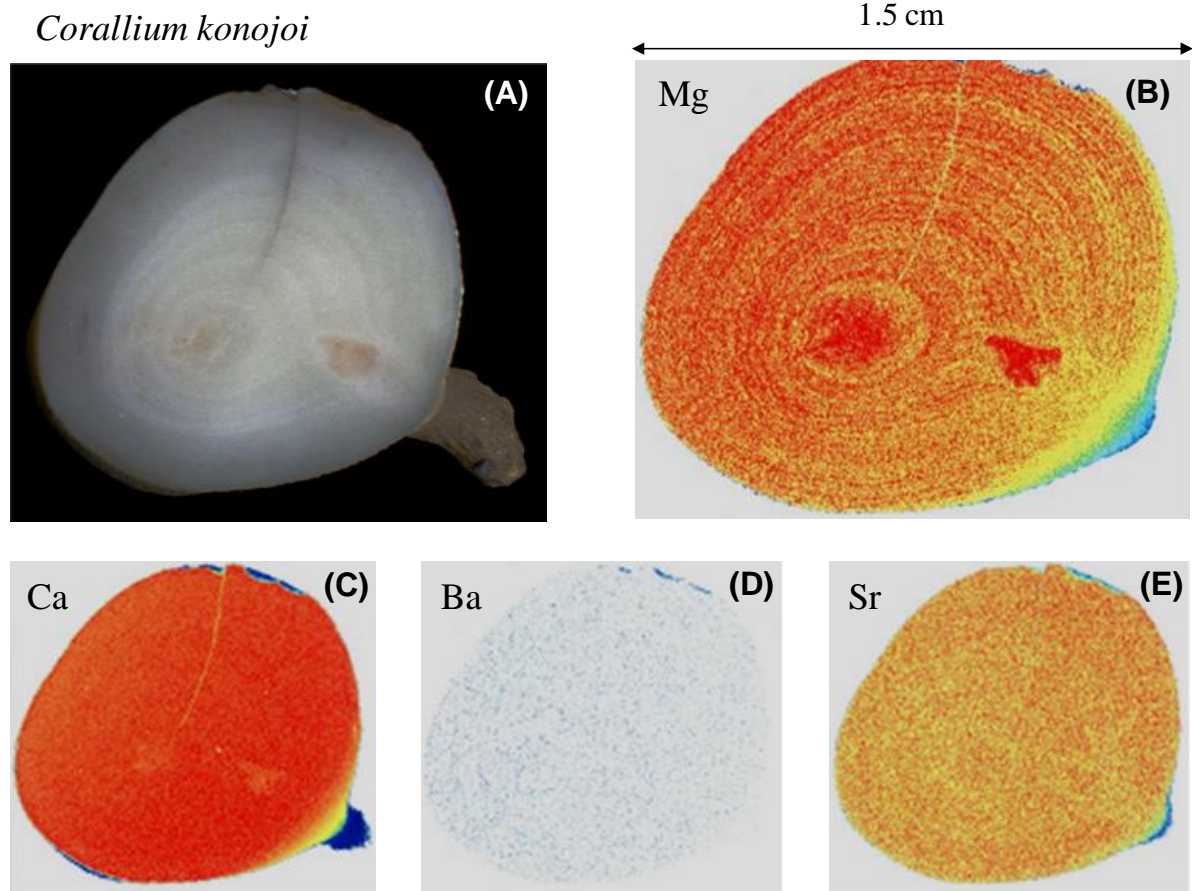


**Fig. 4.1:** Skeleton of Japanese white coral. Photograph of white coral (A), mapping analysis of Mg (B), Ca (C), Ba (D), and Sr (E) in the skeleton of precious white coral by EPMA.

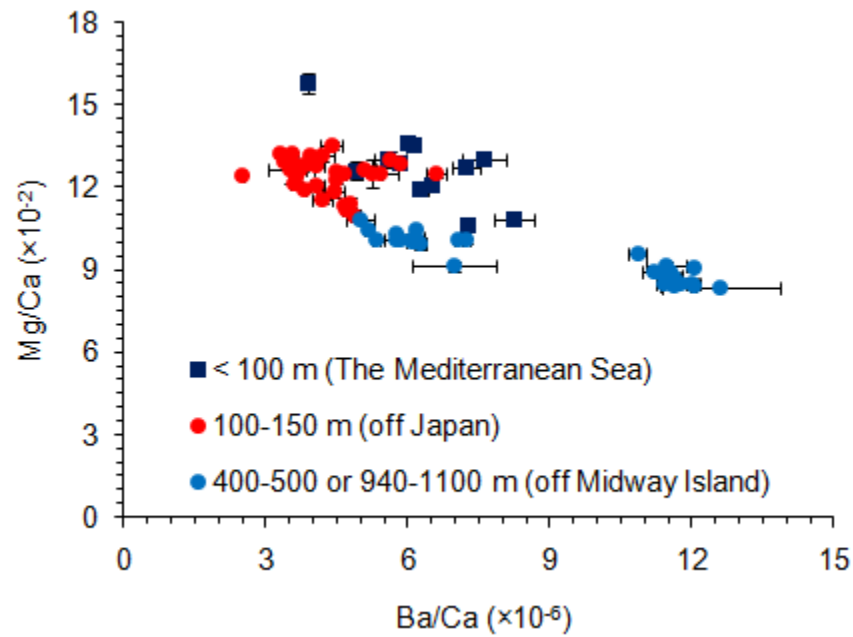


**Fig. 4.2:** Distribution of Mg and Ba in skeleton of precious corals collected from different depth and geographical locations indicating the origin of the corals. Values are mean  $\pm$  SD.

**REFERENCES**

- Boyle, E.A., Sclater, F., Edmond, J.M., 1976. On the marine geochemistry of cadmium. *Nature* 263(5572), 42-44.
- Chow, T.J., Goldberg, E.D., 1960. On the marine geochemistry of barium. *Geochim. Cosmochim. Acta* 20(3-4), 192-198.
- FAO, 2007. Report of the second FAO Ad hoc expert advisory panel for the assessment of proposals to amend appendices I and II of CITES concerning commercially-exploited aquatic species. Food and Agriculture Organization of the United Nations, Rome, pp. 133.
- FAO, 2010. Report of the third FAO expert advisory panel for the assessment of proposals to amend appendices I and II of CITES concerning commercially-exploited aquatic species. Food and Agriculture Organization of the United Nations, Rome, pp. 150.
- Grigg, R.W., 1974. Growth rings: Annual periodicity in two gorgonian corals. *Ecology* 55(4), 876-881.
- Grigg, R.W., 1993. Precious coral fisheries of Hawaii and the US Pacific Islands. *Mar. Fish. Rev.* 55(2), 50-60.
- Hasegawa, H., Iwasaki, N., Suzuki, A., Maki, T., Hayakawa, S., 2010. Distribution of trace elements in biogenic carbonate minerals of precious corals by X-ray fluorescence analysis. *Bunseki Kagaku* 59(6), 521-530.

- Iwasaki, N., Hasegawa, H., Suzuki, T., Yamasa, M., 2009. Biology of Japanese *Corallium* and *Paracorallium*. In: Bruckner, A.W., Roberts, G.G. (Eds.), Proceedings of the First International Workshop on Corallium Science, Management, and Trade. NOAA Technical Memorandum NMFS-OPR-43 and CRCP-8, Silver Spring, MD, Hong Kong, China, pp. 153.
- Iwasaki, N., Suzuki, T., 2010. Biology of precious corals. In: Iwasaki, N. (Ed.), Biohistory of Precious corals- Scientific, Cultural and Historical Perspectives. Tokai University Press, Tokai, Japan.
- Maté, P., Revenge, S., Masso, C., 1986. Estudio preliminar de la composición química del coral rojo (*Corallium rubrum* L.) de distintas zonas del Mediterráneo Español. Bol. Inst. Esp. Oceanogr. 3, 53–60.
- Mitsuguchi, T., Matsumoto, E., Abe, O., Uchida, T., Isdale, P.J., 1996. Mg/Ca thermometry in coral skeletons. Science 274(5289), 961.
- Mitsuguchi, T., Matsumoto, E., Uchida, T., 2003. Mg/Ca and Sr/Ca ratios of porites coral skeleton: Evaluation of the effect of skeletal growth rate. Coral Reefs 22(4), 381-388.
- Mitsuguchi, T., Uchida, T., Matsumoto, E., Isdale, P.J., Kawana, T., 2001. Variations in Mg/Ca, Na/Ca, and Sr/Ca ratios of coral skeletons with chemical treatments: Implications for carbonate geochemistry. Geochim. Cosmochim. Acta 65(17), 2865-2874.
- Nonaka, M., Muzik, K., Uchida, S., 2004. Capture, study and display of precious corals,

- 10<sup>th</sup> International Coral Reef Symposium, Okinawa, Japan, pp. 38-42.
- Seki, K., 1991. Study of precious coral diver survey with open circuit air SCUBA diving at 108 m. *Ann. Physiol. Anthropol.* 10(3), 189-192.
- Shen, G.T., Boyle, E.A., 1988. Determination of lead, cadmium and other trace metals in annually-banded corals. *Chem. Geol.* 67(1-2), 47-62.
- Tsounis, G., Rossi, S., Grigg, R., Santangelo, G., Bramanti, L., Gili, J.M., 2010. The exploitation and conservation of precious corals. *Ocean. Mar. Biol.* 48, 161-212.
- Velimirov, B., Böhm, E., 1976. Calcium and magnesium carbonate concentrations in different growth regions of gorgonians. *Mar. Biol.* 35(3), 269-275.
- Vielzeuf, D., Garrabou, J., Baronnet, A., Grauby, O., Marschal, C., 2008. Nano to macroscale biomineral architecture of red coral (*Corallium rubrum*). *Am. Mineral.* 93(11-12), 1799-1815.
- Weber, J.N., 1973. Incorporation of strontium into reef coral skeletal carbonate. *Geochim. Cosmochim. Acta* 37(9), 2173-2190.
- Weber, J.N., Woodhead, P.M.J., 1970. Carbon and oxygen isotope fractionation in the skeletal carbonate of reef-building corals. *Chem. Geol.* 6, 93-117.
- Weinbauer, M.G., Brandstatter, F., Velimirov, B., 2000. On the potential use of magnesium and strontium concentrations as ecological indicators in the calcite skeleton of the red coral (*Corallium rubrum*). *Mar. Biol.* 137(5), 801-809.
- Weinbauer, M.G., Velimirov, B., 1995. Calcium, magnesium and strontium

concentrations in the calcite sclerites of Mediterranean gorgonians (Coelenterata: Octocorallia). *Estuar. Coast. Shelf Sci.* 40(1), 87-104.

# CHAPTER 5

## RESULTS AND DISCUSSION

### DISTRIBUTION OF TRACE ELEMENTS IN JAPANESE RED CORAL (*Paracorallium japonicum*) BY $\mu$ -XRF AND SULFUR SPECIATION BY XANES: LINKAGE BETWEEN TRACE ELEMENT DISTRIBUTION AND GROWTH RING FORMATION

#### 5.1 INTRODUCTION

Corals of the genus *Corallium* and *Paracorallium* (Subclass Octocorallia; Order Alcyonacea; Family Coralliidae) have been considered as precious corals because

of their use in jewelry, medicine, and for fabricating other valuable products (Tsounis *et al.*, 2010a). The precious corals (PCs) have been harvested from the Mediterranean sea for many years (Grigg, 1975), and have attracted interest of traders and consumers worldwide. In Japan, the PC fishery began in Kochi during the 19<sup>th</sup> century (Kosuge, 1993), and expanded in the areas of Kochi, Kagoshima, and Ryukyu Archipelago in recent years. Therefore, compared to PCs of other geographical origin, little is known about the biochemical compositions of Japanese precious corals (JPCs).

The growth rings along the thin cross section (CS; about 100 – 120  $\mu\text{m}$ ) of JPCs skeleton reveal that the growth rate of this corals is very slow (few  $\mu\text{m}$  in diameter per year) (Hasegawa and Yamada, 2010; Luan *et al.*, 2013). It is well established that the mineralised hard tissues of PCs are the composite structure of inorganic and organic components (Kobayashi and Samata, 2006; Robach *et al.*, 2006), and calcium carbonate ( $\text{CaCO}_3$ ) is the main constituent of the skeletal axis and the spicules of PCs (Hasegawa and Iwasaki, 2010). Trace elements are also important constituents of coral skeleton which can be used as indicators of the origin and habitat of the PCs (Hasegawa *et al.*, 2012). The geochemical and isotopic data derived from the coral skeleton may also improve our understanding of past environmental conditions of the aquatic systems (Roark *et al.*, 2006a).

Paleoenvironmental studies using cutting-edge instruments and technologies have recently been employed in order to obtain authentic data of past environmental conditions from biochemical compositions of the coral skeleton. For example, micro X-ray fluorescence ( $\mu\text{-XRF}$ ) (Weinbauer *et al.*, 2000; Hasegawa *et al.*, 2010) and electron-probe X-ray microanalysis (EPMA) (Vielzeuf *et al.*, 2008; Hasegawa *et al.*, 2012) were used to explore chemical compositions of red coral (*Corallium rubrum*).

The results showed that the magnesium (Mg) and strontium (Sr) distributions in calcite skeleton of *C. rubrum* can be used as the paleoenvironmental indicator of the coral habitat (Weinbauer *et al.*, 2000). The variations of Mg/calcium (Ca) and Sr/Ca ratios in Mediterranean corals were found to be related to water depth. A direct relationship between Mg concentration in coral skeleton and water temperature was observed, and the Mg/Ca ratio increased substantially with the ambient water temperature (Weinbauer and Vellmirov, 1995). Bond *et al.* (2005) used secondary ion mass spectrometry (SIMS) ion microprobe to analyze trace elements in the skeleton of a shallow water gorgonian, *Plexaurella dichotoma*, and found a positive correlation between Mg/Ca ratio and annual sea surface temperature suggesting that Mg calcite in the coral skeleton can be potential for paleothermometry. Hasegawa *et al.* (2012) studied the trace element concentrations in the skeletons of *Corallium* spp. from different locations of the Mediterranean Sea (off Italy) and Pacific Oceans (off Japan and off Midway Island) using EPMA and found that the trace elements were attributable to their habitat and origin. This study also showed that trace elements in the coral skeletons can be used as ecological indicator of the corals, and are expected to play an important part in the cultural study and sustainable management of PCs. A negative correlation between Mg concentration and organic matrix (OM) content in the skeleton of Japanese white coral (*Corallium konojoi*) using ICP-AES and EPMA mapping indicates that Mg concentration corresponds to the annual growth rings (AGRs) of the coral (Hasegawa and Iwasaki, 2010; Hasegawa *et al.*, 2012).

Several studies have reported the biochemical compositions of AGRs of a wide range of PCs from divers origin (Grigg, 1984; Kaczorowska *et al.*, 2003; Marschal *et al.*, 2004; Debreuil *et al.*, 2011b). Using EPMA system, Vielzeuf *et al.* (2008) found a

negative correlation between Mg concentrations and OM in Mediterranean red coral (*C. rubrum*), except the central part of the skeleton, indicating that Mg distribution corresponded to the AGRs. In a recent study, we reported that Ca and Mg are the major constituents of the skeleton of Japanese white coral (*C. konojoi*), and Ca is distributed homogeneously, while Mg is distributed concentrically forming growth rings (Hasegawa *et al.*, 2012). However, little is known about the distribution of trace elements in axial skeletons of other JPCs.

Beside this, sulfur (S) is considered as a minor element in the skeleton of red corals of a wide range of taxa (Grillo *et al.*, 1993; Dauphin and Cuif, 1999; Cuif *et al.*, 2003). XANES technique has been widely used for determining the local geometric and/or electronic structure of matter (Tamenori *et al.*, 2011). Since the core electrons are localized around the atoms to which they originally belonged, X-ray core-electron transitions allow investigating the chemical properties of specific elements in complex materials, and provides information about the geometric arrangement of the elements of interest. Using XANES system, Cuif *et al.* (2003) examined the S chemical speciation and the localization of organic sulfate in three scleractinian coral skeletons. They reported that the sulfated form (S-sulfate) extremely dominants in coral aragonite, and mapping of S-sulfate in centres and fibres provides direct evidence of high concentration of organic sulfate in the centres of calcification tissues of the coral skeleton. However, there is no report on the speciation and localization of organic S molecules along the AGRs of *P. japonicum*.

## 5.2. FOCUS

In the present study, we investigated the distribution of Mg, P, Sr, and S in the axial skeleton of *P. japonicum* using  $\mu$ -XRF mapping analysis. Furthermore, we determine the S chemical state and localization along the axial skeleton of *P. japonicum* using XANES system and have examined the linkage between the distribution pattern of trace elements and the formation of AGRs along the coral skeleton.

## 5.3. MATERIALS AND METHODS

### 5.3.1. Sample collection and preparation

Two colonies of *P. japonicum*, colony 1 (DPC-18) and colony 2 (DPC-19), were collected from 207 and 212 m depth, respectively, near the Amami Islands, Kagoshima Prefecture, Japan (28° 16.894' N, 129° 46.03'W) on March 08, 2009. The samples were then dried at room temperature ( $25 \pm 2$  °C).

One to three mm thick CSs of the coral skeleton of each colony were made using a NSK Elector Emax (NE 129, Nakanishi Inc. Japan) at different points from the tip to the bottom of the skeleton. The CSs were embedded and coated in epoxy resin that provides a protective cover for cutting, grinding, and polishing them. The CSs were then mounted on glass slides and polished with 1500 and 2000 SiC grid powder and 3M imperial polishing paper. The thin polished CSs (slabs) were then cleaned ultrasonically, rinsed in 100% ethanol, and dried at room temperature ( $25 \pm 2$  °C). Polished surface of the slabs were kept free from dust prior to examine under the VHX-1000 digital microscope (Keyence, Japan). Two clear CSs from the DPC-18 and DPC-19 were

slected for  $\mu$ -XRF and XANES analysis. Copper rings of one mm diameter were used to fix two positions on the slab of DPC-19 in order to determine the distribution of trace elements using  $\mu$ -XRF system. For XANES analysis, the coral skeleton was grinded in an agate mortar and then the powder was sprayed on conductive double-sided carbon adhesive tape using industrial cotton swabs.

### 5.3.2 Extraction of organic matrix from fraction

In order to separate the OM from the mineral fraction, procedures were adapted from (Debreuil *et al.*, 2011a). A 5.21 g sample (tip of the axial skeleton) of DPC-19 was soaked in 30 mL of 0.25 M ethylenediaminetetraacetic acid (EDTA; Kanto Chemicals Co. Japan) solution (pH 7.8) for 48-72 h at 4 °C in order to demineralize the calcium carbonate. After mineralization, the soluble OM was washed with deionized (DI) water (using an E-pure system, Barnstead). The soluble OM was then dried at 25 °C and was subjected to XANES analysis.

### 5.3.3 $\mu$ -XRF and XANES analysis

$\mu$ -XRF and XANES analysis were carried out at the b-branch of the soft X-ray photochemistry beam line (BL27SU) at the SPring-8, Japan. The radiation from the undulator was monochromatized by using a double crystal Si(111) monochromator ensuring an energy resolution of 350 meV. Photon flux on the sample was  $1 \times 10^{11}$  Ph/s at 2500 eV. The Kirkpatrick-Baez (K-B) mirror focused the photon beam on the sample, and the horizontal and vertical beam size at focus point were 16.3 and 13.7  $\mu$ m, respectively. For the  $\mu$ -XRF analysis, full XRF data were obtained at each mapping point, and the elemental imaging data were extracted from the XRF data set. For  $\mu$ -XRF

mapping measurements, the polished sample (slab) was fixed on an aluminium sample holder by carbon tape which was then installed in a vacuum chamber ( $10^{-1}$ Pa) and fixed on a motorized XYZ stages. The  $\mu$ -XRF measurements were taken at an excitation photon energy of 2481.3 eV along transect from the inner shell layer at 10  $\mu$ m intervals with an acquisition time of 5 s.

For XANES measurements, all samples were powdered to ensure that sample orientation and inhomogeneity did not influence the results. Powdered samples were fixed with conductive double-sided carbon tape onto a sample holder and the sample holder was fixed on a linear and rotatable manipulator and installed in an analysis chamber. Spectra were recorded by partial-fluorescence yield (PFY) method by using a silicon drift detector (SDD) (Tamenori *et al.*, 2011). The SDD was mounted perpendicularly to the axis of the incident photon beam. Monochromatic light was irradiated at an angle of about  $80^\circ$  to the sample normal to minimize contamination by elastic scattering.

## 5.4. RESULTS AND DISCUSSION

### 5.4.1. $\mu$ -XRF analysis for trace element distribution in Japanese red coral skeleton

Figure 5.1 showed  $\mu$ -XRF spectrums of trace elements in powdered skeletal sample of DPC-19 measured at 2500 eV photon energy. In the present measurement, we were unable to distinguish the  $\mu$ -XRF signals of C  $K\alpha$  and Ca  $L\alpha$  due to insufficient energy resolution of SDD detector.  $\text{CaCO}_3$  is the main component in the skeleton of PCs (Hasegawa and Iwasaki, 2010; Hasegawa *et al.*, 2012), however, in the present study  $\mu$ -XRF signals of C, Ca, and O were found to be much weaker than those of other major

trace elements (Fig. 5.1). This might be because – (i) the fluorescence deterioration probability following the inner-shell electron excitation was low, and (ii) the X-ray transmission of X-ray window attached to the SDD steeply decreased in the lower photon energy region. For example, the transmission of 2500 eV (S  $K\alpha$ ) was > 70%, while it was about 47% for 300 eV (C  $K\alpha$ ). Furthermore, in the present study, we have obtained XRF data in the vicinity of sulfur K-edge region. Therefore, the intensity of sulfur was higher than that of other trace elements, and it does not reflect the concentrations of the trace elements.

The highest XRF spectrums were observed for S  $K\alpha$  followed by Mg  $K\alpha$ , and Sr  $La\beta$  (Fig. 5.1). [Hasegawa, et al. \(2012\)](#) also reported the distribution of Mg and Sr in the skeleton of Japanese white coral (*C. konojoi*) by EPMA analysis. The incorporation of Mg and Sr in carbonate minerals can be explained by the displacement of Ca by Mg or Sr, as reported by [Hasegawa, et al. \(2012\)](#). In addition to these trace elements, the present study confirms the incorporation of Na and P in carbonate mineral of *P. japonicum* skeleton (Fig. 5.1). Although [Hasegawa et al.\(2010\)](#) reported the distribution of Ba, Mo, and I in the skeleton of *C. konojoi* using XRF analysis, these elements were not observed in the skeleton of *P. japonicum* in the present study. This may be due to the fact that the concentrations of these elements were lower than the detection limit of our system.

The trend of trace element distribution in the axial skeleton of *P. japonicum* was also determined in the present study by  $\mu$ -XRF (Fig. 5.2). The contrasting peaks of Mg and S in the  $\mu$ -XRF spectrums (Fig. 5.2C) indicate a negative correlation between the Mg and S distributions in the skeleton. On the other hand, peaks of P and S in the  $\mu$ -XRF spectrums showed a matching pattern (Fig. 5.2D) indicating a positive

correlation between their distribution in the skeleton of *P. japonicum*. Two-dimensional  $\mu$ -XRF mapping images (Figs. 5.3 and 5.4) can also explain the distribution pattern of Mg and S in the coral skeleton. Pearson correlation coefficient analysis of  $\mu$ -XRF two-dimensional mapping data showed a strong positive correlation ( $r = 0.6$ ) between P and S, while a relatively weak negative correlation ( $r = -0.2$ ) was observed between Mg and S in the coral skeleton (Fig. 5.4). A negative correlation between Mg and S in calcite shells was reported by [England et al. \(2007\)](#) that elucidates the relationship between the OM and the Mg distribution in the shells.

Assuming that every peak of Mg, P and S in  $\mu$ -XRF spectrum (Fig. 5.2B) was formed annually, we can estimate growth rates of *P. japonicum* based on the number of peaks and diameter of the skeleton. For example, the  $\mu$ -XRF spectrum of Mg and S showed 27 peaks within 7 mm of diameter, indicating a growth rate of 0.26 mm per year for *P. japonicum* (DPC-19). This growth rate of DPC-19 is similar (range 0.23 – 0.28 mm per year) to that of the same coral calculated based on the petrographic method using high resolution VHX-1000 digital microscope ([Luan et al., 2013](#)). Variation in the distribution of certain elements, particularly Mg, in the skeleton may also provide information about the paleoenvironmental conditions of the coral habitat. For example, [Bond et al. \(2005\)](#) observed a positive correlation between Mg/Ca ratio in calcite skeleton of *Plexaurella dichotoma* and water temperature of the habitat. Weinbauer and [Velimirov \(1995\)](#) reported that Mg/Ca ratio in the skeleton of Mediterranean *C. rubrum* decreased substantially with depth of the coral habitat, indicating a dependency of Mg/Ca ratio with water depth. [Hasegawa et al. \(2012\)](#) also found the Mg/Ca ratio in the skeleton of different PC species of diverse origin to be habitat specific.

### 5.4.2 Distribution of trace elements and the formation of annual growth rings

Spatial distribution of Mg and S in the skeleton of *P. japonicum* (DPC-18) using  $\mu$ -XRF is shown in Figure 5.3. Different colors in the maps reflect the varied distribution of the elements. For instance, blue and red color correspond to lower and higher distributions, while the black and red color regions in the maps indicate the lowest and highest distribution, respectively, of Mg and S. The two-dimensional maps of Mg and S distribution (Fig. 5.3C) clearly illustrate a contrasting correlation between these two elements.

$\mu$ -XRF mapping images of axial skeleton of *P. japonicum* (DPC-19) in Figure 5.4 show the spatial distribution of Mg, S, P and Sr. The distribution pattern of trace elements can be explained by the formation of growth bands in AGRs along the coral skeleton. The AGRs of PCs is characterised by growth band consisting of two layers, one is thick light color and the other is thin dark color (Marschal *et al.*, 2004). It has been reported that the dark color band indicate the high OM zone, while the light color band indicate the low OM zone in the coral skeleton (Luan *et al.*, 2013). In the present study, dark and light color growth bands in the microscopic image of the coral skeleton (Figs. 5.4A, E) seems to be linked with the distribution patterns of S, Mg and P in the  $\mu$ -XRF mapping images of the skeleton (Figs. 5.4B, C, D, G, and H). The dark band/region in the microscopic image of the coral skeleton (Fig. 5.4A) corresponds to the high S and P region in the  $\mu$ -XRF mapping images (Figs. 5.4D, B) indicating that the OM-rich dark growth bands in JPC skeleton may contain S and P. Previous studies have also reported high concentration of S in OM of carbonate shells of marine bivalve mollusc (Lorens and Bender, 1980; Putten *et al.*, 2000), while the S has been reported to be a minor element in the skeleton of the red coral (*C. rubrum*) of Mediterranean origin

(Maté *et al.*, 1986a; Grillo *et al.*, 1993).

Light growth bands in the microscopic image of axial skeleton of *P. japonicum* (DPC-19) (Fig. 5.4E) correspond to the area of Mg map in the XRF image (Fig. 5.4C) of the coral skeleton. From a negative correlation between Mg concentration and OM content in axial skeleton of Mediterranean red coral *C. rubrum*, Vielzeuf *et al.* (2008) suggested that Mg corresponds to light bands of the AGRs, which is in agreement with the present study. The present study also reveals that, in addition to Mg, S and P are important elements in growth bands in *P. japonicum* (DPC-19), and the chemical composition of dark growth bands differ for the origin and habitat of PCs. The formation and arrangement of growth bands in PC skeleton is assumed to demonstrate the annual periodicity of active and inactive growth (Marschal *et al.*, 2004) as well as the seasonality of the key environmental factors (e.g., temperature, trophic content) (Coma *et al.*, 2000). Trace element distributions, particularly the S, P and Mg, and their linkage with the formation of AGRs (dark and light bands) in the axial skeleton of *P. japonicum* can be potential archives of past environmental conditions.

An instinct dark band around the central growing part of the skeleton indicates high deposition of OM in the first growth ring. Since the development of the first growth ring in the PC skeleton has been estimated to be about 3-4 years (Marschal *et al.*, 2004), the dark OM-rich growth ring around the central growing part of the skeleton of *P. japonicum* is assumed to respond the lowest growth rate. Thus, trace element distribution may also explain the growth characteristic of Japanese PCs. Strontium was observed to be distributed homogenously across the CS of the axial skeleton of *P. japonicum* (Fig. 5.4f). Hasegawa *et al.* (2010; 2012) also reported homogenous distribution of Sr in the skeleton of *C. konojoi*.

### 5.4.3 Speciation of S in Japanese red coral using XANES

The characterization of S in the *P. japonicum* (DPC-19) skeleton was studied using XANES fluorescence. XANES spectra were recorded from six reference S-bearing organic molecules (Yoshimura *et al.*, 2013): two amino acids (H-S-C bonds in cysteine and C-S-C bonds in methionine), two sulfated sugars (chondroitin and protamine), saccharine, and gypsum (Fig. 5.5A). The amino acids (cysteine and methionine) spectra displayed a single peak at 2472.5 eV, while each of the two sulfated sugars (protamine and chondroitin) and gypsum exhibited similar peak at 2482 eV. Saccharine showed a peak at 2478 eV.

OM extracted from the *P. japonicum* (DPC-19) showed a main peak at 2472 eV and 2 minor peaks at 2475.8 and 2480 eV (Fig. 5.5A). The energy position of the main peak was similar to that of the two amino acids. The feature at an energy of 2475.8 eV in the S K-edge XANES spectra provide indirect evidence for the presence of S-H bonds, which allows to detect S-H bonds in a “C-S-H environment” typical for biological samples (Prange *et al.*, 2002). XANES spectra of the *P. japonicum* (DPC-19) skeleton also showed a major peak at 2482 eV, which is similar to that of the two sulfated sugars (protamine and chondroitin) and gypsum. Disappearance of sulphate peak in the XANES spectrum of OM strongly suggests that the sulphate may not be a macro organic molecule in the coral skeleton as protamine is. Therefore, it can be conclude that the major S species in the *P. japonicum* (DPC-19) is inorganic sulphate ( $\text{SO}_4^{2-}$ ), which concurs with the result of Cuif *et al.* (2003) for scleractinian coral skeleton. Using XANES, Cusack *et al.* (2008) also reported that shells of *Terebratulina retusa* (benthic lamp shell) contain S as sulfur-containing amino acids as well as

sulphate, and the present XANES mapping analysis of the S K-edge at 2482.6 eV revealed that the S was mainly inorganic sulphate.

XANES spectra of *P. japonicum* (DPC-19) skeleton also showed a minor peak at 2472.2 eV, which was very close to the main peak of OM and two amino acids cysteine and methionine (Fig. 5.5A). The intensity of the minor peak was very small (about 0.5) compared to that of the main peak (about 9.0) in the skeleton (Fig. 5.5B) indicating very little amount of organic sulphate with a ratio of 1:20 for organic and inorganic sulphate in the skeleton of *P. japonicum* (DPC-19). Previous studies also reported the presence of organic molecules (proteins and sugars including sulfated sugars) in both axis and spicules of the Mediterranean red coral (*C. rubrum*) (Allemand *et al.*, 1994), however, the mean protein content of the soluble OM obtained from dry mass of powdered skeleton of *Corallium* spp. is very low (about 0.01%) (Debreuil *et al.*, 2011b).

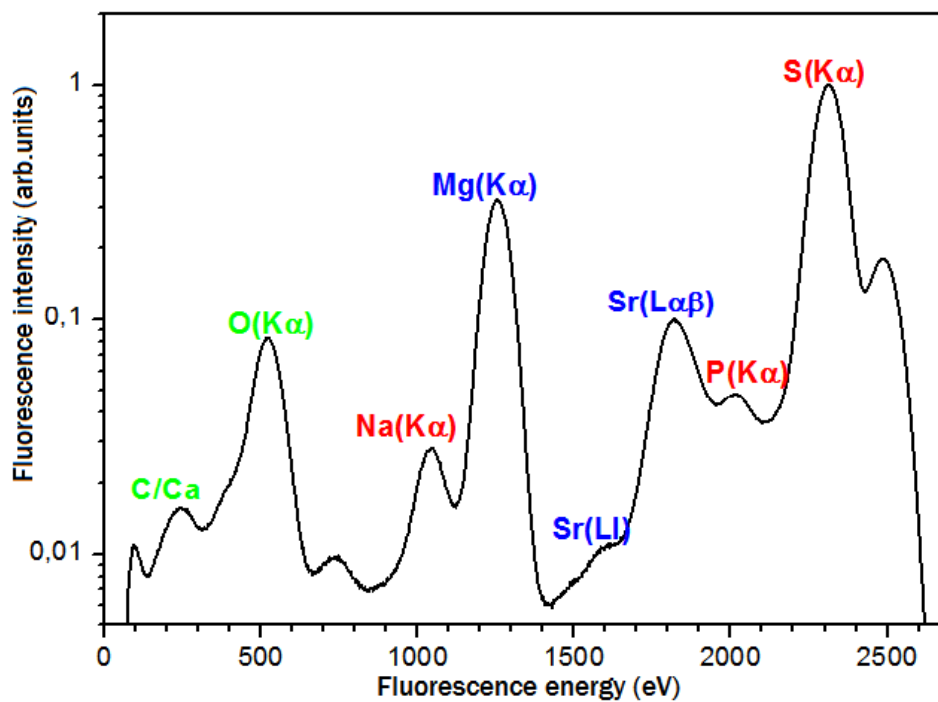


**Fig. 5.1:** X-ray fluorescence spectrum of trace elements (Na, S, P, Mg and Sr) in powdered sample of Japanese red coral (DPC-19) skeleton measured at 2500 eV of excitation photon energy.

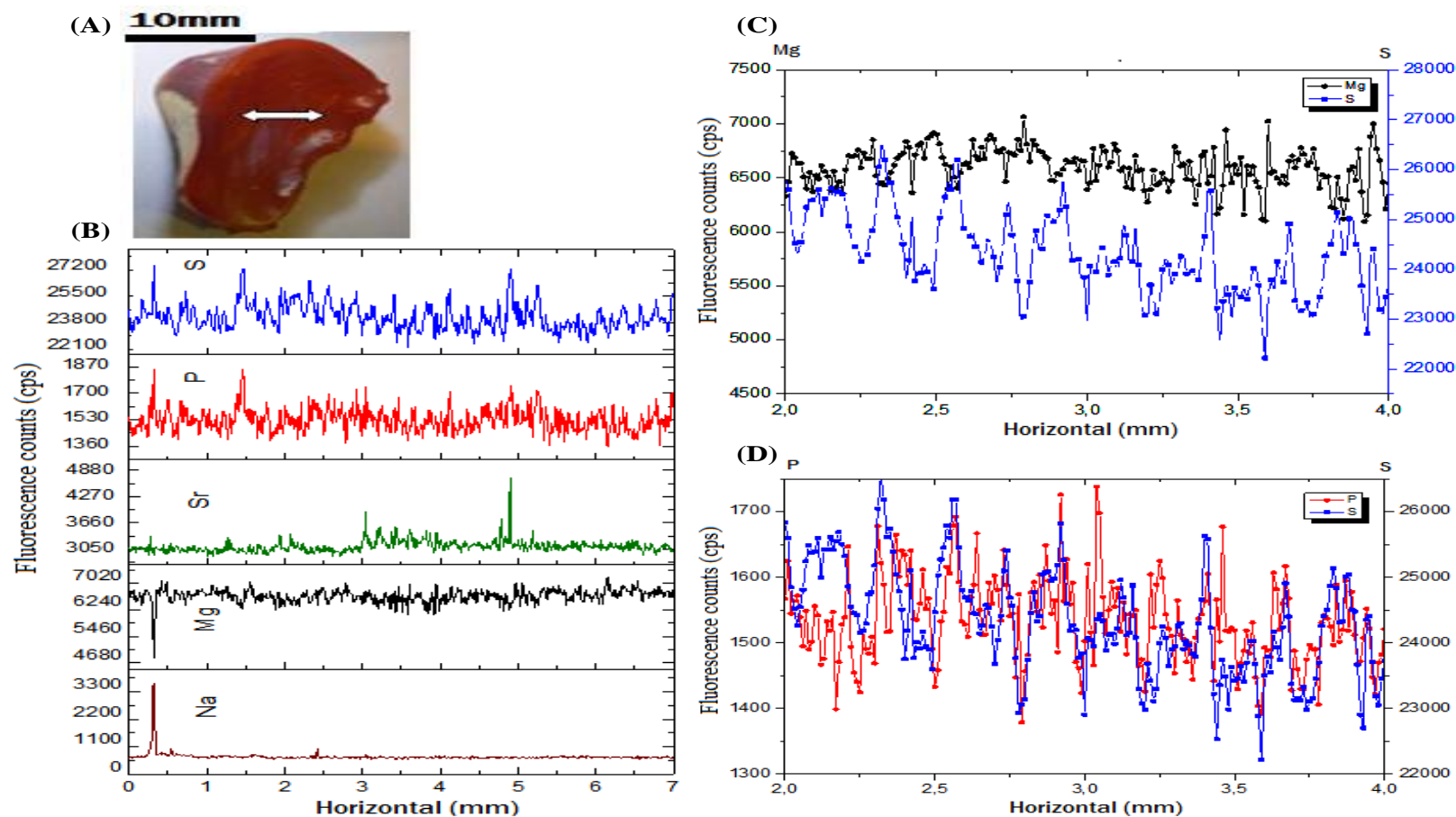


**Fig. 5.2:** X-ray fluorescence spectrum of trace elements (Na, S, P, Mg and Sr) in Japanese red coral skeleton (DPC-19) using 2500 eV energy, 5s/point measuring time, and 10  $\mu$ m step size. White arrow (7 mm) is the position from where the section was taken for  $\mu$ -XRF analysis (A). Trace element spectrum in the sample (B). Relationship between the distributions of S and Mg (C) and S and P (D) in the skeleton of DPC-19

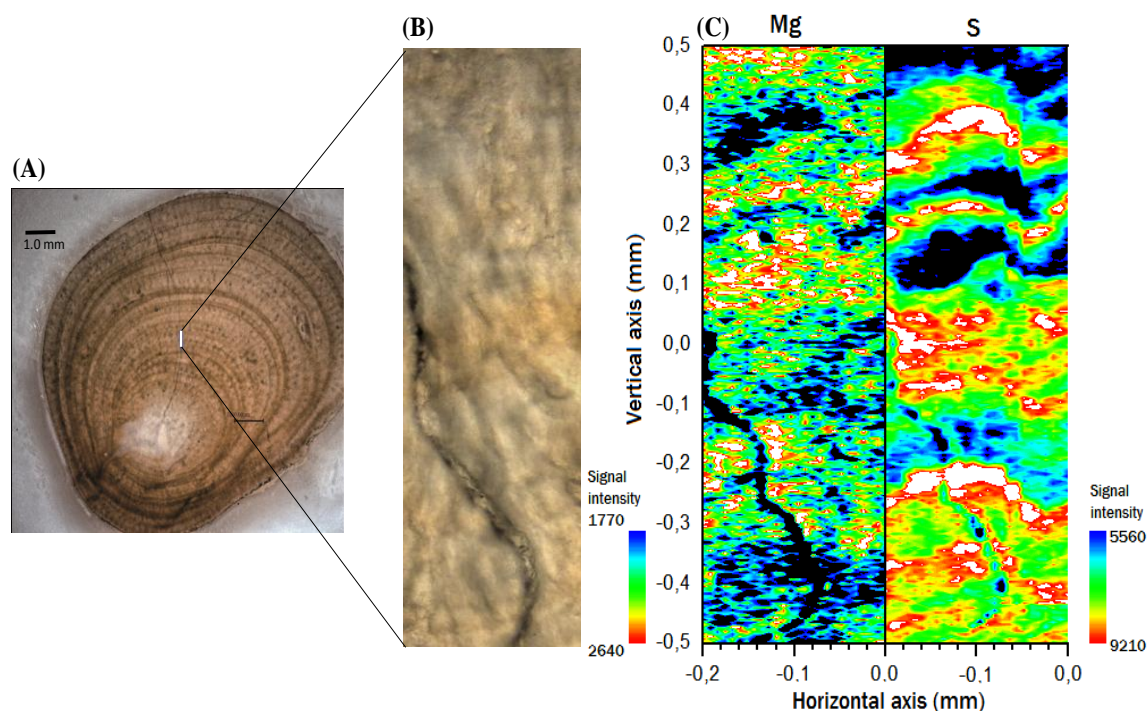


**Fig. 5.3:** Micro-XRF mapping analysis of Mg and S in axial skeleton of Japanese red coral (DPC-18). Cross section of DPC-18 skeleton showing the position where the  $\mu$ -XRF analysis was performed (a). The magnification of the region of  $\mu$ -XRF analysis (b). Distribution maps of Mg and S in the skeleton of the coral (c). The colour bar represents the signal intensity with the blue and red color correspond to lower and higher distributions, and the black and red color regions in the maps indicate the lowest and highest distribution of the elements, respectively. Micro-XRF signal was collected at 10  $\mu$ m step size

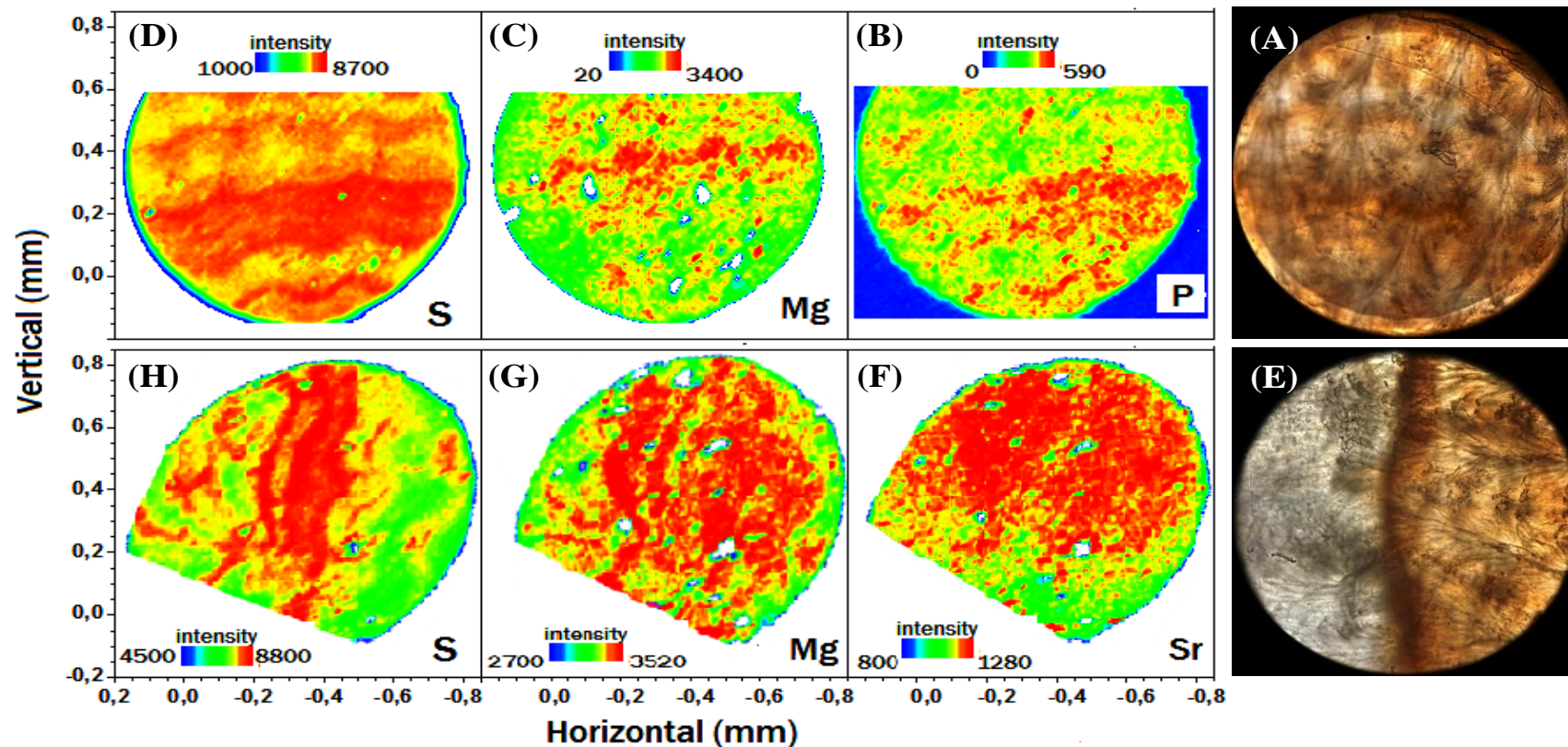


**Fig. 5.4:** Micro-XRF mapping analysis of trace elements in polished cross section of Japanese red coral skeleton (DPC-19). Two copper rings of one mm diameter were used to select two positions on the cross section of the coral skeleton where the distribution of trace elements were detected. The colour bars represent the signal intensity with the blue and red color correspond to lower and higher distributions, and the black and red color regions in the maps indicate the lowest and highest distribution of the elements, respectively. Micro-XRF signal was collected at 10  $\mu\text{m}$  step size

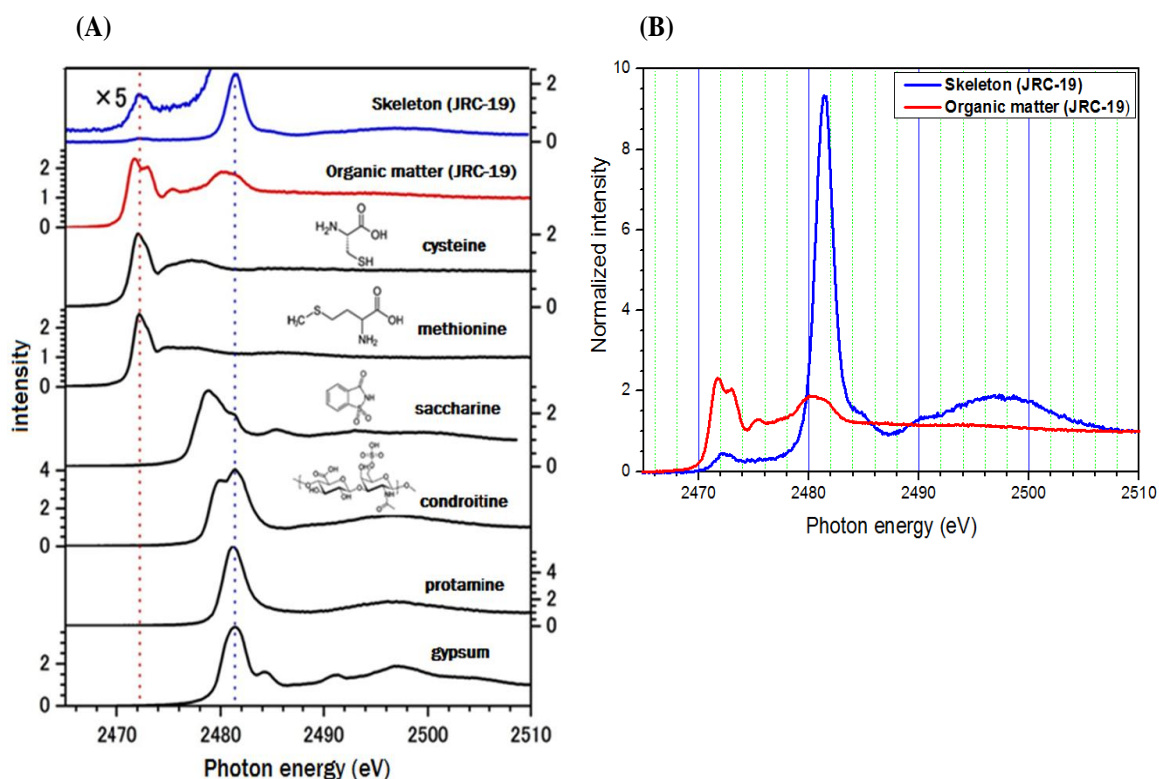


**Fig. 5.5:** XANES spectra of sulfur (S) in axial skeleton and organic matter extract of DPC-19. XANES spectra of S reference compounds (A). Each of the cysteine and methionine spectra display a single peak at 2473 eV photon energy, while chondroitine, protamine, and gypsum show peaks at 2482 eV photon energy. Saccharine exhibits a single peak at 2477.5 eV photon energy. Magnified view ( $\times 5$ ) of XANES spectra of S in axial skeleton and organic matter of DPC-19 (B) showing that sulfate is the main species of S and organic matter content in the DPC-19 skeleton is very low.

## REFERENCES

- Allemand, D., Cuif, J.P., Watabe, N., Oishi, M., Kawaguchi, T., (1994). The organic matrix of skeletal structures of the Mediterranean red coral, *Corallium rubrum*. *Bull. Inst. Oceanogr.* **14**, 129-139.
- Bond, Z.A., Cohen, A.L., Smith, S.R., Jenkins, W.J., (2005). Growth and composition of high-Mg calcite in the skeleton of a Bermudian gorgonian (*Plexaurella dichotoma*): Potential for paleothermometry. *Geochem. Geophys. Geosys.* **6**, 1-10.
- Coma, R., Ribes, M., Gili, J.-M., Zabala, M., (2000). Seasonality in coastal benthic ecosystems. *Trends Ecol. Evol.* **15**, 448-453.
- Cuif, J.-P., Dauphin, Y., Doucet, J., Salome, M., Susini, J., (2003). XANES mapping of organic sulfate in three scleractinian coral skeletons. *Geochim. Cosmochim. Acta* **67**, 75-83.
- Cusack, M., Dauphin, Y., Cuif, J.-P., Salomé, M., Freer, A., Yin, H., (2008). Micro-XANES mapping of sulphur and its association with magnesium and phosphorus in the shell of the brachiopod, *Terebratulina retusa*. *Chem. Geol.* **253**, 172-179.
- Dauphin, Y., Cuif, J.-P., (1999). Relationship between mineralogy and microstructural patterns of calcareous biominerals and their sulfur contents. *Annales des Sciences Naturelles - Zoologie et Biologie Animale* **20**, 73-85.
- Debreuil, J., Tambutté, S., Zoccola, D., Segonds, N., Techer, N., Allemand, D.,

- Tambut ,  ., (2011a). Comparative analysis of the soluble organic matrix of axial skeleton and sclerites of *Corallium rubrum*: Insights for biomineralization. *Comp. Biochem. Physiol., Part B: Biochem. Mol. Biol.* **159**, 40-48.
- Debreuil, J., Tambut , S., Zoccola, D., Segonds, N., Techer, N., Marschal, C., Allemand, D., Kosuge, S., Tambut ,  ., (2011b). Specific organic matrix characteristics in skeletons of *Corallium* species. *Mar. Biol.* **158**, 2765-2774.
- England, J., Cusack, M., Lee, M.R., (2007). Magnesium and sulphur in the calcite shells of two brachiopods, *Terebratulina retusa* and *Novocrania anomala*. *Lethaia* **40**, 2-10.
- Grigg, R.W., 1975. The commercial potential of precious corals in the western Caroline Islands, Micronesia. Sea Grant Tech Rep UNIHI-SEAGRANT-AR-75-03, Hawaii University.
- Grigg, R.W., (1984). Resource Management of Precious Corals. *Mar. Ecol.* **5**, 57-74.
- Grillo, M.C., Goldberg, W.M., Allemand, D., (1993). Skeleton and sclerite formation in the precious red coral *Corallium rubrum*. *Mar. Biol.* **117**, 119-128.
- Hasegawa, H., Iwasaki, N., (2010). *Chemical analyses of carbonate skeletons in precious corals*, Biohistory of Precious corals.
- Hasegawa, H., Iwasaki, N., Suzuki, A., Maki, T., Hayakawa, S., (2010). Distribution of trace elements in biogenic carbonate minerals of precious corals by X-ray fluorescence analysis. *Bunseki Kagaku* **59**, 521-530.
- Hasegawa, H., Rahman, M.A., Luan, N.T., Maki, T., Iwasaki, N., (2012). Trace

- elements in *Corallium* spp. as indicators for origin and habitat. *J. Exp. Mar. Biol. Ecol.* **414-415**, 1-5.
- Hasegawa, H., Yamada, M., (2010). *Biology of precious coral*, in: Iwasaki, N. (Ed.), *Biohistory of Precious corals-Scientific, Cultural and Historical Perspective*. University Press, Tokai, Japan, pp. 43-60.
- Kaczorowska, B., Hacura, A., Kupka, T., Wrzalik, R., Talik, E., Pasterny, G., Matuszewska, A., (2003). Spectroscopic characterization of natural corals. *Anal. Bioanal. Chem.* **377**, 1032-1037.
- Kobayashi, I., Samata, T., (2006). Bivalve shell structure and organic matrix. *Mater. Sci. Eng., C* **26**, 692-698.
- Kosuge, S., (1993). History of the precious coral fisheries in Japan. *Precis. Coral. Octocor. Res.* **1**, 30-38.
- Lorens, R.B., Bender, M.L., (1980). The impact of solution chemistry on *Mytilus edulis* calcite and aragonite. *Geochim. Cosmochim. Acta* **44**, 1265-1278.
- Luan, N.T., Rahman, M.A., Maki, T., Iwasaki, N., Hasegawa, H., (2013). Growth characteristics and growth rate estimation of Japanese precious corals. *J. Exp. Mar. Biol. Ecol.* **441**, 117-125.
- Marschal, C., Garrabou, J., Harmelin, J.G., Pichon, M., (2004). A new method for measuring growth and age in the precious red coral *Corallium rubrum* (L.). *Coral Reef.* **23**, 423-432.
- Maté, P., Revenge, S., Masso, C., (1986). Estudio preliminar de la composicion quimica

- del coral rojo (*Corallium rubrum* L.) de distintas zonas del Mediterraneo Español. *Bol. Inst. Esp. Oceanogr.* **3**, 53-60.
- Prange, A., Dahl, C., Trüper, H.G., Behnke, M., Hahn, J., Modrow, H., Hormes, J., (2002). Investigation of S-H bonds in biologically important compounds by sulfur K-edge X-ray absorption spectroscopy. *Europ. Phys. J. D Atom. Molecul. Optic. Plasm. Phys.* **20**, 589-596.
- Putten, E.V., Dehairs, F., Keppens, E., Baeyens, W., (2000). High resolution distribution of trace elements in the calcite shell layer of modern *Mytilus edulis*: Environmental and biological controls. *Geochim. Cosmochim. Acta* **64**, 997-1011.
- Roark, E.B., Guilderson, T.P., Dunbar, R.B., Ingram, B.L., (2006). Radiocarbon-based ages and growth rates of Hawaiian deep-sea corals. *Mar. Ecol. Prog. Ser.* **327**, 1-14.
- Robach, J.S., Stock, S.R., Veis, A., (2006). Mapping of magnesium and of different protein fragments in sea urchin teeth via secondary ion mass spectroscopy. *J. Struct. Biol.* **155**, 87-95.
- Tamenori, Y., Morita, M., Nakamura, T., (2011). Two-dimensional approach to fluorescence yield XANES measurement using a silicon drift detector. *J. Sync. Rad.* **18**, 747-752.
- Tsounis, G., Rossi, S., Grigg, R., Santangelo, G., Bramanti, L., Gili, J.M., (2010). The exploitation and conservation of precious corals. *Ocean. Mar. Biol.* **48**, 161-212.
- Vielzeuf, D., Garrabou, J., Baronnet, A., Grauby, O., Marschal, C., (2008). Nano to macroscale biomineral architecture of red coral (*Corallium rubrum*). *Am. Mineral.*

93, 1799-1815.

Weinbauer, M.G., Brandstatter, F., Velimirov, B., (2000). On the potential use of magnesium and strontium concentrations as ecological indicators in the calcite skeleton of the red coral (*Corallium rubrum*). *Mar. Biol.* **137**, 801-809.

Weinbauer, M.G., Velimirov, B., (1995). Calcium, magnesium and strontium concentrations in the calcite sclerites of Mediterranean gorgonians (Coelenterata: Octocorallia). *Estuar. Coast. Shelf Sci.* **40**, 87-104.

Yoshimura, T., Tamenori, Y., Suzuki, A., Nakashima, R., Nozomu, I., Hasegawa, H., Kawahata, H., (2013). Element profile and chemical environment of sulfur in a giant clam shell: Insights from micro X-ray fluorescence and X-ray absorption near-edge structure. (*Personal communication*).

# CHAPTER 6

## CONCLUSION

In the chapter 3, Japanese precious corals are recognised as ecologically as well as economically important natural resources of Japan, and are characterised by slow growth rates compared to other precious corals of other geographical locations. Although Japanese red, pink, and white corals are not included in the list of endangered species in Japan, the red coral (*P. japonicum*) is considered to be at risk of declining in number. Authentic biological and ecological data such as growth characteristics, age and growth rate can be of great relevance for developing proper management and conservation plans for these valuable species. The present study showed that the widely employed OMS method would not be suitable for obtaining relevant biological and ecological data of Japanese precious corals probably due to the low concentration of

organic matrix in these corals. We propose that the non-destructive method (without acetic acid treatment and without staining the organic matrix by toluidine blue) using the high resolution VHX-1000 will be more suitable for studying Japanese precious corals.

In the chapter 4, Apart from Mg concentrations that vary slightly with annual rings, trace elements in precious coral skeletons are distributed homogeneously. Our study reveals that the trace elements in skeletons of precious corals are habitat-specific rather than species-specific. The Mg/Ca and Ba/Ca ratios in skeletons of precious corals, particularly, are the indicators of their habitats and environments and, therefore, can be used to identify the harvested areas of coral products. X-ray fluorescent analysis is another useful method that can serve to identify the bathymetrical and geographic origin of coral (and other) products.

The proposal to list all species in the family Corallidae in Appendix II of the *Convention on International Trade in Endangered Species of Wild Fauna and Flora* was rejected in the Conferences of the Parties (CoP) 14 (FAO, 2007) and CoP 15 (FAO, 2010). The difficulties in the identification of coral products in trade have been highlighted in the debate about the feasibility to enforce such a listing effectively. Identification of raw coral to species level is easy to the coral specialists, and a taxonomic reference guide has been recently published by World Wildlife Fund Canada (WWF Canada) to help customs officials to identify raw coral to species level, however, it is likely that identification might not be possible when coral products such as jewelries of *Corallium* sp. and of other species that are resembled to *Corallium* sp. after dying (FAO, 2007, 2010). The findings of the present study would guide to a possible solution to this problem, and would contribute in developing a nondestructive analytical method,

such as XRF, for the identification of raw corals as well as coral products. Further research is necessary to develop a fully functional, cost-effective and readily applicable method.

In the chapter 5, Using  $\mu$ -XRF mapping analysis showed the spatial distribution of trace elements (S, P, Mg, and Sr) in the skeleton of *P. japonicum*. The distribution pattern of the trace elements, particularly Mg, S and P, illustrates linkage between the trace element distribution and the formation of growth bands in the coral skeleton. The dark band in the microscopic image of *P. japonicum* skeleton corresponds to the high S and P regions in the  $\mu$ -XRF mapping images. This observation confirms that, in addition to Mg, the dark bands in the AGRs along the skeleton of *P. japonicum* contained S and P. Furthermore, XANES analysis showed that, compared to organic sulphate ( $\text{SO}_4^{2-}$ ), inorganic sulphate is the major S species in the skeleton of *P. japonicum* with a ratio of 1:20 for organic and inorganic sulphate. The present study will contribute in enhancing our understanding of biochemistry as well as the accumulation and distribution of trace elements in the skeleton of JPCs, and will provide important information about the past environmental conditions of the marine systems.

# Appendix

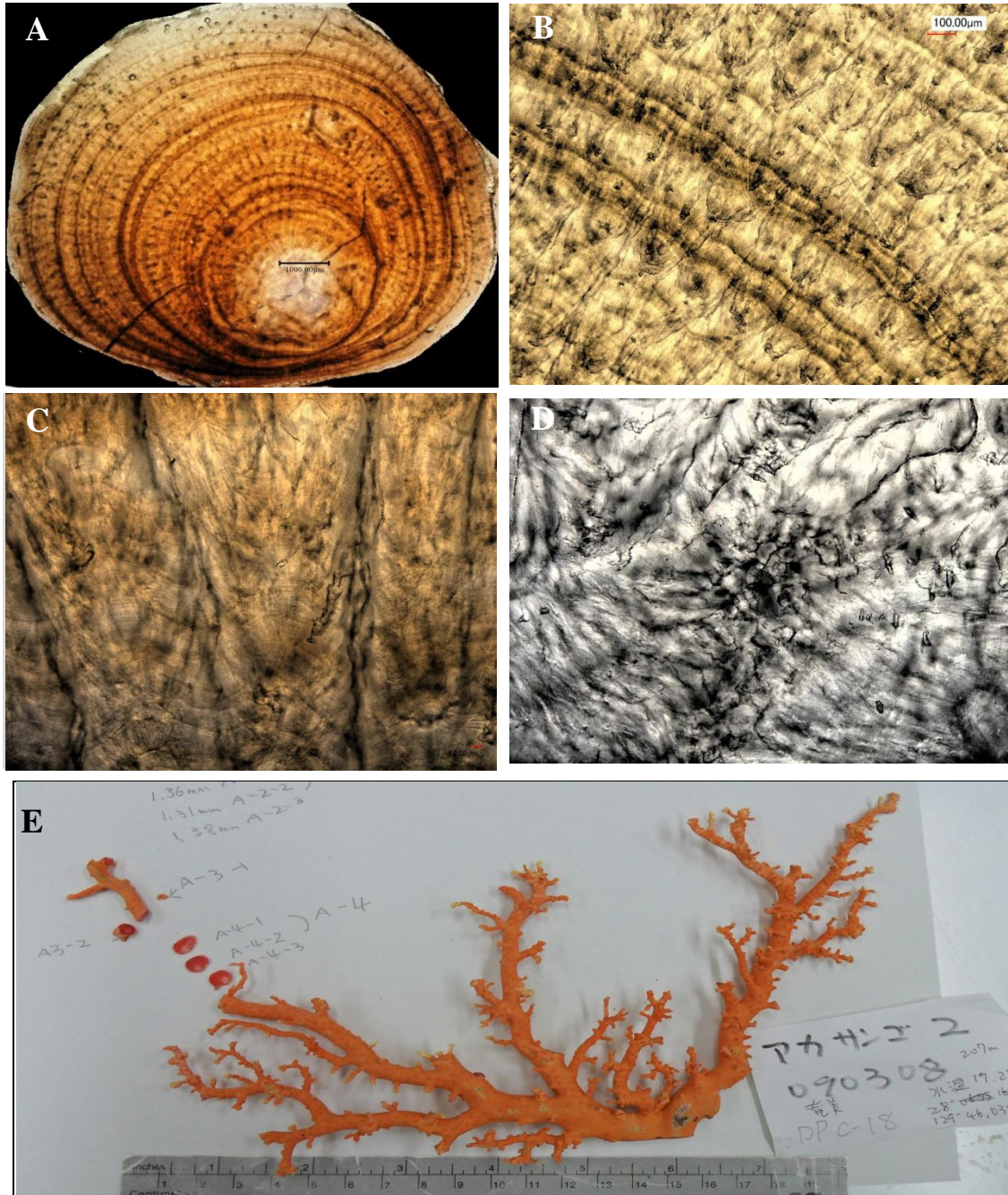


**Fig. A1.** (A): a thin cross-section of the axial skeleton of Japanese red corals (DPC-18) under the VHX-1000 digital microscope. (B): the wide of growth band of skeleton is not similar. (C) and (D): growth rings display wavelets and the structure of center medullar zone is complex, respectively. (E): Cross sections were cut from axial skeleton of Japanese red coral *Paracorallium japonicum* (DPC-18).

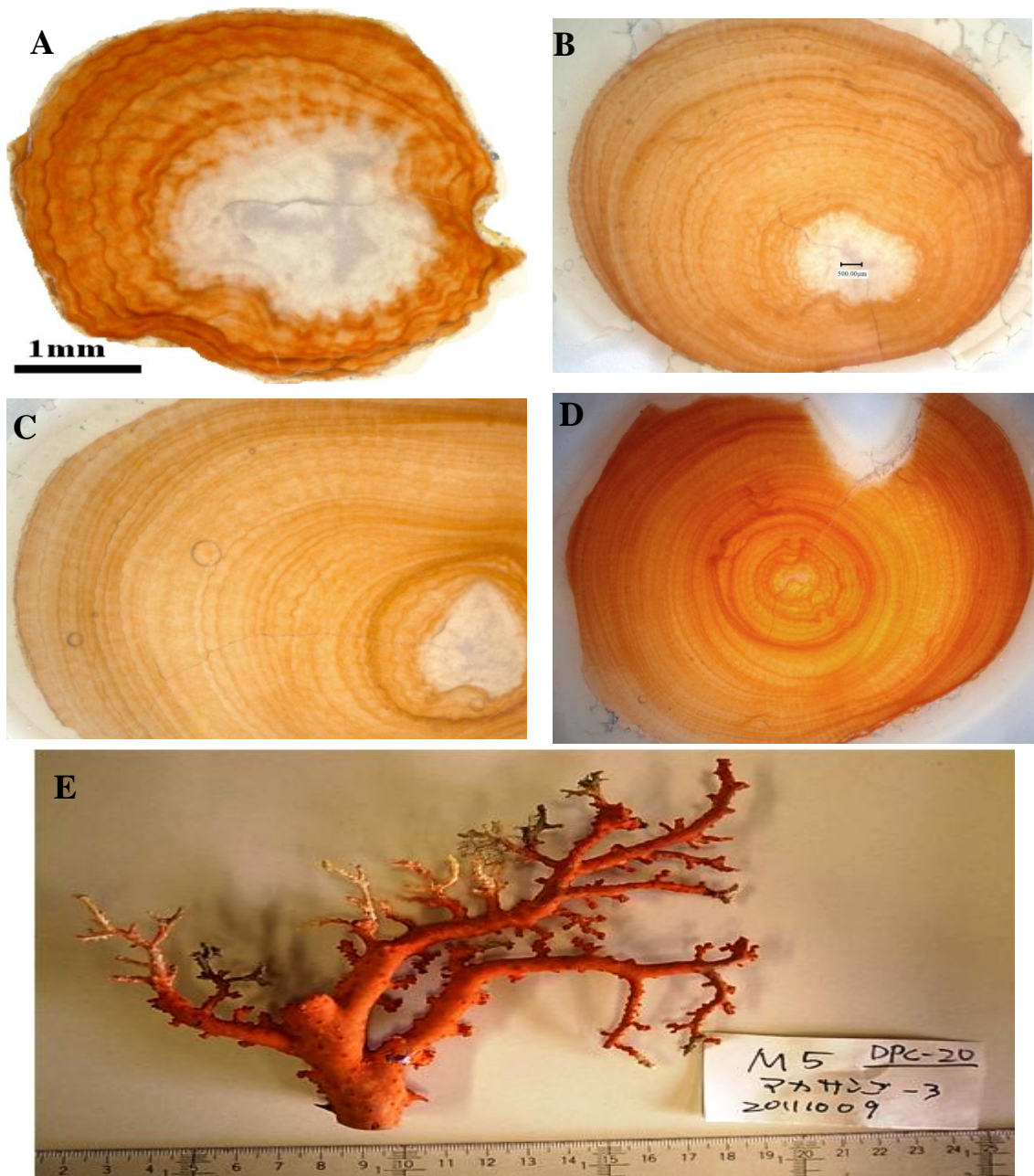


**Fig. A2. (A), (B), (C) and (D):** thin cross-sections of the axial skeleton of Japanese red corals (DPC-20) under the VHX-1000 digital microscope. **(E):** axial skeleton of Japanese red coral *Paracorallium japonicum* (DPC-18).

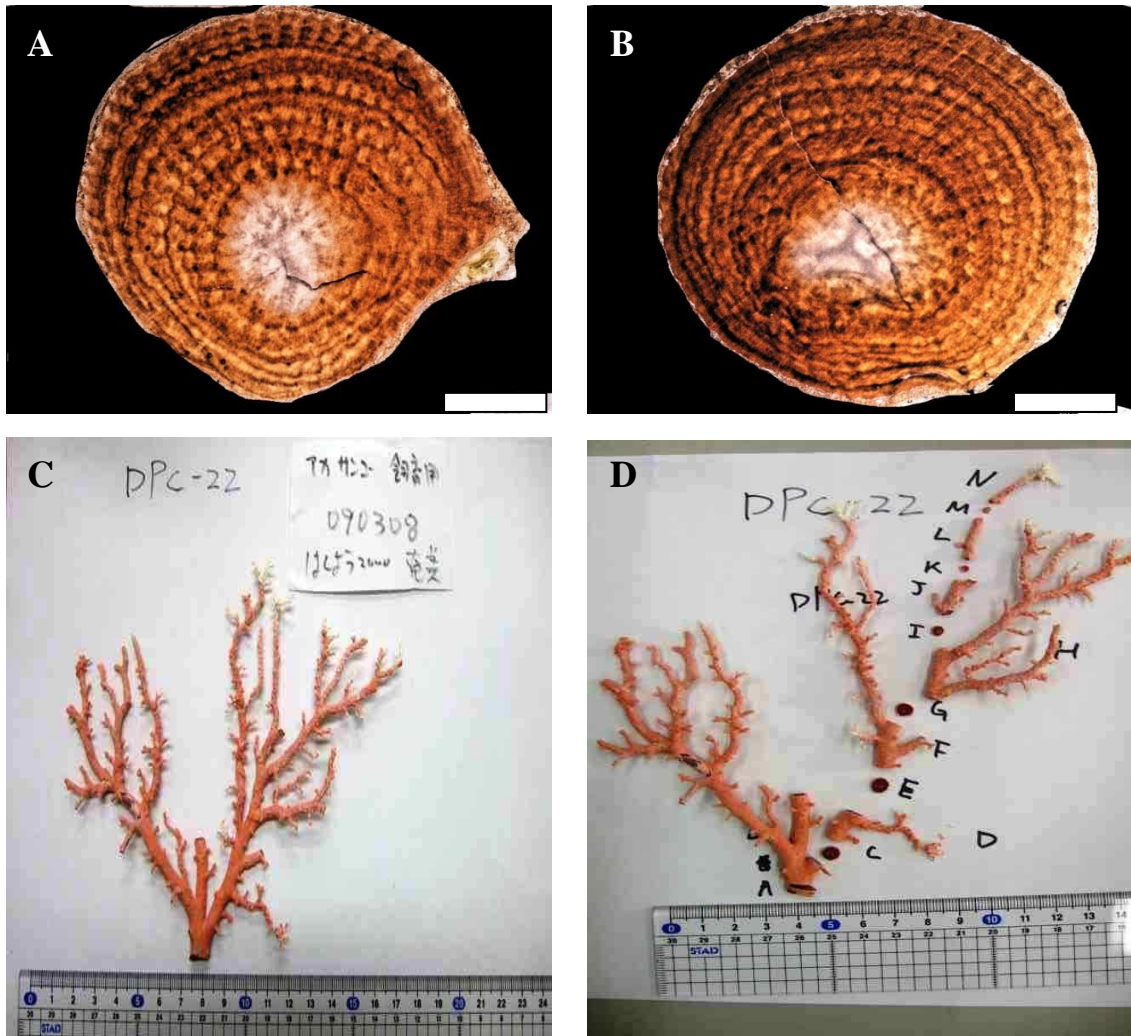


**Fig. A3. (A) and (B):** thin cross-sections of the axial skeleton of Japanese red coral (DPC-22) under the VHX-1000 digital microscope, respectively. **(C) and (D):** axial skeleton of Japanese red coral *Paracorallium japonicum* (DPC-22) and cross sections were cut from axial skeleton of this specie, respectively. White bar (1mm)

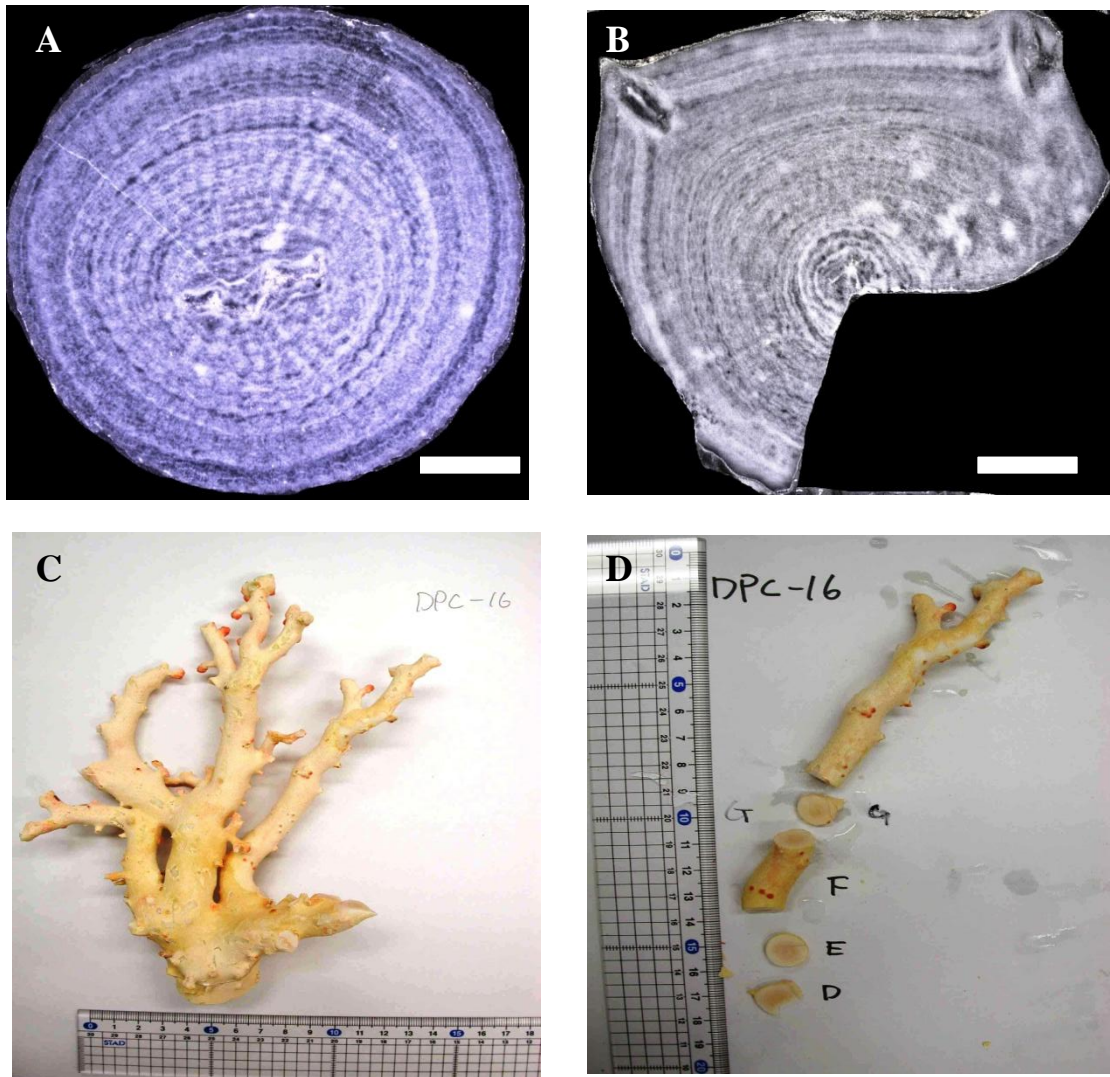


**Fig. A4. (A) and (B):** thin cross-sections of the axial skeleton of Japanese white coral (DPC-16) under the VHX-1000 digital microscope, respectively. **(C) and (D):** axial skeleton of Japanese white coral (DPC-16) and cross sections were cut from axial skeleton of this species, respectively.

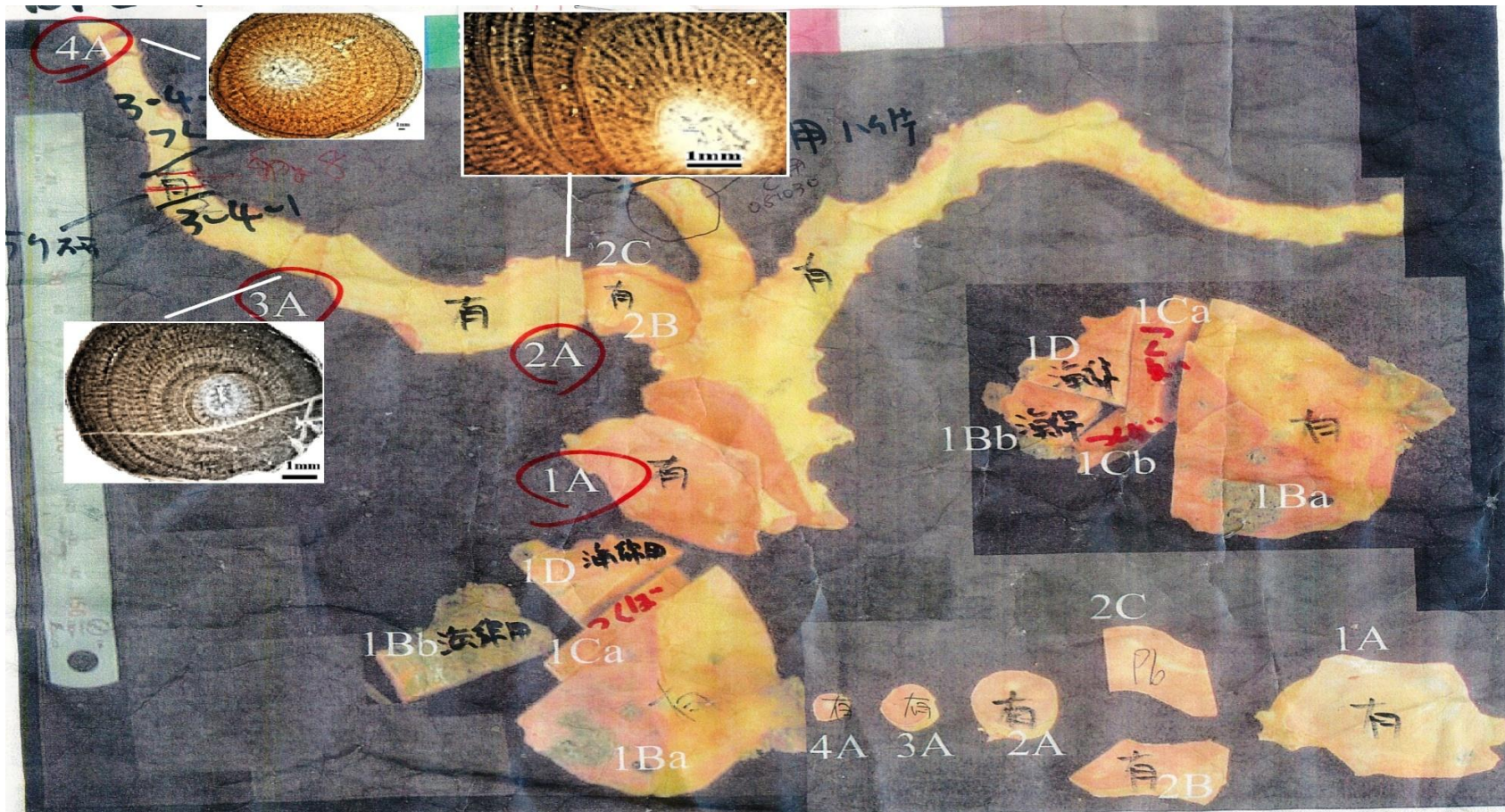


**Fig. A5. (A):** axial skeleton of Japanese pink coral (DPC-10) and cross sections were cut from axial skeleton of this species.

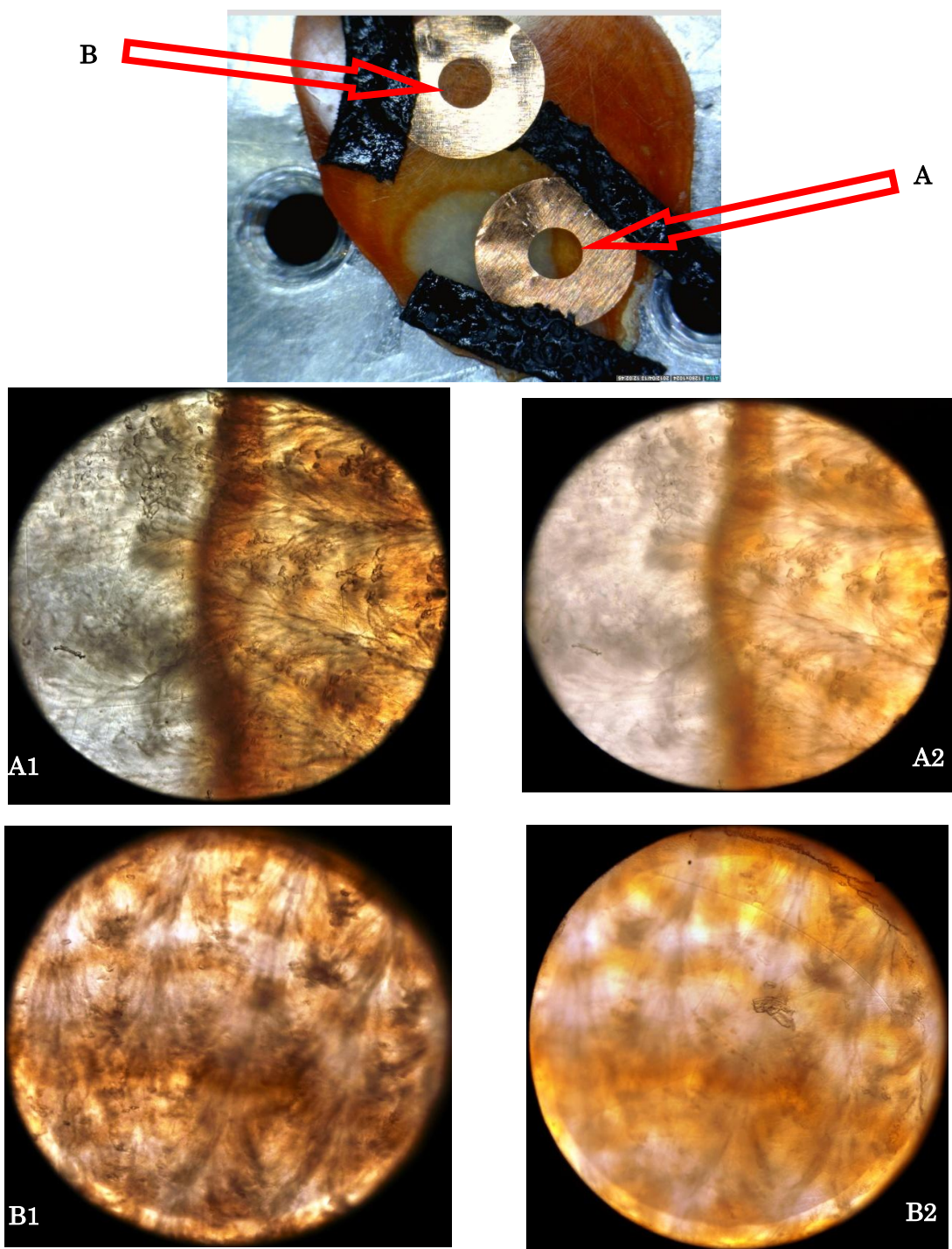


**Fig A6** : 1000 VHX digital microscope images of cross section of DPC – 19. A & B: the points where were fixed by sheet mesh (diameter = 1mm) in order to indentify inorganic distribution through X-ray Fluorescence (XRF) analysis. A1 & A2 images taken from the position A with High Dynamic Range (HDR) and normal mode of microscope and B1 & B2 taken from the postion B with HDR and normal mode of microscope, respectively